NTNU – Trondheim
Norwegian University of
Science and Technology

Fatigue in Jacket Structures With Impaired Integrity

Arve Flesche

Marine Technology
Submission date: June 2012
Supervisor: Bernt Johan Leira, IMT
Co-supervisor: Professor Jørgen Amdahl, IMT
Nils-Christian Hellevig, Aker Solutions
Junbo Jia, Aker Solutions

Norwegian University of Science and Technology
Department of Marine Technology

NTNU
Norwegian University of Science and Technology
Department of Marine Technology

Master Thesis, Spring 2012
for
Stud. Techn. Arve Flesche

Fatigue in jacket structures with impaired integrity

Utmatting av Jacket Konstruksjoner med Initiell Skade

Present regulation for the Norwegian Continental shelf has a requirement for ALS and FLS redundancy in the damaged state, but the requirement is far more well-defined for the ALS case than for the FLS.

By performing a case study for one or a number of typical North Sea jacket structures, removing single members in a systematic manner (in a systematic manner similar to ALS redundancy) and performing fatigue analysis, the sensitivity towards damage can be established.

The results shall be generalized for adjacent members and members in the same frame and parallel frames. The calculations shall be performed for the jacket as a system, but also consider local structural elements like a conductor or caisson with supports.

It is the objective that the work shall contribute to an increased understanding of the totality of the factors which will influence the safety of offshore structures. In particular, improvements related to methods for estimation of the risk of accelerated fatigue due to an initial damage on a given structure are aimed at. This risk can then be compared e.g. with the risk of failure due to extreme environmental action and the risk of single-component fatigue failure leading to reduced capacity and increased risk of failure due to overload.

The following subjects are to be addressed as part of this work:

1. A review of definitions which are proposed in the literature for the concept of "structural redundancy" is to be made. Both definitions based on deterministic and probabilistic approaches are to be considered. Methods for quantification of the various measures of redundancy are also to be highlighted.

2. A numerical model of a specific jacket structure is to be established. An initial damage of this structure is to be introduced based on discussion with the advisors. Computation of the load-carrying capacity before and after the initial damage is introduced shall be performed by application of a Finite Element Computer Program which is decided upon in cooperation with the advisors.

3. Based on the structural model in Item 2, fatigue analyses are performed based on a given scatter diagram which applies for the relevant site. Critical members of the structure are identified based on these calculations and the consequences with respect to residual fatigue damage due to the impaired integrity (i.e. initial damage) are to be discussed.

4. Parametric studies with are performed based on an established "matrix of variations". The factors to be varied can e.g. be those related to sea-state variation, load parameters and load modeling, fatigue parameters and fatigue analysis methodology. It may also be relevant to study additional jacket structures if the time allows. Furthermore, it is highly relevant to evaluate the results from the deterministic analysis within a probabilistic framework. The "variation matrix" is to be discussed and agreed upon with the advisors prior to start of the analysis itself.

The work scope may prove to be larger than initially anticipated. Subject to approval from the supervisor, topics may be deleted from the list above or reduced in extent.

In the thesis the candidate shall present his personal contribution to the resolution of problems within the scope of the thesis work.
Theories and conclusions should be based on mathematical derivations and/or logic reasoning identifying the various steps in the deduction.

The candidate should utilise the existing possibilities for obtaining relevant literature.

The thesis should be organised in a rational manner to give a clear exposition of results, assessments, and conclusions. The text should be brief and to the point, with a clear language. Telegraphic language should be avoided.

The thesis shall contain the following elements: A text defining the scope, preface, list of contents, summary, main body of thesis, conclusions with recommendations for further work, list of symbols and acronyms, references and (optional) appendices. All figures, tables and equations shall be numbered.

The supervisor may require that the candidate, in an early stage of the work, presents a written plan for the completion of the work. The plan should include a budget for the use of computer and laboratory resources which will be charged to the department. Overruns shall be reported to the supervisor.

The original contribution of the candidate and material taken from other sources shall be clearly defined. Work from other sources shall be properly referenced using an acknowledged referencing system.

The thesis shall be submitted in 3 copies:

- Signed by the candidate
- The text defining the scope included
- In bound volume(s)
- Drawings and/or computer prints which cannot be bound should be organised in a separate folder.

Supervisors: Professor Bernt J. Leira /Professor Jørgen Amdahl

Contact person at AkerSolutions: Nils-Christian Hellevig

Deadline: June 6th 2012

Trondheim, January 16th, 2012

Bernt J. Leira

Preface

This report is written as a result from a master thesis within the field of marine structural engineering. Aker Solutions MMO AS C&T in Bergen was the provider of the proposal forming this thesis. The work was undertaken during the spring semester 2012 at the Norwegian University of Science and Technology (NTNU), Department of Marine Technology. A large portion of the thesis was performed at Aker Solutions MMO AS in Bergen.

The thesis look into the effect of damage in a structural member, and how that will affect the fatigue life of the structure. To do this, a case study has been performed on two jacket structures. Members were removed in a systematic manner, similar to ALS redundancy check, and fatigue life calculations was carried out using the SESAM software package.

The Finite Element models and input files for SESAM was provided by Aker Solutions (AKSO). Therefore, the fatigue life calculations imposed no large amount of work. However, a significant portion of the work was used for processing and interpretation of the results, including writing a MATLAB script to do so. Nevertheless, the work has been both challenging and motivating putting large portion of the theoretical knowledge I have obtained during the years at NTNU into practical application. I have also extended my knowledge in the use of software which is frequently adapted in the engineering industry, and I am grateful for this experience.

There was some convergence issues regarding the pushover analyses of the 4L-jacket, which reduced the number of wave directions that could be presented in this report. It is time consuming to perform several hundred analyses, and trying to manually fix the runs which posed numerical problems would simply take too much time and require more effort than I wanted to put into the pushover analyses.

Further, I must point out that the FE models used in this thesis has an internal classification, and thus there will be no electronic copies available. This will make it difficult for the reader to fully grasp the results, but I hope the level of description in the thesis and the number of result plots is sufficient to understand the conclusions I have drawn.

I would like to thank Nils-Christian Hellevig at Aker Solutions for a master thesis proposal and supervising, as well as Ole Johan Sletten for his involvement in searching through AKSO for a thesis subject for me. I am also grateful for the help I got from Junbo Jia, my second supervisor at AKSO, when Nils-Christian was unavailable. Your help and guidance was and still is much appreciated. Further, I am thankful for the help I got from Håkon Vidar Sylta regarding use of the software. I would also like to thank my supervisor at NTNU, Professor Bernt Johan Leira, and my co-supervisor Professor Jørgen Amdahl, for your help and guidance whenever I felt stuck or lost.

Finally, I would like to express my gratitude towards the C&T department in

AKSO for giving me my own office and allowing me to take advantage of employee privileges. My roughly two months long stay was nothing but pleasurable thanks to all the friendly and helpful employees.

Trondheim, June 6, 2012

Arve Flesche

Abstract

Present regulations for offshore structures on the Norwegian continental shelf have a requirement for Accidental Limit State redundancy and Fatigue Limit State redundancy in a damaged state. However, the requirement is far more defined for the Accidental Limit State than for the Fatigue Limit State. An increased understanding of factors governing fatigue redundancy would create a basis to form a comprehensive definition.

In literature, the term redundancy is defined in several ways. The different methods can be divided into two major categories, namely deterministic and probabilistic approaches. In general, redundancy may be defined as the absence of members whose failure would lead to global collapse. Within both the deterministic and the probabilistic framework, several redundancy factors are usually defined, and there are resemblance between some of them. In probabilistic methods, the reliability method is commonly applied through the First Order Reliability Method.

Fatigue damage is a primarily concern regarding the integrity for offshore structures. A near constant subjection to cyclic loadings from wind, current and waves initiates a cumulative damage process which leads to a certain fatigue life for the members in the structure. The lifetime may be calculated using either a fracture mechanics approach or a SN-curve approach. There exists several approaches to calculate the stress levels to be used in the fatigue analyses, and the choice of method is mainly based on whether or not the structure under consideration is dynamically behaving or may be regarded as quasi-static. Also, there may be non-linearities that needs to be accounted for and naturally this will affect the choice of analysis method. However, large uncertainties are associated with fatigue calculations regardless of analysis approach. Thus, a probabilistic framework is highly relevant in order to estimate the risk of failure due to fatigue.

A study on how impaired integrity affects the fatigue life has been performed for two jackets; one highly redundant four-legged jacket and one less redundant three-legged jacket. The main goal has been to investigate the fatigue redundancy of the structures, in order to link up the risk of accelerated fatigue due to damage with the risk of failure due to extreme environmental actions, which may eventually lead to structural collapse. A stochastic fatigue analysis approach was chosen, and the analyses was in agreement with the standards governing the Norwegian continental shelf at the time of this thesis. Pushover analyses has been performed on the jackets to give an insight in their redundancy, and a calculation of changes in the natural periods under impaired integrity has also been done.

The four-legged jacket was proven to be highly redundant, and had small changes in the natural period under impaired integrity. The three-legged jacket on the other hand, had some damage cases with a rather large increase. Also, the redundancy factor R_4 was significantly lower for the three-legged jacket, thus confirming it to be less redundant than the four-legged jacket. A large change in the natural period will alter the dynamic response, thus the fatigue life is vastly connected to changes in global stiffness.

Trying to explain the changes in fatigue life for the two jackets under impaired integrity without using a deterministic approach, i.e. calculate the fatigue life for the specific damage case, was proven to be very difficult. There seems to be no easy way to isolate the severity of the fatigue life reduction since large changes are occurring throughout almost the entire structure for several damage cases, as well as large spread in the values them self. However, there was also found some trends in the results. One of them, was that the closer a member is to the damaged element, the larger is the expected reduction in fatigue life. Another trend, is that a large fatigue accelerator factor is expected in almost every damage case, thus one may expect large changes for most of the damage scenarios.

Another vastly occurring phenomenon were the location of the damaged members who gave the lowest fatigue life in the structures. For the four-legged jacket, this involved damage in the caisson supports. The three-legged jacket, however, had the lowest fatigue lives occurring for damage cases in the top frame where there is a lack of deterministic redundancy.

There seems to be no fatigue redundancy for the jackets, as there are large fatigue accelerator factors occurring. There is also the very low calculated fatigue life in the most extreme cases. However, there has been found a slight correlation between a large reduction in fatigue life and a large initial fatigue life. What should also be taken into account though, is both the risk related to the fatigue lives found, and the accuracy of the values due to the linearised analysis.

Sammendrag (Norwegian Abstract)

Nåværende forskrifter for offshore konstruksjoner på norsk sokkel har et krav til redundans i skadet tilstand. Imidlertid er kravet langt mer definert for styrkemessige betraktninger enn for utmatting. En økt forståelse av faktorene som styrer utmattingsredundans vil skape et grunnlag for å danne en omfattende definisjon i forskriftene.

I litteraturen er begrepet redundans definert på flere måter. De ulike metodene kan deles inn i to hovedkategorier, nemlig deterministiske og probabilistiske metoder. Generelt kan redundans defineres som fravær av medlemmer som ved svikt vil føre til global kollaps. Innenfor både deterministiske og probabilistiske rammeverk, er flere redundansfaktorer definert, og det er likheter mellom noen av dem. I probabilistiske metoder, er pålitelighetsanalyse vanligvis anvendt gjennom første ordens pålitelighets metode.

Utmattingsskade er en ofte kritisk faktor for offshore konstruksjoner. En konstant utsettelse for sykliske belastninger fra vind, strøm og bølger medfører en kumulativ skadeprosess som fører til materialtretthet for medlemmene i strukturen. Levetiden kan beregnes ved hjelp av enten en bruddmekanisk tilnærming eller en SN-kurve tilnærming. Flere metoder for å beregne spenningsnivået som skal brukes i de utmattingsanalyser finnes, og valg av metode er i hovedsak basert på hvorvidt strukturen er oppfører seg dynamisk eller kan anses som kvasi-statisk. Dessuten kan det være ikke-lineariteter som må tas hensyn til, og naturligvis vil dette påvirke valg av analysemetode. Det er i midlertidig store usikkerheter knyttet til utmattingsberegninger uavhengig av analysemetode. Dermed er et probabilistisk rammeverk svært relevant for å estimere risikoen for svikt på grunn av utmattelse.

En studie av hvordan skade i en konstruksjon vil påvirke levetiden for to jacketkonstruksjoner er blitt utført, en svært redundant firebent jacket og en mindre redundant trebenet jacket. Hovedmålet har vært å undersøke utmattingsredundans av konstruksjonene, for å knytte opp risiko for akselerert utmatting på grunn av skade med fare for svikt på grunn av ekstreme naturkrefter, som vil medføre global kollaps. En stokastisk utmattingsanalyse ble valgt, og de involverte variabler følger standarder for norsk sokkel. Progressiv kollaps analyser har blitt utført på jacketene for å gi innsikt i deres redundans, og en kontroll av endringer i egenperioder under skadet tilstand har også blitt gjennomført.

Den firbente jacketen ble påvist å være svært redundant, og hadde små endringer i sin egenperiode under skadetilstander. Den trebeinte jacketen derimot, hadde noen skadetilfeller med en ganske stor økning i egenperiode. I tillegg var redundans faktoren R_4 betydelig lavere for den trebente jacketen, noe som bekrefter at den er mindre redundant enn den firbente jacketen. En stor økning i egenperioder vil lede til endringer i dynamisk respons, og levetid er derfor sensitiv til endringer i global stivhet.

Å forklare endringene i levetiden til de to jacketene under skade uten å bruke en deterministisk tilnærming, dvs. beregne levetiden for det bestemte skadetilfellet, ble påvist å være svært vanskelig. Det ser ikke til å finnes en måte beskrive endrin-

gene i levetid generelt sett, siden det var store forandringene gjennom nesten hele konstruksjonen for flere skadetilfeller, samt stor spredning i tallverdier. Imidlertid ble det også funnet noen trender i resultatene. En av dem, var at jo nærmere et medlem var til det skadede elementet, jo større var forventet reduksjon i levetid. En annen trend, var en stor utmattingsakselerator i nesten alle skadetilfeller, og dermed kan man forvente store endringer for de fleste skadescenarier.

Et annet fenomen som ble funnet var plasseringen av skade scenariene som ga den laveste levetiden. For den firebente konstruksjonen, gjaldt dette involvert skader i caisson-innfestningene. Den trebente jacketen hadde imidlertid de laveste levetidene for skader scenarioer i den øverste rammen hvor det er manglende redundans.

Det ser ut til å være en mangel på utmattingsredundans for jacketene, siden det er veldig store ekstremverdier for utmattingsakselerator-faktoren. Det er også svært lav beregnet levetid i de mest ekstreme tilfellene. Det har imidlertid blitt funnet en svak sammenheng mellom en stor reduksjon i levetid og en stor uskadet levetid. Det bør tas hensyn til både risikoen knyttet til de lave levetidene, og nøyaktigheten av verdiene på grunn av linearisert analyse, før en endelig konklusjon trekkes.

Contents

List of Figures

List of Tables

NOMENCLATURE

β Reliability index

γ Peak enhancement factor in JONSWAP spectrum

3L The three legged jacket

4L The four legged jacket

ADAEOSL Accumulated Damage At End Of Service Life

AKSO Aker Solutions AS

ALARP As Low As Reasonable Possible

ALS Accidental Limit State

C&T Concept & Technology

CDF Cumulative Distribution Function

DAF Dynamic Amplification Factor

DF Damage Factor

DNV Det Norske Veritas

E Young's modulus

e-mod Short for Elastic Modulus or Young's Modulus

EDAF Equivalent DAF

FAF Fatigue Accelerator Factor

FE Finite Element

FEA Finite Element Analysis

FEM Finite Element Method

FLS Fatigue Limit State

FORM First Order Reliability Method

FRAMEWORK Program for post-processing of framed structures, part of SESAM

GeniE Finite Element program, part of SESAM

H_S Significant wave height

JONSWAP Joint North Sea Wave Project, wave spectrum

KC Keulegan-Carpenter

LC Load Capacity

MANAGER Graphical User Interface to run SESAM analyses/programs, part of SESAM

MATLAB MATrix LABoratory, a programming environment for algorithm development, data analysis, visualization, and numerical computation

MMO Maintenance Modification and Operation

MPa Mega (10^6) Pascal

MT Metric tonnes

NORSOK NORsk SOkkels Konkurranseposisjon, standards for the Norwegian continental shelf

NTNU Norges Teknisk Naturvitenskapelige Universitet (Norwegian University of Science and Technology)

PDF Probability Density Function

PM Pierson-Moskowitz, wave spectrum

PREFRAME Program for creating spaced frame structures, part of SESAM

PRESEL Program for combining super elements pre FEA, part of SESAM

R_n Redundancy Factor n

RBI Risk Based Inspection

RIFLEX Beam based FE program suitable for slender structures

RSR Reserve Strength Ratio

SCF Stress Concentration Factor

SESAM Software package by Det Norske Veritas (DNV)

SESTRA Program for solving the FE equations, part of SESAM

SL Service Life

SLS Serviceability Limit State

SN Stress-Cycle relationship between cyclic stress range S and magnitude of cycles before failure, e.g. SN-curve

T_P Peak period for wave spectrum

ULS Ultimate Limit State

USFOS Non-linear Finite Element program

WAJAC Program for calculating wave loads on jacket structures, part of SESAM

y Year

1

Introduction

Safety regarding marine structures are naturally an important aspect in both the design phase of a structure and during operating phase. The structure needs to withstand forces acting from the environment during its lifespan without danger to human life. This implies resistance against extreme loads during abnormal environmental situations, but also resistance against the frequently occurring fatigue damage loads. Due to the random nature of the loads, ensuring adequate strength is best solved using a probabilistic approach where the risk of structural collapse or failure should be As Low As Reasonable Possible (ALARP). The risk of an event may be expressed as the product of the probability of an event and the consequence of the event. Thus, if an event has a high consequence, the probability of this event must be low to reduce the associated risk.

For the Norwegian continental shelf, there is a set of NORSOK standards that define how to design structures and how to inspect them in order to have a safe structure during its service life time. For the structural integrity, there are three different limit states that must be checked. These are named Ultimate Limit State (ULS), Accidental damage Limit State (ALS) and Fatigue Limit State (FLS), where ULS and ALS are actions corresponding to a probability of occurrence of 10^{-2} and 10^{-4}, respectively.

Present rules for the Norwegian continental shelf requires that after an ALS event has occurred, i.e. under impaired integrity, the structure should withstand ULS actions and have adequate residual fatigue life. However, very little guidance is given on how to calculate the latter. The former requirement is for filled provided that the structure has sufficient redundancy, so that when one member fails other members have sufficient capacities to carry the added loads. This may however lead to large changes in the fatigue life for the members. In the most extreme cases, the stress redistribution may cause failure of several more members due to fatigue, and eventually a collapse of the structure may occur. It is therefore not given that the adequate redundancy in strength implies sufficient fatigue redundancy.

In the following chapters, some different methods for defining structural redundancy will be reviewed. The basic principles behind fatigue and fatigue calculation will be described. Two numerical models of two different jackets will be presented along with a description of a fatigue analysis which has been performed. The effect of damage on the structural integrity will be investigated along with how impaired integrity affects the fatigue life for the structures. The scope of work forming the chapters has been to not only find the fatigue life for a damaged structure, but also try to explain the changes in a general manner.

2

Redundancy

Redundancy in a structure is one way to keep a low risk of collapse after an abnormal damage scenario. For instance, say the structure looses the load carrying capacity in one member. If the rest of the members will redistribute the load without the structure collapsing, there will be no change in the consequence for the given load level. Hence, the risk of structural collapse will not increase and will even be less for the damaged structure, as the probability of the structure existing in a damaged state is less than existing in the intact state.

It ought to be obvious that all offshore structures should be considered a safe place for human beings, and impose no threat to the environment or the economy. This is why redundancy is usually required by design specifications or owners, and by rules and regulations governing the field where the offshore structure should be. However, how to define structural redundancy is not a well defined property, and in literature there are several different approaches to do so. A general definition of redundancy is the absence of members whose failure would lead to global collapse. Digging deeper, two main categories could be defined namely deterministic and probabilistic methods. In the following sections some of these different ways of defining redundancy will be presented.

2.1 Deterministic

Deterministic redundancy is simply put a mathematical way to describe how well a structure can respond to damage of its members, given that all quantities are known. A classical deterministic way to define structural redundancy is to base it on static indeterminacy for a truss work [Fu and Frangopol, 1990]. The measurement is commonly known as degree of redundancy, and is defined as

$$R_1 = F - E \tag{2.1}$$

where F is the number of unknown reactive forces and E is the number of independent equilibrium equations.

This degree of redundancy is illustrated by the two truss works in figure 2.1. Here, 2.1a is a statically determine structure, and thus have no redundancy; while 2.1b is a statically indetermined structure with one degree of redundancy: It can survive failure of any single member. Hence, the truss work can be classified as a *fail-safe* structure. It must be emphasized though, that the degree of redundancy in a structure (based on static indeterminacy), is *not* a measure for overall system strength as it does not express whether or not the remaining members will cope with the redistributed loads. Also, when the structure becomes complicated, it may have certain parts which are redundant and certain which are not even though

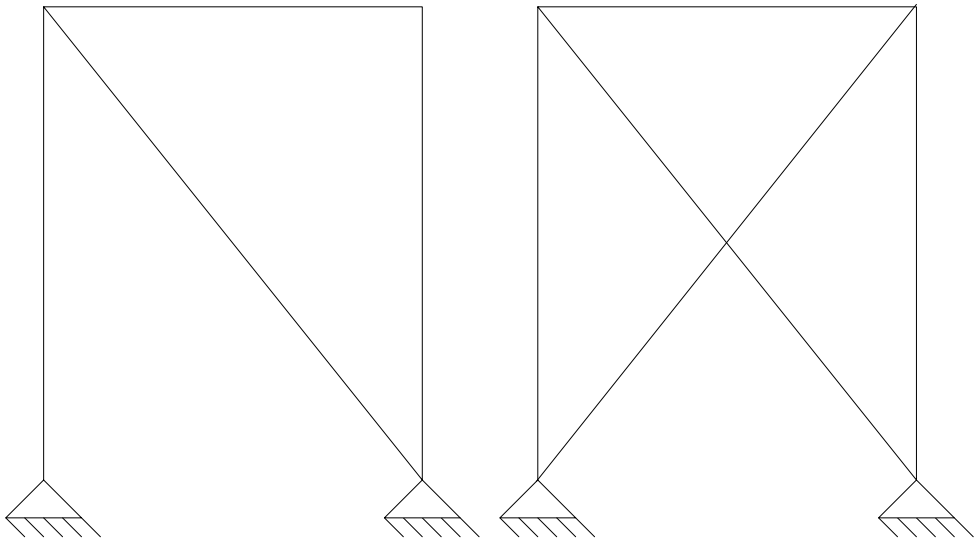

(a) Statically determine trusswork **(b)** Statically indetermine trusswork

Figure 2.1: Two simple truss works with pinned joints

the structure as a whole is statically indeterminate. This can be illustrated by an example with a 10 bar truss [Furuta et al., 1985],[Frangopol and Curley, 1987]. The main results are briefly repeated here:

> The truss has six joints [...] and one degree of redundancy due to the presence of one additional member connecting two intermediate joints. It is shown that the capacity of the system depends on which member will fail first. If any of the four members connecting the lateral and the intermediate joints fail, the structure fails immediately. On the other hand, if any of the six members connecting the intermediate joints fail, the structure may survive because of an alternative load path.

This clearly shows that measuring redundancy with respect to degree of static indeterminacy, does not give an adequate way to define system strength. One must either look at a different parameter, or one has to also include member behaviour and overall system strength as a redundancy measure.

To deal with this problem, the following factors are proposed [Furuta et al., 1985].

1. Reserve redundant factor defined as

$$R_2 = \frac{L_{intact}}{L_{design}} \tag{2.2}$$

where L_{intact} and L_{design} are collapse load for intact structure and design load, respectively.

2. Residual redundant factor defined as

$$R_3 = \frac{L_{damaged}}{L_{intact}} \tag{2.3}$$

where $L_{damaged}$ is the collapse load for damaged structure.

3. Strength redundant factor defined as

$$R_4 = \frac{L_{intact}}{L_{intact} - L_{damaged}} \tag{2.4}$$

4. Redundancy factor R_{cy} [Yoshida, 1990]

$$R_{cy} = \frac{Q_{col} - Q_{yiel}}{Q_{col}} = \frac{L_{intact} - L_{yiel}}{L_{intact}} \tag{2.5}$$

where Q_{col} and Q_{yiel} or L_{yiel} are collapse load of an undamaged structure and first yielding load, respectively.

From these parameters, one may notice that equations (2.2)-(2.5) give a better measurement of redundancy than equation (2.1), as they take the overall structural strength into account. This was the weakness for the degree of redundancy, as shown with the ten-bar truss example. On the other hand, R_2 does not necessarily give a measure for redundancy, as it does not express any connection between local failure and global failure. In regard to this matter, R_{cy} is a better choice as it will go towards zero when the structure looses redundancy, i.e. a structure failing without stress redistribution would have $L_{intact} = L_{yiel}$ and thus $R_{cy} = 0$.

It could also be noted that the product R_3R_4 actually gives a way to check if the structure will survive the design load in damaged condition, i.e. R_3R_4 should be larger than 1 in order for the structure to survive.

2.1.1 Example: Ten-bar Truss

Take the ten-bar symmetric truss shown in figure 2.2 [Frangopol and Curley, 1987]. The members are assumed brittle, i.e. when member load reaches yield, the member fails completely. Five different member states are introduced as follows:

1. “Intact” member: no reduction in Load Capacity (LC), Damage Factor (DF)=0
2. “Slight” damage: 25 % reduction in LC, DF=0.25
3. “Moderate” damage: 50 % reduction in LC, DF=0.5
4. “Severe” damage: 75 % reduction in LC, DF=0.75
5. “Complete” damage: 100 % reduction in LC, DF=1.0

Damage factor	Member number									
	1	2	3	4	5	6	7	8	9	10
0.00	1.00	1.00	1.00	1.00	1.00	1.00	1.00	1.00	1.00	1.00
0.25	0.75	1.00	1.00	0.99	1.00	1.00	1.00	1.00	0.75	1.00
0.50	0.50	1.00	0.88	0.71	1.00	1.00	1.00	0.88	0.50	1.00
0.75	0.25	1.00	0.71	0.71	1.00	1.00	1.00	0.71	0.25	1.00
1.00	0.00	1.00	0.71	0.71	1.00	1.00	1.00	0.71	0.00	1.00

Table 2.1: Redundancy factor R_3 for the ten-bar truss

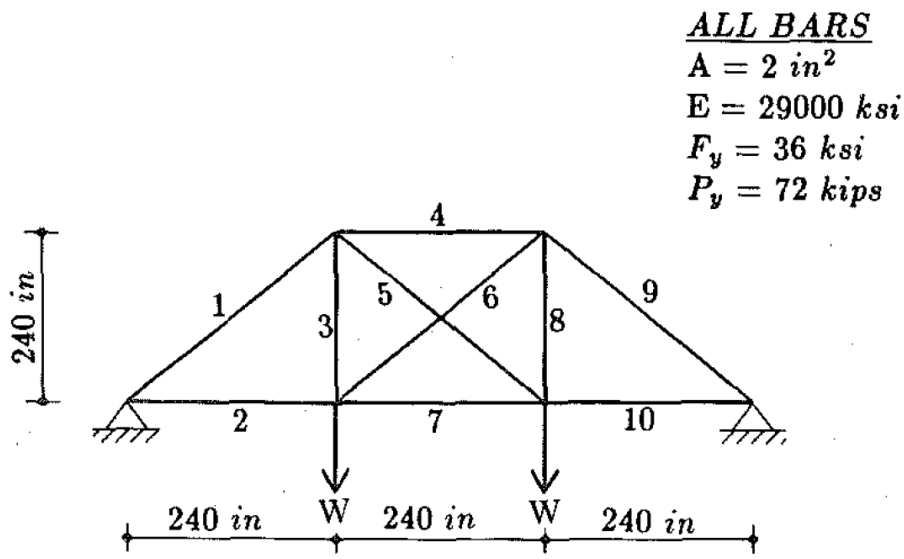

Figure 2.2: Ten-bar truss with geometric and material properties shown

By looking at single member failure, i.e. applying the five different member damage states on each member individually, and thereby calculating maximum load W, the residual redundant factor R_3 (equation (2.3)) can be calculated. The numbers are given in table 2.1.

From these numbers, one can see the following. Members 2, 5, 6, 7 and 10 have no influence on system strength, while members 1 and 9 are critical components, whose failure would lead to structural collapse. The remaining members 3, 4 and 8 have some impact on the system strength, but still, they can fail completely without global collapse, i.e. the structure can still carry a load W. However, these numbers are only valid for single member failure. A similar approach can be done while looking at two and two members failing at the same time, to identify a more complex redundancy property for the structure. The results are presented in

Damage factor	Members								
	3&1	3&2	3&4	3&5	3&6	3&7	3&8	3&9	3&10
0.00	1.00	1.00	1.00	1.00	1.00	1.00	1.00	1.00	1.00
0.25	0.75	1.00	0.96	1.00	1.00	1.00	1.00	0.75	1.00
0.50	0.50	0.88	0.65	0.83	0.83	0.87	0.97	0.50	0.88
0.75	0.25	0.71	0.33	0.44	0.44	0.71	0.65	0.25	0.71
1.00	0.00	0.71	0.00	0.00	0.00	0.71	0.00	0.00	0.71

Table 2.2: Redundancy factor R_3 for the ten-bar truss, two members with damage

table 2.2.

No one see that member 3 together with members 1, 4, 5, 6, 8, and 9 are critical for the system strength, and that the combination of 3&1 and 3&9 are the worst, i.e. smallest value for R_3 for a small value of DF.

2.2 Probabilistic

In the previous section, a deterministic concept of redundancy was described, meaning that all quantities were assumed to be known and constant. This gives a general assessment to identify members which should be inspected more frequently. However, many of the involved variables, e.g. the loading and the material strength, is of a random nature. This is especially true for offshore structures, which are subjected to random wind, current and wave loads. To account for this, a probabilistic approach for system redundancy should be applied, meaning that one look at the probability of failure.

2.2.1 Reliability

For a simple structure, one may express a performance function Z describing the relation between the system loading S and the system resistance R. By defining a positive Z as safe, one have that the structure will survive the loads S if $Z \geq 0$, i.e. the structure will not collapse as long as the system resistance is larger than or equal to the external loading.

$$Z = R - S \tag{2.6}$$

The probability of failure can then be expressed as the probability that R is less than or equal to S, which can be written as follows:

$$p_f = P\left(R \leq S\right) = P\left(R - S \leq 0\right) = P\left(Z \leq 0\right) \tag{2.7}$$

R and S are random variables, so they each have a Probabilistic Density Function (PDF) f_R and f_S, respectively. The joint PDF, f_{RS} is used to identify the probability of failure:

$$p_f = P\left(R - S \leq 0\right) = \int_D \int f_{RS}(r,s)drds \tag{2.8}$$

By assuming that R and S are independent, one get that $f_{RS}(r,s) = f_R(r)f_S(s)$ and thus the probability of failure is

$$p_f = P\left(R - S \leq 0\right) = \int_{-\infty}^{\infty} \int_{-\infty}^{s \geq r} f_R(r)f_S(s)drds \tag{2.9}$$

It can be shown that since R and S are independent of each other, equation (2.9) can be expressed as [Melchers, 1999]:

$$p_f = \int_{-\infty}^{\infty} F_R(x)f_S(x)dx \tag{2.10}$$

One have that $F_R(x)$ is the probability that $R \leq x$, i.e. the probability that the resistance is less than some value x. Thus one have a quantity that can denote failure. By further assuming that R and S are normally distributed random variables with means μ_R and μ_S and variances σ_R^2 and σ_S^2 respectively, one have the following properties for the Z variable.

$$\mu_Z = \mu_R - \mu_S \tag{2.11a}$$
$$\sigma_Z^2 = \sigma_R^2 + \sigma_S^2 \tag{2.11b}$$

Now the failure probability can be expressed in terms of Z, which is also a normally distributed random variable

$$p_f = P\left(Z \leq 0\right) = \Phi\left(\frac{0 - \mu_Z}{\sigma_Z}\right) \tag{2.12}$$

where $\Phi(\ldots)$ is the standard normal distribution function. This can also be written as

$$p_f = \Phi\left(-\beta\right) \tag{2.13}$$

where $\beta = \mu_Z/\sigma_Z$ is defined as the *safety index* or *reliability index*. β is a measure of how many standard deviations σ_Z the mean value μ_Z is from the origin $Z = 0$ (failure boundary) in a Gaussian space. Thus, β is a direct measure of the safety for the system described by the performance function Z. The higher β is, the lower the probability of failure is. This is illustrated in figure 2.3.

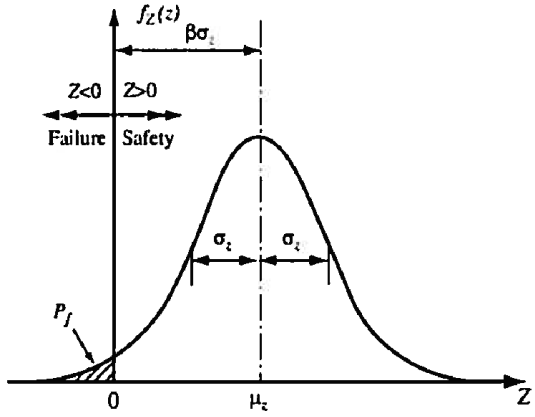

Figure 2.3: Illustration of β

A Reliability Example

How one can use the reliability index in practise can be illustrated by a little example. Take a simply supported steel beam with length $10[m]$. This beam is subjected to a random loading, uniformly distributed over the length of the beam, with a mean of $0.5[kN/m]$ and a variance of $0.01[kN^2/m^2]$. The bending strength of the beam has been found to have a mean value of $50[kNm]$ and a variance of $1[kNm^2]$. From simple beam theory, the largest bending moment occurring is $M_{Max} = qL^2/8$. This leads to a mean value for the external loading $\mu_S = \mu_q \cdot 10^2/8$ and a variance $\sigma_S^2 = \sigma_q^2 \cdot \left(10^2/8\right)^2$. Now, one can find the mean and variance for the performance function Z from equation (2.11): $\mu_Z = 50 - 6.25 = 43.75$ and $\sigma_Z^2 = 156.25 + 1 = 157.25$. Thus, one have that $\beta = 43.75/157.25 = 0.278$ (if one assume normally distributed values), and from tables it can be found that the failure probability is $p_f = \Phi(-\beta) = \Phi(-0.278) = \underline{\underline{0.0027}}$.

2.2.2 First Order Reliability Method - FORM

In the previous section, it was stated how to calculate the reliability index for a system given that the involved parameters for the performance function were normally distributed. In general, this is not always true and thus one cannot use the standard normal distribution function as showed in equation (2.12). However, this can be solved by transforming the involved parameters from the physical space into a space consisting of independent, standard Gaussian variables. The performance

function could be linearised in the Gaussian space using a first-order Taylor series expansion, hence the name First Order Reliability Method (FORM). A short introduction to this method can be done by looking at the normal tail transformation. Say that one have a non-normal distributed random variable X. The transformation of this variable to an equivalent standardized normally distributed random variable Y can be expressed mathematically as

$$p = F_X(x) = \Phi(y) \Rightarrow y = \Phi^{-1}\left[F_X(x)\right] \tag{2.14}$$

where p is some probability connected to $X = x$ and thus $Y = y$. One can know introduce an equivalent normal variable U, with a cumulative distribution function F_U, to represent X. The choice of U is somewhat ambiguous, as it depends on the choice of μ_U and σ_U. An appropriate choice is found by linearising the failure surface using a Taylor series expansion of equation (2.14) around some point x^e, i.e. using FORM. The results are as follows [Melchers, 1999]:

$$y = \frac{u - \mu_U}{\sigma_U} \tag{2.15a}$$

$$\text{if} \quad u = x \tag{2.15b}$$

$$\text{with} \quad \mu_U = x^e - y^e \sigma_U \tag{2.15c}$$

$$\sigma_U = \frac{\phi(y^e)}{f_X(x^e)} \tag{2.15d}$$

$$y^e = \Phi^{-1}\left[F_X(x^e)\right] \tag{2.15e}$$

Thus, the transformation given in (2.14) can be expressed by the new random variable U which is normally distributed with mean μ_U and standard deviation σ_U given by (2.15c) and (2.15d) above. Also, by combining (2.14), (2.15a) and (2.15b), it follows that $F_X(x^e) = F_U(x^e)$. Introducing the transformation $f_Y(y) = f_X(x)|\frac{dx}{dy}|$ and using (2.15d), (2.15a) and (2.15b) it also follows that $f_X(x^e) = f_U(x^e)$. Thus, by setting the tail probability for U equal to that of X, i.e. $1 - F_X = 1 - F_U$, one has performed the so-called *normal tail approximation.*

It can be shown that the expansion point x^e is identical to the checking point x^* by demanding β to be stationary [Melchers, 1999]. The so called checking point, also known as the design point, is the point along the failure boundary curve (or plane) in the Gaussian space which is perpendicular to β. β will be a circle in a two dimensional Gaussian space and a sphere in a three dimensional Gaussian space. x^* represents the most probable point along the failure boundary, hence the name design point. It should be noted that some errors will occur when using FORM. Since each variable are individually approximated by a normal distribution at the checking point, the point of maximum joint probability density is not necessarily at the same place as the checking point. However, any resulting errors are assumed to be small. The linearisation that is performed of the performance function will

also introduce some errors. But if one is mostly dealing with small probabilities, it turns out that FORM is a very good approximation in practise [Haver, 2011].

Rosenblatt Transformation

If the joint probability density function is known and the involved variables are dependent, then a Rosenblatt transformation can be performed in order to apply FORM. Consider a set of random variables represented by the vector $\mathbf{X}$ and the equivalent standardized normal variables denoted by the vector $\mathbf{Y}$. Then, a Rosenblatt transformation from the physical space into the Gaussian space is done as follows:

$$\begin{aligned} \Phi(y_1) &= F_1(x_1) \\ \Phi(y_2) &= F_2(x_2|x_1) \\ &\cdots \\ \Phi(y_n) &= F_n(x_n|x_1,\ldots,|x_{n-1}) \end{aligned} \tag{2.16}$$

$$\begin{aligned} y_1 &= \Phi^{-1}\left[F_1(x_1)\right] \\ y_2 &= \Phi^{-1}\left[F_2(x_2|x_1)\right] \\ &\cdots \\ y_n &= \Phi^{-1}\left[F_n(x_n|x_1,\ldots,|x_{n-1})\right] \end{aligned} \tag{2.17}$$

$$\begin{aligned} x_1 &= F_1^{-1}\left[\Phi(y_1)\right] \\ x_2 &= F_2^{-1}\left[\Phi(y_2|x_1)\right] \\ &\cdots \\ x_n &= F_n^{-1}\left[\Phi(y_n|x_1,\ldots,|x_{n-1})\right] \end{aligned} \tag{2.18}$$

Now, one also have to transform the performance function into the Gaussian space. This is done by utilizing that a probability density function defined in $\mathbf{x}$ space is transformed into $\mathbf{y}$ space as shown in (2.19), and that this transformation holds for every continuous functions in $\mathbf{X}$ and $\mathbf{Y}$.

$$\begin{aligned} f_{Y_1Y_2}(y_1,y_2) &= f_{X_1X_2}(x_1,x_2)|\mathbf{J}| \\ &\Downarrow \\ G(\mathbf{x}) &= g(\mathbf{y})|\mathbf{J}| \end{aligned} \tag{2.19}$$

where $\mathbf{J}$ is the Jacobian matrix with elements $j_{ij} = \partial y_i/\partial x_j = \frac{1}{\phi(y_i)}\frac{\partial F_i(x_i|x1,\ldots,x_{i-1})}{\partial x_j}$

2.2.3 Probabilistic Redundancy Factors

Another approach to probabilistic redundancy is to simply use the deterministic factors described earlier, and extend them into the world of probabilistic uncertainty. Take for example the strength redundant factor R_4. The known quantities can be replaced with probabilities and thus one may introduce R_5 as shown in equation 2.20, where $P(C)$ is the probability of system collapse, and $P(D)$ is the probability of failure of a structural component [Fu and Frangopol, 1990].

$$R_5 = \frac{P(D) - P(C)}{P(C)} \tag{2.20}$$

One also may use the concept of the reliability index to describe redundancy factors for the system. Some of these probabilistic redundancy factors found in literature are listed in the following [Frangopol et al., 1992].

- Redundancy factors with respect to failure of the weakest member

$$R_6 = \frac{\beta_C}{\beta_{WM}} \tag{2.21a}$$

$$R_7 = \beta_C - \beta_{WM} \tag{2.21b}$$

$$R_8 = \frac{\beta_C - \beta_{WM}}{\beta_C} \tag{2.21c}$$

  where β_{WM} is the reliability index of the weakest member, and β_C is the reliability index of the intact system with respect to collapse.

- Redundancy factors with respect to any first member failure

$$R_9 = \frac{\beta_C}{\beta_{AM}} \tag{2.22a}$$

$$R_{10} = \beta_C - \beta_{AM} \tag{2.22b}$$

$$R_{11} = \frac{\beta_C - \beta_{AM}}{\beta_C} \tag{2.22c}$$

  where β_{AM} is the reliability index of the intact system with respect to any first member failure.

2.3 Using Redundancy Factors in Design

Identifying which one of the factors or methods described in this chapter that should be used in order to define the redundancy for a system, is not a self-explaining task. This is reflected in the fact that there are several approaches fluctuating in literature. One example may be presented. Take for instance the truss system shown in figure 2.4a (each member has a cross section area equal to A/n where A is a constant and n is the number of members). One may compare the calculated redundancy factors R_{10} and R_{11} for this system, and identify the most convenient

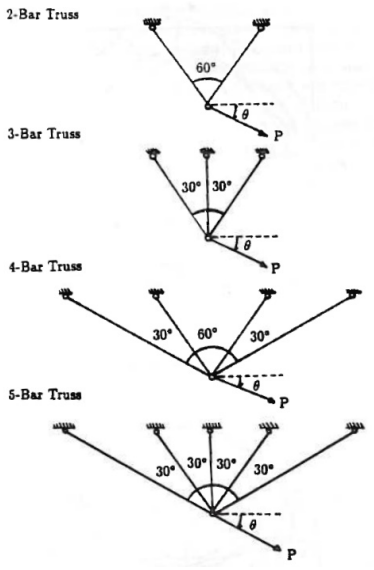

(a) Four truss systems

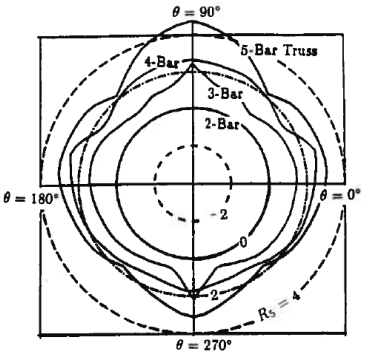

(b) R_{10} for the truss system in figure 2.4a

Figure 2.4: A truss system example

of them [Frangopol et al., 1992]. The conclusion found by Frangopol et al. was that R_{10} is the better measurement since it distinguished between the different trusses for all load directions. This can be seen in figure 2.4b[1]. However, this may not be the case for all types of structures.

It is important to identify how safe a structure is, in order to ensure that the risk of fatalities are according to the ALARP-principle, and also make sure no environmental and/or financial damage may occur due to collapse or failure of structures. This is why one needs redundancy measures so a structure can be classified as "safe". As indicated earlier there are very much to be said and investigated around redundancy, and since this is not the main topic of this thesis the reader is encouraged to study the references for more information.

[1]Note: In the figure it says R_5 instead of R_{10} due to different notations on the figure and in this thesis

3

Fatigue

One important mechanism to consider when designing metal structures is fatigue. A material, say steel, subjected to a cyclic loading will be exposed to a cumulative damage process which will lead to crack growth and eventually failure of the material, and thus the load-bearing capacity. For offshore structures, especially in the North-Sea, fatigue loading is often a governing design aspect to consider due to an almost continuous exposure to cyclic loadings from waves. The following text is mainly based on [Berge, 2006].

3.1 Basic Fatigue Formulation

Fatigue damage is classified into two categories: *low cycle fatigue* and *high cycle fatigue*. The difference being a fatigue life below 10^5 cycles or above 10^5 cycles, respectively. Low cycle fatigue mainly occurs when the material is subjected to yielding, and most marine structures will not be in this range.

3.1.1 Crack

The fatigue crack process may be separated into three different stages: Initiation, crack growth and final failure. This is shown in figure 3.1, where the three stages are referred to as *Region A*, *Region B* and *Region C*, respectively. ΔK is the cyclic stress intensity factor, and is defined as

$$\Delta K = \Delta S \sqrt{\pi a} F \tag{3.1}$$

where ΔS is the nominal stress range, a the crack length and F is a form factor which is often a function of external loading, geometry, crack length, crack geometry and configuration of loading.

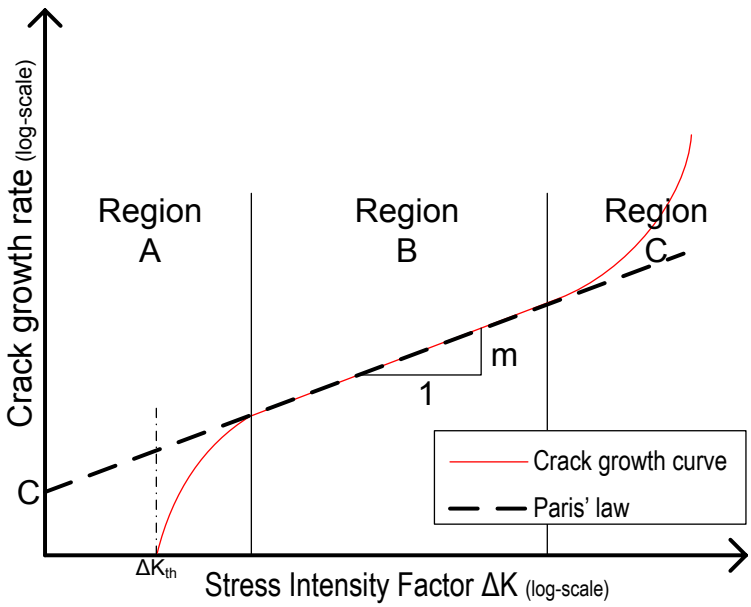

Figure 3.1: Paris law for a material, say steel

From figure 3.1, one notice that for a given ΔK_{th}, there is no crack growth. This limit, known as the threshold limit, is a material property where if the loading is below this level the material will have "infinite" fatigue life. This threshold will not be present for steel when subjected to corrosive environments.

3.1.2 SN Curves

SN-curves are very often used during design to determine the number of cycles a specific material will have. In design codes, there have been established a set of SN-curves that depends on both the environment, e.g. corrosive, air or cathodic protected, and the geometry of the joint. These curves are based on empirical testing and curve fitting. From figure 3.1 one see that in region B, there is a linear relationship between the ΔK and da/dN when plotted in a log-log diagram. This is described with Paris' law given in equation (3.2). Linear relationship is assumed to be a good fit as most of the cycles are found in region B. Also, if the threshold limit is ignored, Paris' law is assumed to be conservative.

$$\frac{da}{dN} = C\Delta K^m \Rightarrow \log\left(\frac{da}{dN}\right) = \log\left(\Delta K\right) \cdot m + \log\left(C\right) \Leftrightarrow y = ax + b \qquad (3.2)$$

The straight line obtained from Paris law can be translated directly into a SN-curve, where the stress range for the cyclic loading is on the y-axis and number

of cycles until failure is on the x-axis. The relationship is given by equation (3.3). From this, one notice that the slope m in Paris' law is the inverse slope for the SN curve. Typical SN curves are shown in figure 3.2. SN curves usually include the effect from welds on the stresses, and thus one shall not account for the so called *notch stress* (see fig. 3.6) to find the appropriate curve based on the structural details as defined in e.g. [DNV, 2010].

$$\log \Delta S = -\frac{1}{m} \log N_g - \frac{1}{m} \log A' + \frac{1}{m} \log I \tag{3.3a}$$

$$N_g = \sum_i n_i \tag{3.3b}$$

$$A' = C\pi^{m/2} \tag{3.3c}$$

$$I = \int_{a_i}^{a_f} \frac{da}{(\sqrt{a}F)^m} \tag{3.3d}$$

Equation (3.3) may be rewritten into a more simpler form, from which the SN curve from empirical testing can be defined as

$$N\left(\Delta S\right)^m = \text{Const} \Rightarrow \log N = \log \bar{a} - m \cdot \left(\Delta S \left(\frac{t}{t_{ref}} \right)^k \right) \tag{3.4}$$

where a thickness correction has been introduced: t_{ref} is the reference thickness, t is the thickness through which crack growth most likely will occur and k is a thickness exponent given in standards. This correction is due to the local geometry of the weld toe relative to the thickness of the adjacent plates, and its impact on the local stress distribution through the thickness.

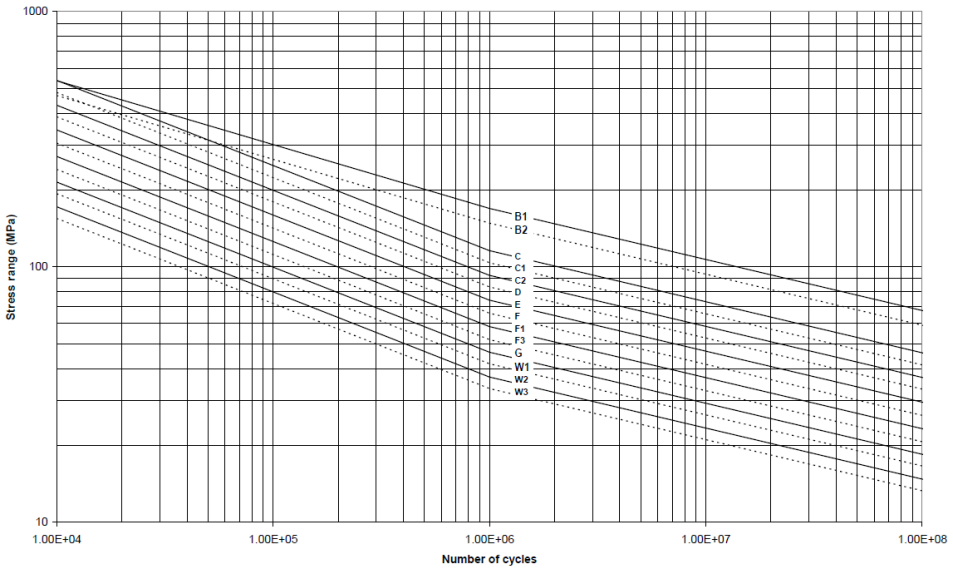

Figure 3.2: SN curves in seawater with cathodic protection [DNV, 2010]

3.1.3 Miner Sum

When using SN curves in design, it may be obvious that for marine structures subjected to fluctuating wind and wave loads, the stress range amplitude will not be a constant. Therefore, some way of calculating the cumulative damage from a given stress time series or stress range histogram must be applied. In literature, several proposals are found, but a simple method is to use the Miner summation. This method has proven itself to be no worse than any other method, and due to its simplicity virtually all fatigue design of steel structures is based on this method [Berge, 2006]. Miner summation assumes that each load cycle produces a "damage" on the structure given as

$$D = \frac{1}{N} \tag{3.5}$$

where N is the number of cycles before failure for the given load cycle. Thus, one find that failure will occur when $D = 1$. For a non-constant stress range amplitude loading, the Miner damage turns into a summation

$$D = \sum_i \frac{n_i}{N_i} \tag{3.6}$$

where n_i is the number of cycles for a given stress range i, and N_i is the number of cycles before failure for the stress range i which can be found from e.g. SN-curves.

3.1.4 Counting Algorithms

In order to determine the Miner damage when the loading is not of a constant amplitude and period, some sort of counting algorithm must be applied to extract cycles from a stress time series. The problem associated with cycle counting is shown in figure 3.3, where a narrow banded process and a broad banded process is shown. For the narrow banded process, a stress cycle is easily found as there exists only one peak for every zero-crossing. Most counting algorithms when applied to this process will yield similar results. On the other hand, for a broad banded process each large cycle is interrupted by several smaller cycles, and the cycle count is largely dependent on the algorithm applied.

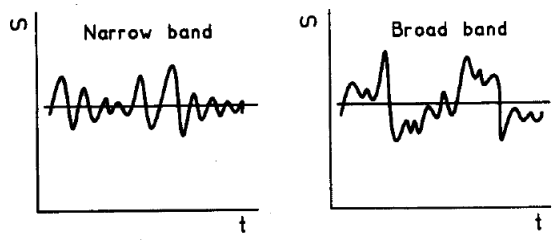

Figure 3.3: Definition of narrow-banded and broad-banded processes

Rainflow

The rainflow counting algorithm is thought to be superior to other methods, both in low cycle fatigue and in high cycle fatigue, and is the most popular as of 2008 [Næss, 1985], [Wikipedia, 2011]. Strictly speaking, rainflow counting is used as a common name for a large class of methods (e.g. Hayes method, hysteresis loop counting), but the final count is similar for all methods and in some special cases they yield identical results. If one examine the method that is actually known as the rainflow counting, one find a procedure designed to count cycles that is reflecting how the material is responding in regards of a stress-strain relationship. The rainflow counting method is recommended for use when the loading is broad banded [Næss, 1985].

Stress Concentration Factor

A very important mechanism in fatigue calculations is local stress concentrations which are described by the *Stress Concentration Factor*. SCF is the ratio between the nominal stress and the local stress amplitude. When looking at the stress close to changes in geometry, e.g. cut outs and welds, one will find that the local stress is in most cases larger than the nominal stress, occasionally as much as 3 times and even higher ratios are not unusual. It is obvious then that using SCF is necessary in order to find the correct stress range to be used in fatigue analysis. For instance, if the nominal stress vary between say 10 [Mpa] and 20 [MPa] corresponding to a

stress range of 10 [MPa], a SCF of 3 would lead to the local stress vary between 30 [MPa] and 60 [Mpa], i.e. a stress range of 3x10 [MPa]=30 [MPa]. Inspecting equation (3.4), one notice that the fatigue life is the inverse ratio to the stress range in the m'th power. For welded steel structures, m may be taken as - say - 3, and it then follows that a small change in stress range will lead to a large change in fatigue life. For instance will an increase in stresses with a factor 2 lead to a decrease in fatigue life with a factor of $2^3 = 8$. It is then obvious that variation in both the nominal stress and the SCF will have large influence on the fatigue life.

3.1.5 Tubular Joints

Tubular joints are commonly found in offshore structures. Tubular members are the preferred structural component for jacket structures, but is also found used as the bracing for semi-submersibles, jack-up legs and flare booms. The low drag coefficient of tubes, good strength properties and small outer area to be surface treated is essentially the three reasons why they are so frequently used. Geometry and definitions for a tubular joint is shown in figure 3.4.

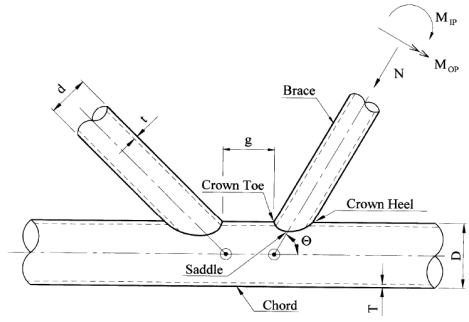

Figure 3.4: Tubular joint and its definitions

Even though tubular members have large advantages for marine structures, there is a large drawback regarding the joints. A tubular member has a very large axial stiffness, but is indulgent towards ovalisation forces. In a tubular joint, the different members will be placed in different directions, giving rise to large difference in relative stiffness going from one member to another. Thus, when the joint is loaded, local stresses known as *hot spot stresses* rise up due to constraints from the incompatible stiffness relationship, and large SCFs are expected. In figure 3.5, one see an example on how the stresses vary around the joint, and one should notice the very high maximum SCF of around 7 at the saddle point.

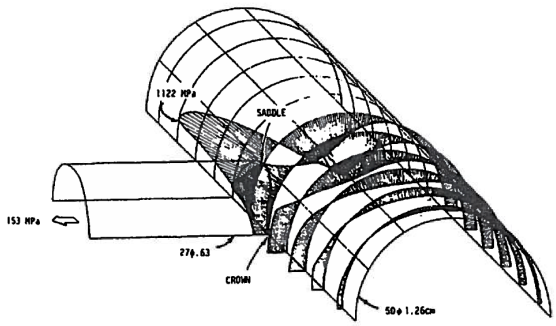

Figure 3.5: Circumferential stress in a tubular joint under axial loading

The SCF for a particular tubular joint may be found in several different ways, e.g. FEA, parametric equations in standards or with strain measurement using steel or acrylic models. An important aspect of tubular joints is that the fatigue life is largely determined by the growth of a crack where the peak stress from weld geometry is of minor significance. Therefore one needs to neglect the *notch stress* when finding the hot spot stress as shown in figure 3.6. Usually, a linear extrapolation is sufficient enough to get good result, but can in some cases be difficult to apply, i.e. the geometric stress is not as linear as one would like i to be.

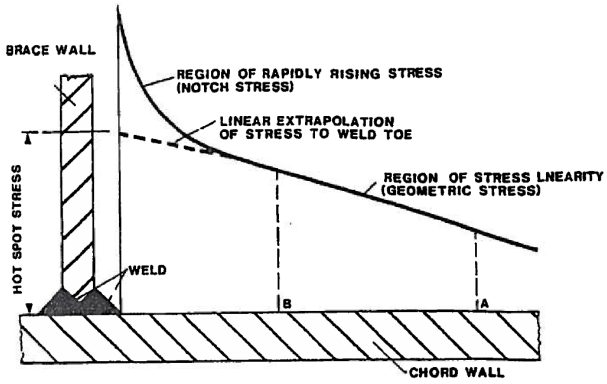

Figure 3.6: Stress distribution along the chord towards the brace wall for a tubular joint

A tubular joint will be subjected to axial loading and in- and out of-plane bending moments, and thus there are several different positions around the joint connection where the largest hot spot stress will occur. If one also take into account that the stress concentration factor is varying for the three types of loadings, then one clearly sees why there is at least eight positions that is checked when analysing a tubular joint. This variation is illustrated figure 3.7. The largest hot spot stresses are

practically always found in the joint itself and not in the members. However, the SCF is usually not identical for the chord and brace side of the weld, as illustrated in figure 3.8. Thus, when performing a stress analysis of a tubular joint, on needs to find the hot spot stresses on both sides of the weld. The nominal stress is in both cases taken as the result from axial forces and in- and out of-plane bending moments in the brace only.

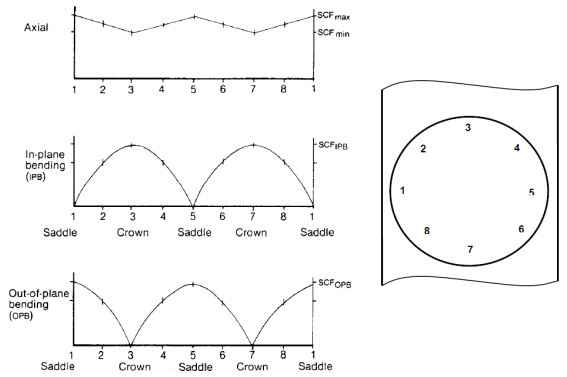

Figure 3.7: SCF variation for a tubular joint

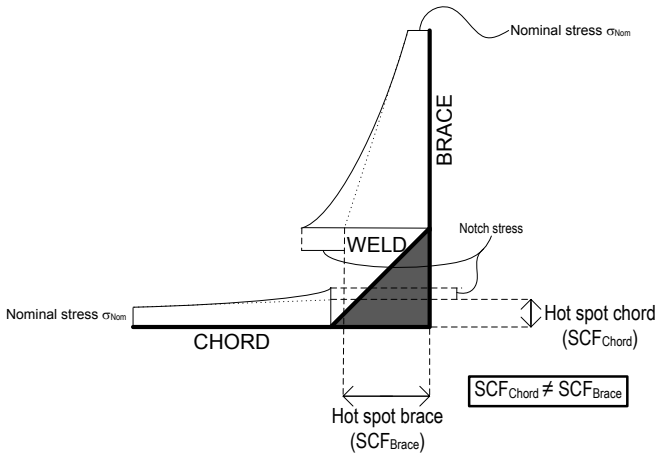

Figure 3.8: Illustration of stress distribution on chord side and brace side of a weld for a tubular joint

3.2 Calculating Fatigue Life

The ocean surface elevation may be modelled by a sum of sinusoidal wave components, where component i has amplitude $\zeta_{A,i}$, frequency ω_i and phase ϵ_i. The

connection between the amplitude and wave frequency is given by a wave spectrum and is expressed as $\zeta_A = \sqrt{2S(\omega)\Delta\omega}$. The phase angle is a uniformly distributed random variable in the range $[0, 2\pi]$ and is stationary. It is assumed that the waves follows a narrow banded process, meaning that only one maxima occurs between every positive zero up crossing (see figure 3.3). Reference is made to [Faltinsen, 1990] for more details regarding the sea environment modelling. Since the forces in a structure is highly dependent on the wave loads, there will naturally be a relationship between the wave process and the stress ranges in the structure.

According to NORSOK N-003, one may perform fatigue analysis without current and wave kinematics factor can be taken to be 1.0.

3.2.1 Spectral Analysis

A spectral fatigue analysis, also known as probabilistic or stochastic fatigue analysis, is a procedure based on combining short term sea states with a frequency domain dynamic analysis to extract partial fatigue damages, and long term sea state probabilities to find the cumulative fatigue damage during the structures lifetime. The method assumes a linear mechanical, linear response system. If this is for filled, then the response component Y from an harmonic excitation force X may be expressed in terms of the transfer function H as shown in (3.7):

$$Y(t) = H_{XY}(\omega)X(t) \tag{3.7}$$

If the excitation spectrum S_{XX} is known, a response spectrum can be found by:

$$S_{YY} = |H_{XY}(\omega)|^2 S_{XX} \tag{3.8}$$

If one have a mass-spring system like $m\ddot{y} + c\dot{y} + ky = xe^{i\omega t}$, the transfer function will be given as

$$H(\omega) = \frac{1}{k - m\omega^2 + i\omega c} \tag{3.9}$$

These connections can be related to, say, wave loading X and corresponding stress Y. Hence, if the wave spectrum is known, the response spectrum may be found by calculating the transfer function.

To include wave spreading in the response, each transfer function for each elementary wave direction θ_i is added up with a spreading weight α_i to generate the transfer function for the main wave direction $\bar{\theta}$.

$$|H_0(\omega,\bar{\theta})|^2 = \sum_{i=1}^{n} \alpha_i |H_0(\omega,\theta_i)|^2 \tag{3.10a}$$

$$\text{where} \qquad \sum_{i=1}^{n} w_i = 1.000 \tag{3.10b}$$

The n'th moment of a spectrum is found by solving the integral

$$m_n = \int_{-\infty}^{\infty} \omega^n S(\omega) d\omega \tag{3.11}$$

By assuming that one have a narrow banded process, the mean zero up crossing period may be approximated as

$$T_z = 2\pi\sqrt{\frac{m_0}{m_2}} \tag{3.12}$$

By applying this formula on the response spectrum, the total number of stress cycles during a time period T can be expressed by

$$n = \frac{T}{T_z} \tag{3.13}$$

Thus, a set of equations to describe the number of stress cycles for a sea state has been found, requiring only that the transfer function between excitation (waves) and response (stress range) is known. However, one still need to find the stress levels for each cycle. The derivation of the damage from a sea state is a rather complicated case. However, by assuming that the stress range within each short term sea state is Rayleigh distributed and narrow banded, the process is simplified somewhat, and the partial Miner damage for a sea state i with wave direction j during a time period T is found by [Pinna, 2009]:

$$d_{ij} = T\frac{1}{2\pi}\left(\frac{m_{2,ij}}{m_{0,ij}}\right)^{1/2} \frac{\left(2\sqrt{2m_{0,ij}}\right)^m}{\bar{a}} \Gamma\left(\frac{2+m}{2}\right) \tag{3.14}$$

where $\Gamma(\ldots)$ is the Gamma function, $m_{n,ij}$ is the n'th moment of the response spectrum for sea state i and direction j, and $\bar{a}$ and m are SN curve properties.

Then, to find the total accumulated damage, each partial damage is added with a probability for each sea state:

$$D = \sum_{i=1}^{n}\sum_{j=1}^{n} p_{s,i} p_{d,j} d_{ij} \tag{3.15}$$

where $p_{s,i}$ is the probability of occurrence of sea state i and $p_{d,i}$ is the probability of occurrence of sea state i

Should the SN-curve consist of, say, 3 linear segments, the partial damage for each sea state is expressed as [Veritas, 1993]

$$d_{ij} = \frac{1}{2\pi}\left(\frac{m_2}{m_0}\right)^{1/2} T\left[(2\sqrt{2m_0})^{m1}\frac{1}{K_1}\Gamma\left\{1+\frac{m_1}{2};\left(\frac{S_1}{2\sqrt{2m_0}}\right)^2\right\}\right.$$
$$+(2\sqrt{2m_0})^{m2}\frac{1}{K_2}\left(\Gamma\left\{1+\frac{m_2}{2};\left(\frac{S_1}{2\sqrt{2m_0}}\right)^2\right\}-\Gamma\left\{1+\frac{m_2}{2};\left(\frac{S_2}{2\sqrt{2m_0}}\right)^2\right\}\right)$$
$$\left.+(2\sqrt{(2)m_0})^{m3}\frac{1}{K_3}\Gamma\left\{1+\frac{m_3}{2};\left(\frac{S_2}{2\sqrt{2m_0}}\right)^2\right\}\right] \quad (3.16)$$

where $\Gamma\{m;s\}$ is $\Gamma(m)-\Gamma_{Incomplete}(m,s)$.

The connection between cycles and stress ranges for the three piece SN-curve is

$$N=\begin{cases}K_1S^{-m1} & \text{if } S>S_1\\ K_2S^{-m2} & \text{if } S_2<S\leq S_1\\ K_3S^{-m3} & \text{if } 0<S\leq S_2\end{cases} \quad (3.17)$$

A spectral fatigue analysis has the advantage of fully taking dynamics into account through the use of the transfer function. On the other hand, it assumes that the response is linear. For jacket structures in moderate to deep water, this may be a reasonable approximation. But for jackets in shallow waters, non-linearities play an important role when it comes to the response, and thus a spectral fatigue analysis is no longer appropriate. However, there has been made some effort to develop a modified approach to be used for shallow water structures [Bishop et al., 1996]. This method is mainly based on developing the transfer function by subjecting the structure to regular waves. The wave height associated to each frequency is found by selecting an appropriate exceedance value for the wave height distribution.

If the hydrodynamic loadings on slender members are calculated using the non-linear Morrison's equation (B.2), a linearisation of this force must be applied in order to calculate the transfer function for a stochastic fatigue analysis. Two methods that can be used in this respect are *linearisation with respect to wave height* and *equivalent linearisation with respect to wave spectrum*. The former method involves selecting a linearisation wave height H_ω for each wave frequency ω. Then, the drag force is linearised with respect to the largest occurring fluid velocity during one wave cycle, and the drag force is expressed as

$$\mathbf{F}_d(\mathbf{r},t)=\frac{1}{2}\rho DC_d\mathbf{v}(\mathbf{r},t)|\mathbf{v}_{max}(\mathbf{r})| \quad (3.18)$$

where $\mathbf{r}$ is coordinate of calculation, $\mathbf{v}$ is the undisturbed water particle velocity, and $\mathbf{v}_{max}$ is the largest occurring fluid velocity for H_ω.

The latter linearisation method is based on the fact that the ocean waves are Gaussian processes. The drag force for a given sea state

$$\mathbf{F}_d(t) = \frac{1}{2}\rho D C_D \mathbf{v}_n(t)|\mathbf{v}_n| \tag{3.19}$$

can be replaced by the linear equivalent drag force

$$\mathbf{F}_d^* = \alpha(\mathbf{u}_n - \mathbf{U}) + E\left[\mathbf{F}_d\right] \tag{3.20}$$

where

$$\alpha = \frac{E\left[\mathbf{F}_d(\mathbf{u}_n - \mathbf{U})\right]}{Cov(u_{n_i}, u_{n_i})} \tag{3.21}$$

where $E[x]$ is the expected value of x, $\mathbf{u}_n$ is the total fluid velocity normal to the member and $\mathbf{U} = E[\mathbf{u}_n]$.

3.2.2 Deterministic Analysis

Deterministic fatigue analysis is based on a wave height exceedance diagram describing the relevant site, from which a long term distribution of hot spot stress range can be developed. The procedure is shown graphically in figure 3.9.

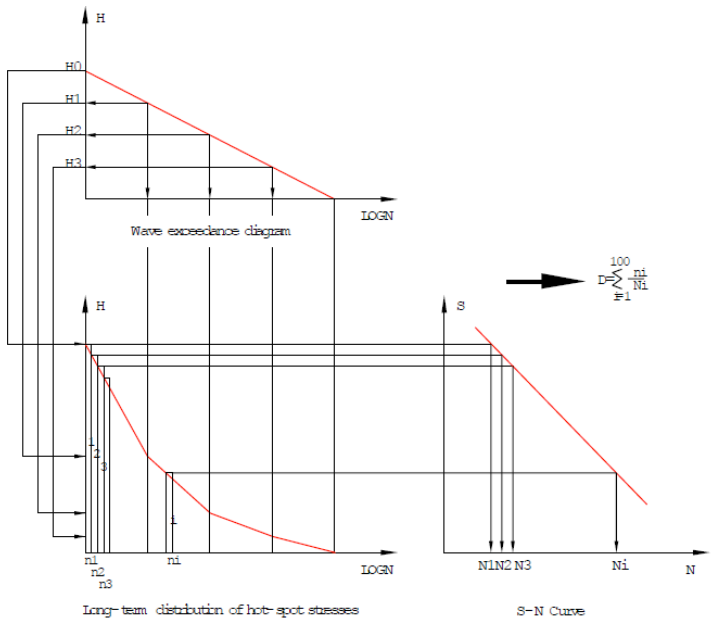

Figure 3.9: Deterministic fatigue analysis procedure [NORSOK-N004, 2004]

According to NORSOK N-004, the analysis should be performed by stepping at least 4 wave heights through the structure from 8 directions, and calculating the stresses for at least ten positions in each wave. If important, dynamics can be included with a Dynamic Amplification Factor (DAF).

3.2.3 Closed Form Analysis

Closely related to the deterministic analysis is the closed form fatigue calculation. Both methods relate the damage to a stress range exceedance diagram, thus the similarity. However, the two methods differs in how the stress range exceedance diagram is found. The closed form method can be very useful in early design phase or when one have a real life measurement of the stress range. The method is derived by assuming stress cycles to be a randomly distributed variable with a probability density function $f(\Delta\sigma)$. The number of cycles within a stress range $(\Delta\sigma + d\Delta\sigma)$ can then be expressed as $n_0 \cdot f(\Delta\sigma) \cdot d\Delta\sigma$ where n_0 is the total number of stress cycles the structure is assumed to be exposed to. From this the Miner Damage will be

$$D = \int_0^\infty \frac{n_0 \cdot f(\Delta\sigma)}{N(\Delta\sigma)} d\Delta\sigma \tag{3.22}$$

where $N(\Delta\sigma)$ is the number of stress cycles before failure for the stress range $\Delta\sigma$.

For offshore structures, the PDF of stress ranges follows a two-parameter Weibull-distribution

$$f(\Delta\sigma) = \frac{h}{q}\left(\frac{\Delta\sigma}{q}\right)^{h-1} exp\left(-\frac{\Delta\sigma}{q}\right)^{h} \tag{3.23}$$

Combining the SN-curve formulation in eq. (3.4) with (3.23) will yield the result in (3.24) [Næss, 1985].

$$D = \frac{n_0}{\bar{a}} q^m \Gamma\left(1 + \frac{m}{h}\right) \tag{3.24}$$

If q is expressed in terms of n_0 and $\Delta\sigma_0$ (the maximum stress range) then (3.24) can be expressed as

$$D = \frac{n_0}{\bar{a}} \frac{\Delta\sigma_0^m}{(\ln n_0)^{m/h}} \Gamma\left(1 + \frac{m}{h}\right) \tag{3.25}$$

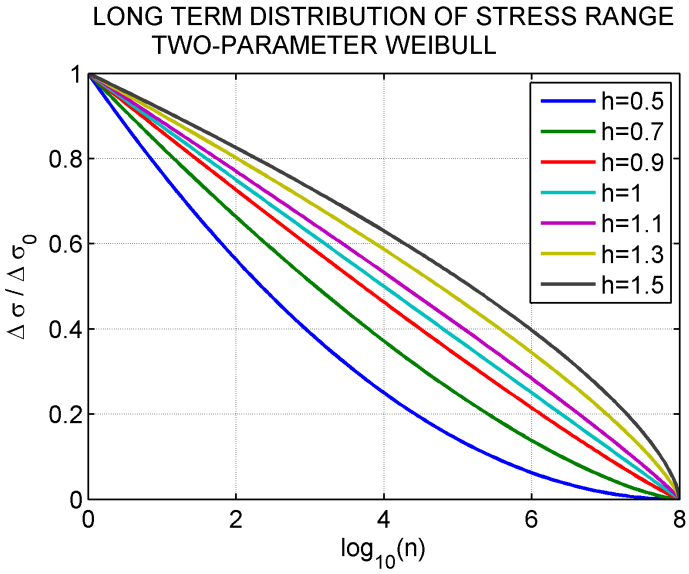

Figure 3.10: Long term distribution of stress ranges

The closed form solutions, i.e. the Weibull PDF for stress ranges, for some values of h can be seen in figure 3.10. However, choosing a suitable value for h is not a straight forward answer if one does not have data to fit a distribution to. A simple method would be to base it on experience from fatigue analyses of similar

structures, or utilize empirical figures or formulas. If no suitable data could be found, then the deterministic approach could be applied. Thus one notice that the difference between the closed form solution and the deterministic approach lies in how the stress range exceedance diagram is created (Weibull PDF vs. point wise interpolation) and how the damage is found (analytical vs. numerical integration).

3.2.4 Time Domain Analysis

Another way to calculate fatigue life, is to utilize time domain simulation. By applying a proper irregular sea state which applies to the relevant site, and using a non-linear FE program, then both dynamic effects and non-linearities associated with wave theory and free-surface effects can be accounted for. Especially non-linearities associated with the drag forces is properly accounted for, which can be very important for structures which have large response. Thus, no approximations is done as for the spectral fatigue case, where one assumes linear response; or as for the deterministic case where all structural response is neglected when calculating drag, i.e. relative velocity in the drag force equation is not accounted for (r in eq. 3.26 is 0). Off course, the latter is not an approximation associated with large errors, as the deterministic method is intended for shallow to moderate water depths where jacket structures have very small responses.

The large downside with a time domain analysis is that it can be very time consuming (CPU-time) to perform when all non-linearities are taken into account, since this will typically involve updating the stiffness and possible the damping matrix at each time step. It could also create vast amounts of data if one should create time series for several members for several load cases.

$$F_D = \frac{1}{2}\rho C_D A \left(u(t) - \dot{r}\right) \left|u(t) - \dot{r}\right| \tag{3.26}$$

3.2.5 Fracture Mechanics Analysis

A fracture mechanics approach differs from the other methods in the previous sections by the fact that it does not use SN-curves directly to find the number of cycles for a given stress range, but it is however closely related as shown in (3.3). The fracture mechanics approach is basically a calculation of crack growth, and thus finding the number of cycles before failure occurs. Two key variables needs to be determined before applying the fracture mechanics approach, namely the initial crack depth a_i and the crack depth at failure a_f. Also, the two fitting parameters m and C needs to be determined and then it is just a matter of solving the integral:

$$N_g = \frac{1}{C\pi^{m/2}\left(\Delta S\right)^m} \int_{a_i}^{a_f} \frac{da}{\left(\sqrt{a}F\right)^m} \tag{3.27}$$

Thus, this method is very useful if a relative large crack is found and one wish to determine if the crack should be repaired, or if it will not grow to the point of fracture within the life time or within the planned repair interval for the structure. On the other hand, fracture mechanics could be applied on critical components to calculate the maximum allowable crack size to avoid fracture during the lifetime, and thus finding a requirement for the accuracy of the measuring equipment or material quality.

However, the fracture mechanics analysis applied on welded joints is not an appropriate method [Berge, 2006]. This is mainly because of the following three reasons.

1. The size and shape of initial defects must be quantified in order to determine the form factor F. This is not easily done for welds
2. Most of the crack growths are in the threshold region, thus involve large uncertainty. An assumption of Paris law behaviour is very conservative.
3. Small cracks ($a < 0.1[mm]$) are outside the validity range for linear-elastic fracture mechanics.

Despite not being appropriate, fracture mechanics may be used as a conservative estimate for sound welds. Another useful application would be for inspection interval planning. In figure 3.11 a typical crack growth is illustrated. If one now assume a_1 to be a reliable detectable crack size, then the residual life $N_R = N - N_1$ can be calculated using fracture mechanics, and thus form an appropriate inspection interval.

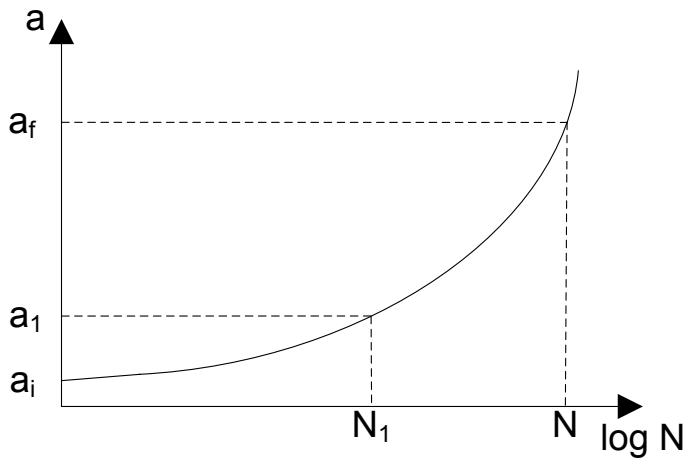

Figure 3.11: Illustration of crack growth

3.3 Uncertainty in Fatigue Calculations

Fatigue life calculations involve large uncertainty due to the large number of variables involved and their inherent uncertainty [Næss, 1985]. For instance, there is variation in parameters like:

- Wave Loads
  - wave height
  - wave period
  - wave theory
  - hydrodynamic coefficients
  - marine growth
- Stress Calculation
  - FEA
  - SCF
  - boundary condition, e.g. soil
- SN-data
  - scatter in testing
  - corrosion
  - selection of SN-curve
  - thickness effect
- Fabrication Tolerances
- Joints (tubular)
  - classification of joint type
  - parametric SCF equations

From testing under variable amplitude loading, there is a considerable variation for the calculated Miner damage at failure [Pinna, 2009]. A typical experimental fatigue test result is shown in figure 3.12.

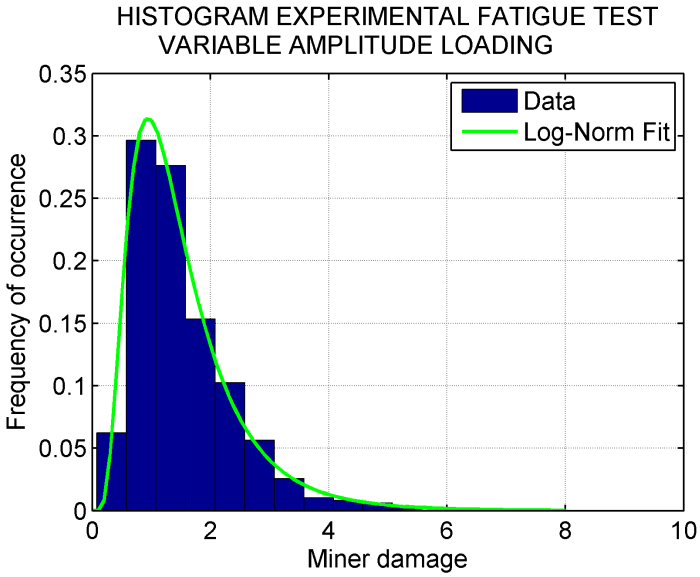

Figure 3.12: Comparison of calculated Miner Damage and failure under variable amplitude testing, [Pinna, 2009]

There is a rather large spread in the testing data which forms the SN-curves. Therefore, design SN-curves is usually two standard deviations below the mean SN-curve. Now assume a standard normal distribution is valid for describing the spread for the SN test data in a log-log diagram. The probability that the fatigue life is larger than that calculated using the design SN-curve is then 97.7 [%] ($P(N > N_D) = 1 - \Phi(\mu - 2\sigma)$). Since it was assumed a normal distribution for the spread, the reliability index for the design SN-curves is $\beta = 2$. However, it must be emphasized that the SN-curves are derived from laboratory experiments, and fabrication tolerances in real life is likely to be larger, thus increasing the uncertainties. Also there are very few experimental SN-data for stress cycles larger than 10^7 due to the time duration of such experiments.

If one take the spread of data in the SN-curves a bit further, one may calculate the probability of failure as a function of accumulated damage. By neglecting the thickness correction, the design SN-curve can be expressed as

$$\log N = \log \bar{a} - m \log(\Delta\sigma) - \beta \log(s) \tag{3.28}$$

where $\log(s)$ is the standard deviation for the SN-curve test data. Finding the number of cycles N_0 for a given stress range from the SN-curve with $\beta = 2$ is per definition the same as finding the number of cycles corresponding to an accumulated damage equal to unity. Thus one can define a reduced number of cycles N_α

corresponding to an accumulated damage of α, i.e. $N_\alpha = \alpha N_0$. Then one may solve for the reliability index:

$$\begin{aligned}\log N_\alpha &= \log(\alpha N_0) = \log\alpha + \log N_0 \\ &= \log\alpha + \log\bar{a} - m\log(\Delta\sigma) - 2\log(s) = \log\bar{a} - m\log(\Delta\sigma) - \beta\log(s) \\ &\Rightarrow \log\alpha - 2\log(s) = -\beta\log(s) \\ \Rightarrow \beta &= 2 - \frac{\log\alpha}{\log(s)}\end{aligned} \tag{3.29}$$

Then, one can calculate the probability of failure for several values of α and against the sensitivity for $\log(s)$ by inserting equation 3.29 into equation (2.13). The results are shown in figure 3.13 for three different standard deviations. Similar curves can be found in NORSOK N-006, where also the uncertainty in Miner Damage (the spread in fig. 3.12) and the uncertainty in stress calculations are taken into account. This will significantly increase the probability of failure for a given accumulated fatigue damage. For instance, take a failure probability of 0.01. For uncertainty in the SN-curve only, this will correspond to a calculated accumulated fatigue damage of about 0.84. On the other hand, for the largest amount of uncertainty given in N-006 this probability will correspond to a calculated accumulated fatigue damage of 0.34.

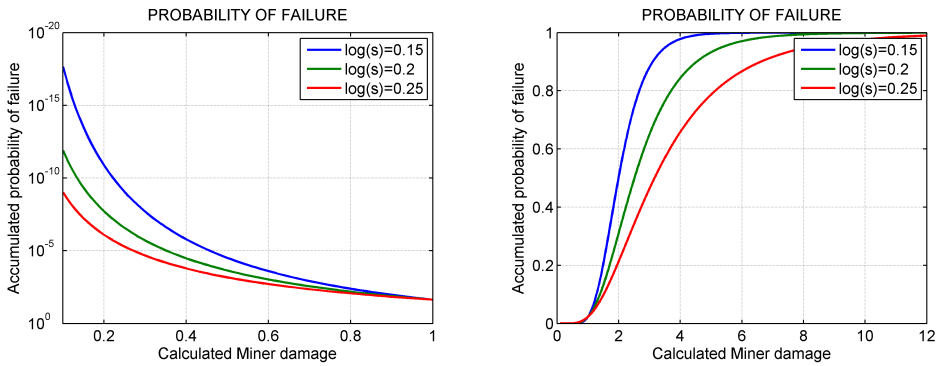

Figure 3.13: Calculated accumulated probability of failure as a function of calculated accumulated fatigue Damage

These failure probability curves can form a basis for the time interval until first inspection. The time until inspection can be calculated by first finding a probability of failure based on the consequence from failure of the joint, e.g. 10^{-3} for a high consequence joint and 10^{-1} for a low consequence joint. With a chosen probability,

the calculated accumulated fatigue damage d_{acc} for this probability is found from the curves. The time until first inspection is then found as

$$T_{insp} = d_{acc} T_{calculated} \tag{3.30}$$

where $T_{calculated}$ is the calculated fatigue life for the joint. It must be emphasized that this Risk Based Inspection (RBI) calculation is no better than the quality of the input data, i.e. the calculated fatigue life.

Probabilistic Example

Say that one have a structure with a Service Life (SL) of 50 [y] and only two failure modes:

1. Joint 1, which have a fatigue life of 100 [y] and Accumulated Damage At End Of SL of 0.5000
2. Joint 2, which have a fatigue life of 150 [y] and Accumulated Damage At End Of SL of 0.3333

Further, assume that if joint 2 is damaged, then joint 1 will only have a fatigue life of 25 [y], or ADAEOSL of 2. One can now calculate the probability of failure from fatigue damage using the curves in figure 3.13 if one assume uncertainty only in the SN-curve.

Now the probability of failure of joint X ($P(X)$) can be calculated by using the curve $y_{s=0.2}$ (log(s)=0.2).

$$\begin{aligned} P(J_1) &= y_{s=0.2}(0.50) = 2.2818\text{E-}4 \\ P(J_2) &= y_{s=0.2}(0.33) = 5.7832\text{E-}6 \\ P(J_2|J_1) &= y_{s=0.2}(2.00) = 0.3104 \end{aligned} \tag{3.31}$$

Finally, the probability of either joints failing can be found as

$$\begin{aligned} P(J_1 \cup J_2) &= P(J_1) + P(J_2) - P(J_1 \cap J_2) \\ &= P(J_1) + P(J_2) - P(J_1) \cdot P(J_2|J_1) \\ &= 2.2818\text{E-}4 + 5.7832\text{E-}6 - 2.2818\text{E-}4 \cdot 0.3104 \\ &= 2.2818\text{E-}4 + 5.7832\text{E-}6 - 7.0815\text{E-}5 \\ &= \underline{1.6314\text{E-}4} \end{aligned} \tag{3.32}$$

From this idealized and simple example, it is shown that there may be a significant increase in the probability of failure by taking into account the stress re-distribution should one member fail. In a jacket structure, there is much more complexity regarding both the number of joints and the dependence between joints, but the basic principle is shown in this example.

4

Analysis

In order to investigate what effect damaged structural members will have on the fatigue life, a case study has been performed on two jackets. The jackets are typical Norwegian continental shelf jackets, i.e. moderate water depth and in agreement with the NORSOK standards. One jacket is a 4-legged X-braced jacket (4L) and the other is a less redundant 3-legged jacket (3L). The analysis approach has been similar to an ALS check, i.e. a fatigue analysis has been performed upon removing structural members one at the time.

4.1 The Fatigue Analysis Procedure

4.1.1 Fatigue Life Calculation

To perform the fatigue calculations, a stochastic fatigue analysis was chosen so that changes in the dynamics due to the impaired integrity would be captured. The jackets analysed have a natural period above that which can be regarded as quasi-static, thus making them suitable for the spectral analysis. A time domain simulation could be appropriate regarding non-linearities, especially for members close to the free surface. But due to the sheer number of analysis needed this form of analysis would require extensive computational time, making it unattractive.

The stochastic analysis was performed using the SESAM package from DNV Software. The sub-models were created with PREFRAME and assembled with PRESEL. WAJAC was used to calculate the wave loads, and SESTRA was used to find the response. Then FRAMEWORK was used to calculate the fatigue life. The entire batch run was performed using a script as described in appendix D.

4.1.2 Fatigue Data

Stress concentration factor are calculated using Efthymiou parametric equations, where the joints are classified using the load path. FRAMEWORK has an extensive library of SN-curves, and the NORSOK T-curve with cathodic protection was used (the SN-curve coefficients are defined in DNV-RP-C203).

4.1.3 Applying Damage

All input files in order to perform a full analysis was provided through AKSO, thus introducing a damaged element was the only modification necessary. However, since a damaged member can effect the natural period of the structure, the wave periods used to create the transfer function should be fine tuned for each damage case. After all, the stochastic analysis results are no better than the accuracy of the transfer function. For simplicity though, it was assumed that the changes in

the eigenvalues could be neglected. An alternative approach would be to have a large number of periods with a small increment around the natural period of the intact structure, but this will however lead to increased computational time.

A simplified approach was applied regarding introducing damage to an element. The software used has the ability to remove one or several elements completely from the stiffness matrix, but still make it attract external loads which will be transferred to the nodes. This is achieved by the command known as *nonstru* (non-structural), and this would have been very suitable to simulate damage. However, when making a member non-structural with this command, the joint connection for this member will no longer exist in FRAMEWORK. Errors are then generated when trying to add cans and stubs etc. to the non-existing joint. Therefore, another approach was used. By reducing the Young's modulus (e-mod) for the damaged element by a factor of 1000, i.e. E=210 [MPa], the stiffness for this element should in practise be zero compared to the rest of the members, but it will still attract external wave loads due to its presence. In other words, this approach should give the same results as the *nonstru* command without the extra work associated with fixing the errors. However, a reduction in the e-mod could lead to an ill-conditioned stiffness matrix which can lead to numerical problems when inverting the matrix.

To ensure this simplified approach is as good as the *nonstru* command, a sensitivity study has been performed. Only one damage scenario was checked, and the conclusion was that the two methods are identical. This can be seen in figure 4.1a where the calculated fatigue life for the two methods are plotted against each other. There is a direct linear relationship (y=x) where any difference in the calculated fatigue life is negligible. Element 1080 is a part of the diagonal bracing in the lower part of the structure, and should therefore be applicable for this sensitivity study. In figure 4.1b a comparison between change in e-mod and complete removal of the damaged element is shown, and one see that some conservatism, i.e. lower fatigue life when changing the e-mod, is presence for a couple of elements. These data points that are deviating from the linear relationship are related to elements 980, 1480 and 1481 which are closely connected to element 1080. Since there are no visible difference in figure 4.1a, the conservatism must be due to load transfer to the nodes, which does not occur when the element is completely removed.

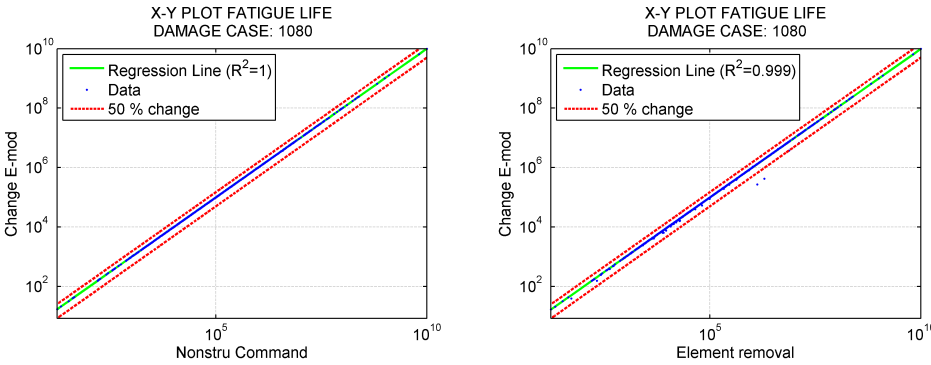

(a) non-stru command vs. e-mod **(b)** element removal vs. e-mod

Figure 4.1: Fatigue life calculation with damaged member, comparison between damage simulation procedures

4.1.4 Waves and Wave Loads

The sea surface elevation is modelled by a JONSWAP spectrum for both jackets, with a constant peak enhancement factor of $\gamma = 3.3$ (which is a mean value [DNV, 2011]). However, there has been performed one sensitivity study regarding the use of a PM spectrum instead. As most of the sea states which are relevant for fatigue analysis are fully developed, a PM spectrum is applicable [Næss, 1985]. This can be confirmed by plotting a histogram showing the ratio between the sea state peak period and the calculated T_P for a fully developed sea state (as defined in (A.1)). The results are shown in figure 4.2 and one see that although most of the sea states are in the vicinity of eq. (A.1), i.e. a ratio close to unity, there are some sea states that can be defined as growing wind seas. The same sea states are applied on both the 3L jacket and the 4L jacket. Reference is made to Appendix A for more details regarding the spectrum.

Drag- and mass-coefficients are according to NORSOK, see B.5b, with a small increase in the drag coefficient to account for the anodes on relevant members. The increase is 5 [%] and 7 [%] for the 4L and the 3L, respectively. Marine growth is also according to the NORSOK standard.

Linearisation of the drag force is done with respect to wave height, and the sea state used for linearisation for both jackets is a JONSWAP spectrum with $H_S = 3.75$ [m], $T_P = 6.5$ [s], spectrum width equal to 0.07 and 0.09 and a peak enhancement factor of 3.3, i.e. default values for the shape parameters.

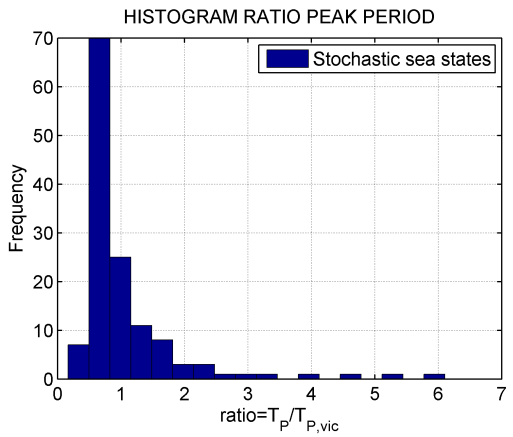

Figure 4.2: Distribution of fully developed sea states

4.2 The FE Models

4.2.1 The Four-legged 4L

The FE model of the NORSOK 4L jacket is shown in figure 4.3. It is seen that the structure is most likely to be highly redundant as it consists of X-bracing, thus have the potential to survive failure of any single member. The jacket stands in 75 [m] deep water, and the largest natural period is 2.77 seconds . The structure will be divided into different sets when referred to later in the thesis. Some of these set names are more or less self-explanatory, e.g. "Elevation +28.5" is the horizontal plane at 28.5 [m] above the sea surface, while the vertical sets are defined in figure 4.3. It should be emphasized that all horizontal bracing elements are a part of the horizontal sets, not the vertical sets. The topside weighs in at 22 500 [MT].

The 4L jacket consists of several hundred members and thus several hundred joints. Almost every member has been included in the damage simulations, and almost all joints are included in the fatigue check. More accurate, the fatigue checks performed consists of 422 damage cases, with 770 joint checks in each damage case. The latter figure is more precisely put 770/2 brace-chord connections as the chord side of the joint and the brace side are separated in the results. All braces, all caisson supports, all members in the riser ladder and some riser/conductor supports was chosen as damage cases. The legs has been excluded as damage scenarios, and due to the structural similarity not all riser supports was included. The pile clusters are also not included in the analysis.

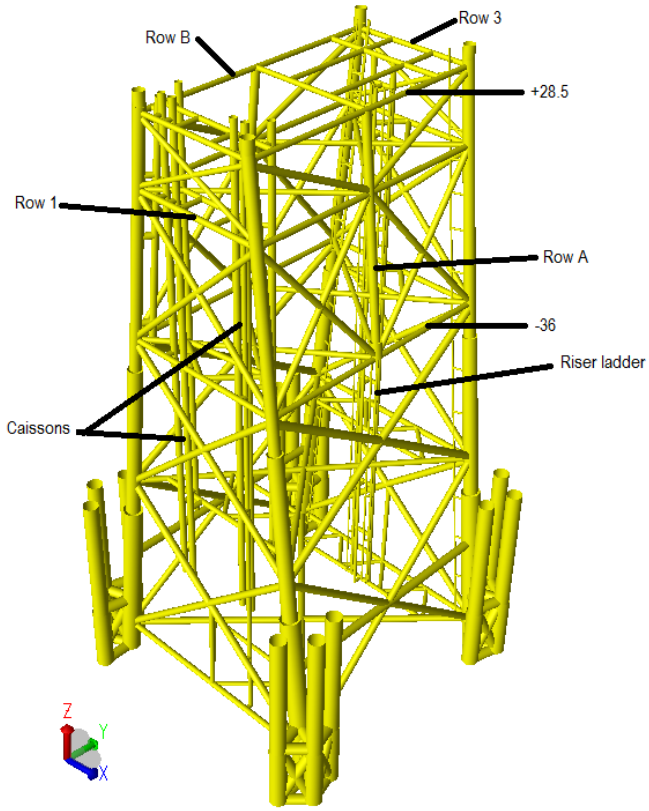

Figure 4.3: Finite element model of a NORSOK 4L jacket

4.2.2 The Three-legged 3L

In figure 4.4, the FE model of the NORSOK 3L jacket is shown. This structure was divided into sets in the same manner as the 4L-jacket, where the vertical naming terminology are also shown in figure 4.4. The biggest difference between the two jacket structures, aside from the number of legs, is the redundancy in the top frame of the 3L-jacket. One see that a lot of the bays are only single braced, and only the lower bay in the top frame is X-braced. Therefore, one would expect less redundancy than the 4L-jacket and thus one would expect larger changes in fatigue life as there are fewer members to redistribute the stresses to. The 3L-jacket with its largest natural period of 2.64 [s] should otherwise be almost equally dynamical behaving as the 4L jacket. The jacket stands in 69.4 [m] deep water, and the topside weighs in at 1733 [MT].

The 3L jacket is not as complex as the 4L regarding the number of members and joints, and has relative few damage cases and joint checks of 211 and 308,

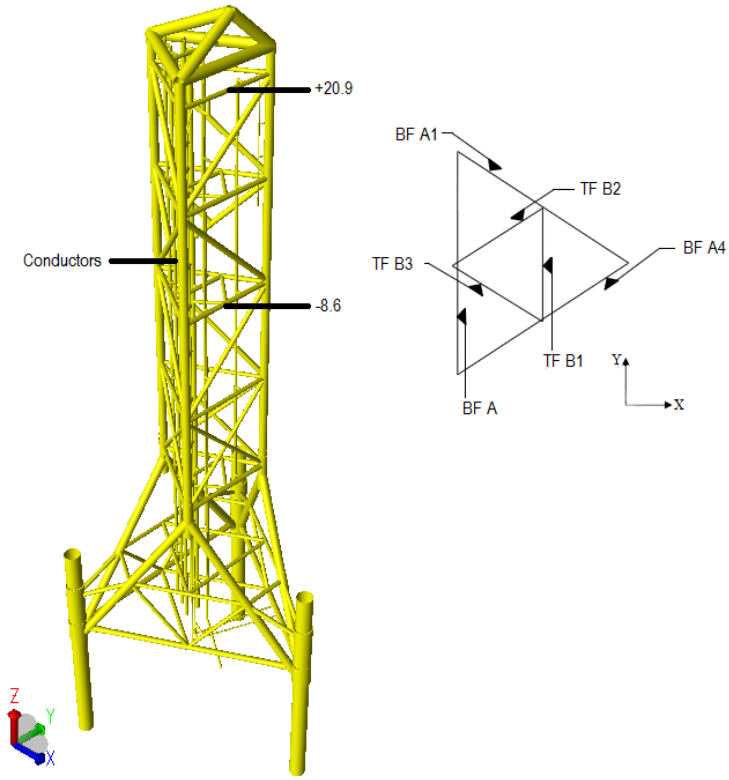

Figure 4.4: Finite element model of a NORSOK 3L jacket

respectively. The same damage implementation analogy was used for the 3L, e.g. no legs or pile clusters are included and most of the braces and supports are included.

4.3 Natural Periods

To calculate the changes in the natural period of the structure after introducing the damage, the FE-models were exported to USFOS. The damaged members were applied using the *non-stru* command. Lanczos solver were chosen to find the 10 lowest eigenfrequencies and their corresponding mode shapes.

4.4 Pushover

To investigate how the structure responds to the damage, and how redundant it is, a simple pushover analysis was performed. USFOS was used in this regard, and the same model used during the eigenvalue analysis was used, i.e. the soil was modelled

by a linear stiffness matrix, thus this analysis does not give the ultimate strength of the platforms, but should reflect the redundancy of the structures. A 28 [m] high Stoke's 5th order wave with a wave period of 12 [s] was chosen to form the basis of the structural load to use during pushover. This wave does not necessary reflect a true 100 year wave (ULS) for the jackets, but is at least a realistic wave event in general (extreme) terms. DAF has not been accounted for. This will give some errors if the natural period is vastly changed when damaged. Otherwise, it will be the same presumption, i.e. error, before and after damage, hence the final answer should not be associated with large errors.

5

Results

Since fatigue life is very sensitive against the stress range, a stochastic fatigue analysis should give some spread in the fatigue life before and after damage as some changes in dynamics are expected. However, the changes should occur locally in accordance with basic mechanical principles: The global load path should remain the same as the structure still is intact globally, i.e. only one brace out of many is no longer carrying loads. On the other hand, changes in stiffness could lead to changes in the load path as more stiff parts of a structure generally attracts more forces. If one also take the complexity of the truss work for a jacket into account, i.e. risers, conductors and caissons "disturb" the structure, the result of a damage scenario is not generally known beforehand without performing a fatigue analysis for the specific case.

5.1 Deterministic Fatigue

5.1.1 XY Plots

To give an overview of the changes in fatigue life that occurs, the following figures shows the fatigue life before damage plotted against the fatigue life after damage (XY-plot). To account for the extreme low fatigue life that occurs for the damaged joint due to the reduced Young's modulus, the fatigue life for these joints are "reset" back to the initial life, thus the joint data should not interfere too much with the XY-plots.

The first plots that are presented shows the fatigue life for all members in a set, and each figure contains data points from all damage cases i.e. each blue dot is a brace-chord connection and is either the brace side or the chord side (two dots in total per joint). In the plots, there are two red lines showing the 50 [%] change limits according to initial fatigue life, as well as a linear regression line for all data points. Due to the similarity in the plots, only some are represented here while all plots are shown in appendix F. In figure 5.1, the fatigue life for the 4L-jacket is shown for the two sets "Elevation -36" and "Row 3", while in figure 5.2 similar plots for the 3L-jacket for the sets "Elevation -39.6" and "Bracing TF B3" are shown.

Immediately, one may notice a very large change or spread in the fatigue life for several joints. There does not seem to be any joint which does not experience a change for any of the damage cases, and there are also large vertical trends for the same joint connection meaning that a single joint responds to several damage cases. When looking at the trend line, it seems to be more or less a straight line with a slope equal to unity. This is especially true for the 4L-jacket, but more vague for the 3L-jacket. This straight line means that there is either symmetry in the data points or several data points must be on the straight line itself meaning

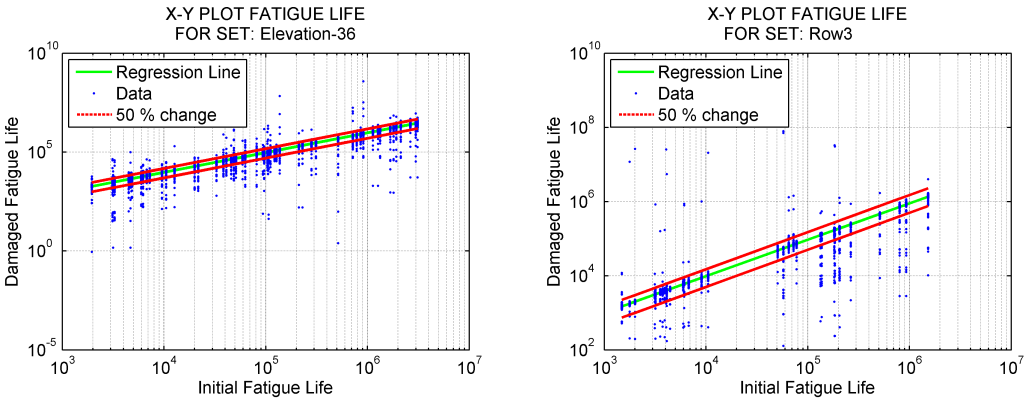

(a) For set "Elevation -36" **(b)** For set "Row 3"

Figure 5.1: Fatigue life changes in XY-plots for two sets, 4L-jacket

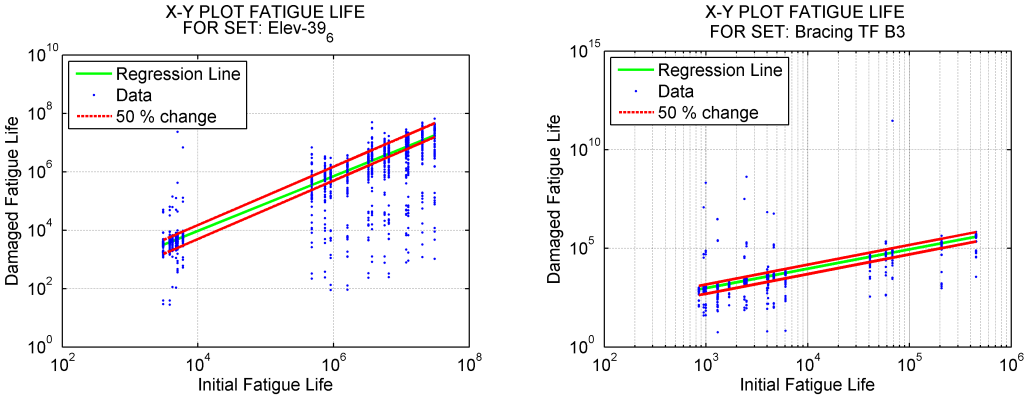

(a) For set "Elevation -39.6" **(b)** For set "Bracing TF B3"

Figure 5.2: Fatigue life changes in XY-plots for two sets, 3L-jacket

no changes for most of the damage cases. By taking into account the fact that a damage scenario should only give local changes, the latter explanation seems to be the most reasonable.

Since a collection of all the data points in one graph makes it difficult to see which points belong to which damage scenario, two of the several hundred damage cases for each jacket are represented in figures 5.3 and 5.4. In these plots all the joints in the structure are plotted for only *one* damage case. One of the plots (a) shows a large spread scenario, while the other plot (b) shows a more refined case. It can be seen that these plots shows somewhat the same trends as the previous did; One notice that large changes occur, and the linear regression line has a slope close to

unity. One also notice that the coefficient of determination (R^2) is close to unity for the 4L-jacket in both the large spread scenario and the more refined case, which confirms that there must be a lot of data points with no change. However, since these plots are dealing with fewer data points than the previous, there are more changes in the slope of the regression line. This combined with very large changes makes it difficult to explain the expected changes in the structure by the use of a simple bias or linear regression.

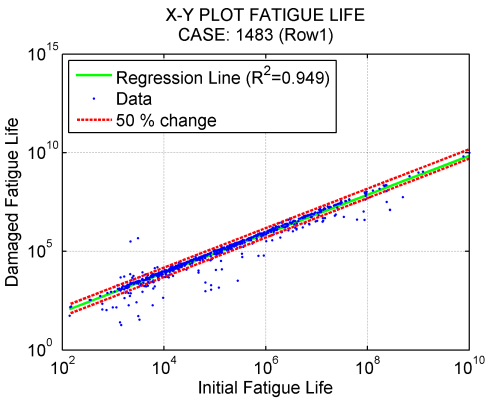

(a) For damage case 1483 (Row 1)

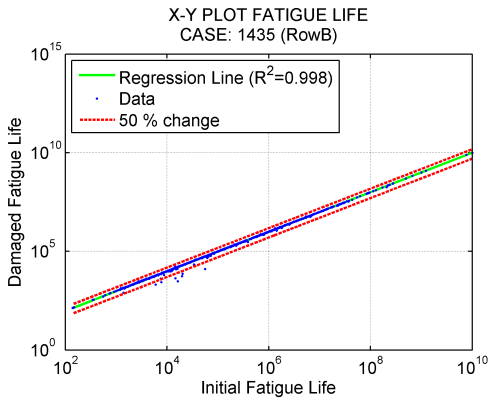

(b) For damage case 1435 (Row B)

Figure 5.3: Fatigue life changes in XY-plots for two damage cases, 4L-jacket

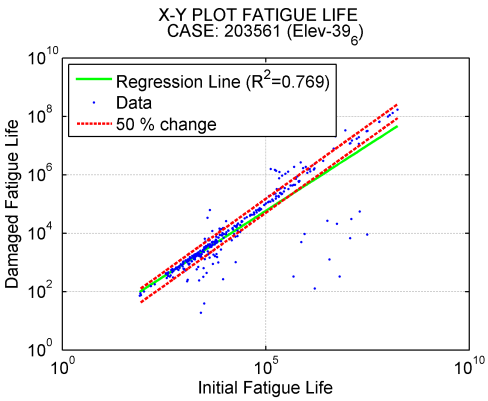

(a) For damage case 203561 (Elevation -39.6)

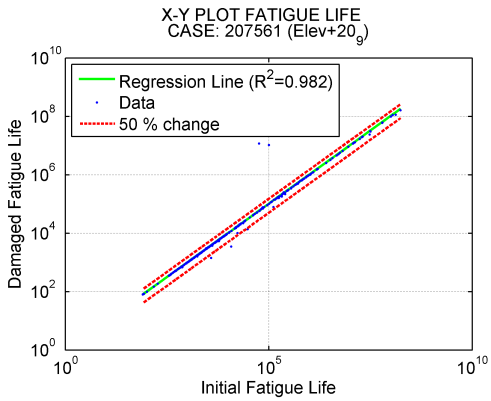

(b) For damage case 207561 (Elevation +20.9)

Figure 5.4: Fatigue life changes in XY-plots for two damage cases, 3L-jacket

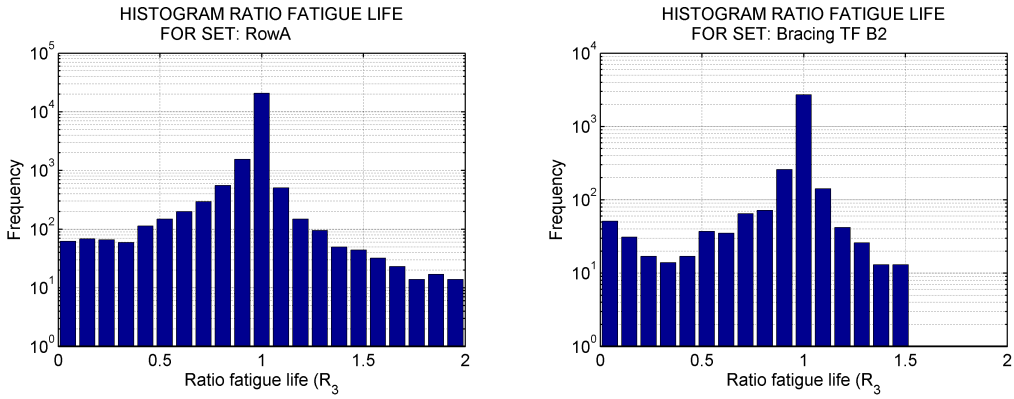

(a) Histogram for set RowA (4L)

(b) Histogram for set BracingTFB2 (3L)

Figure 5.5: Residual Fatigue Redundant Factor R3 histogram for all damage cases

5.1.2 Residual Fatigue Redundant Factor

In chapter 2, some deterministic redundancy factors were described. One of the more simpler ones was the Residual redundant factor ($R3$). Thus, to describe the changes in fatigue life that occurs in a more or less redundant fashion, this factor was used and referred to as the Residual *fatigue* redundant factor. R_3 was plotted in a histogram for values only in the range between 0 and 2. The result is an easy way to see the changes in fatigue life relative to the initial life, but it is difficult to see the extreme values without an extremely small bin size for small values of R_3. On the other hand, the histogram plots make it very easy to see what changes that occur, e.g. if there are a lot of extreme changes (low R_3). In appendix F, a histogram plot for each of the XY-plots are shown, thus making it possible to quantify the data points in the XY-plot. Two of these plots, one for the 4L-jacket and one for the 3L-jacket, are repeated in figure 5.5. From these two plots one can see that one may expect larger changes in the fatigue life for the 3L-jacket than for the 4L-jacket due to the growing number of occurrences as R_3 goes towards zero. It should be noted that these two plots are actually representative for all the plots in the appendix for the respective jacket, as the shape is more or less similar.

Instead of having one plot for each set, one may look at only *one* damage case, and look at the R_3 for *all* the joints. Thus, one may see how sensitive the structure is for a single damage case. The result will be comparable with the XY-plots in figures 5.3 and 5.4 as they both express the same result but in two different presentation methods. As for the XY-plots, only a couple of the results will be shown. In figures 5.6 and 5.7 three different trends are shown for the two jackets: small changes (a), medium changes (b) and large changes (c). Figure 5.7c is definitely a rather exceptional case, but it is not alone. By inspecting the damage cases which

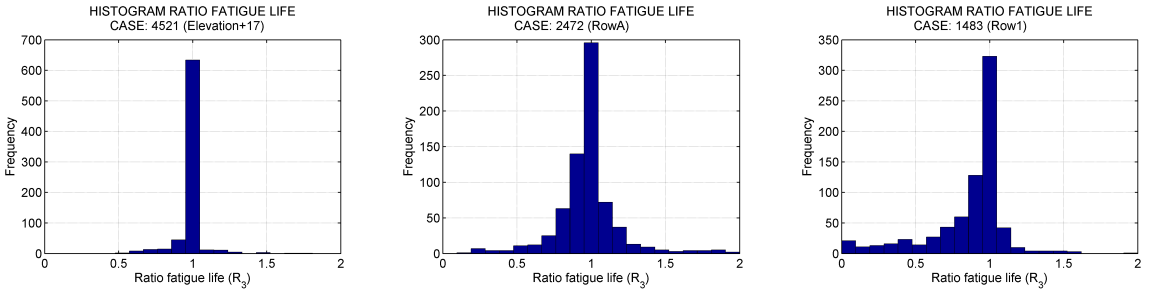

(a) **(b)** **(c)**

Figure 5.6: Residual Fatigue Redundant Factor R3 histogram for all members, 4L-jacket

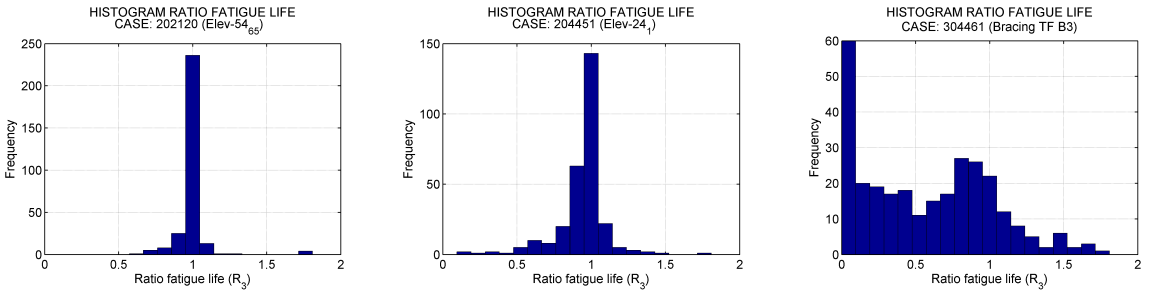

(a) **(b)** **(c)**

Figure 5.7: Residual Fatigue Redundant Factor R3 histogram for all members, 3L-jacket

creates these sort of shapes, one notice that they are a diagonal bracing in the top frame of the structure where no redundancy exist within the bay. This can be seen in figure 5.8 where element 304461 is highlighted as an illustration.

From the previous presented histogram plots, it is easy to see that most off the joint fatigue lives remain unchanged since there is a large peak for $R_3 = 1$. This is the same observation as was found for the slope of the XY-plot regression line. Thus finding a mean value of R_3 would lead to the same conclusion as for the regression line, i.e. more or less equal to unity ergo no change in fatigue life. However, it is possible to extract only values below or equal to, say, 0.8 and find the mean and the standard deviation for these values. If one organize the data so that one can find a mean change in a joint for *all* damage cases instead of splitting the data into sets, one will get the result shown in figure 5.9. Simply put, there are large variations for the joints, but still there seems to be some trends in the data.

Figure 5.8: Location of element 304461 in the 3L-jacket

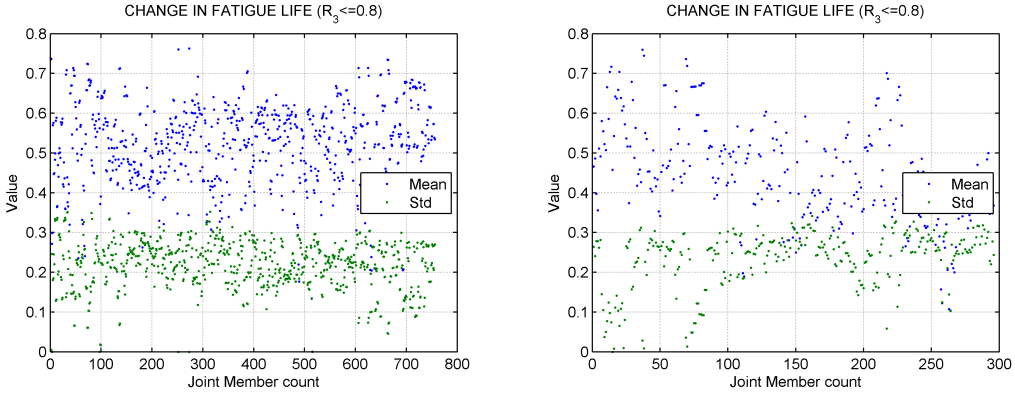

(a) 4L-jacket **(b)** 3L-jacket

Figure 5.9: Mean and standard deviation of all R3 less than 0.8 for each joint

Classification of Members

Instead of looking at a member as just a part in the structure and the joints as just connections in the structure, one may classify them according to their position relative to the damage. This way one can utilize the basic mechanic principle regarding changes in load path, and perhaps find a more general way of describing the changes in fatigue life. There are several ways to do this, and the one used in this thesis is to divide the members into five categories:

1. Adjacent members - Members which share the same node as the damaged element
2. Same set - Members in the same set as the damaged element
3. Adjacent set - Members in sets which are adjacent to the set where the damaged element is
4. Parallel set - Members in a set which one could say is parallel to the damaged element or should not be influenced by the damage
5. Remaining members - Members which does not fall into any of the above categories

This way, it may be possible to find fatigue life changes based on the location relative to the damaged member and perhaps isolate the non-changing members. Now the choice of which set is adjacent and which is parallel will naturally influence the results, and sometimes defining a set may even be difficult without knowing in advance what will happen in the structure. A summary of what was chosen to create the results presented in this thesis is given in appendix E.1.1.

With this classification, the R_3 factor could be found for each of the five categories, and the results are presented in figures 5.10 and 5.11. In these figures all damage cases are added together. In appendix G, a set of figures for each damage set is found, e.g. all damage cases which are in set "Row 1" are plotted in one set of figures: adjacent members, same set, etc. Comparing these figures, it is seen that there is a trend that adjacent members have a larger reduction in the fatigue life, than members in e.g. the parallel set(s). It is also noted that the reduction in fatigue life is smaller when going further away from the damage, i.e. the severity of fatigue life reduction gets less when going from the first category to the last (for the plots, this will be: $a) \rightarrow b) \rightarrow c) \rightarrow d) \rightarrow e)$). On the other hand, one see that the large changes does not get isolated, and it is not easy to find a general value to describe the changes.

A mean value for the R_3 factor for each classification for *each* damage case is shown in figure 5.12. One notice that as for the histogram plots, the lowest mean value is found in adjacent members and the same set, but still there is large spread in the results.

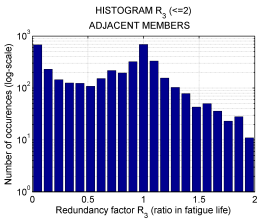

(a) Adjacent members

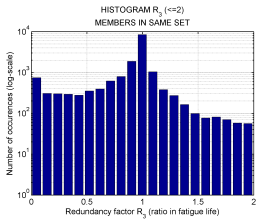

(b) Same set

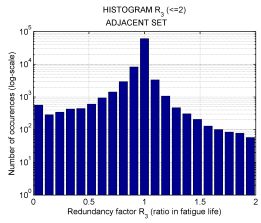

(c) Adjacent set

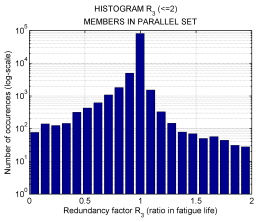

(d) Parallel set

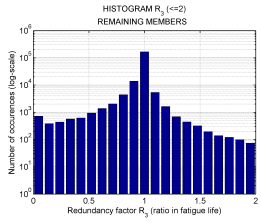

(e) Remaining members

Figure 5.10: Residual Fatigue Redundant Factor for 4L-jacket separated according to member classification

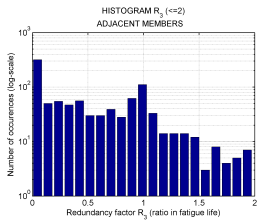

(a) Adjacent members

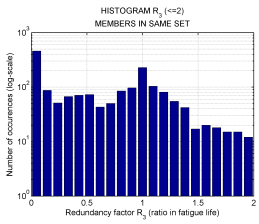

(b) Same set

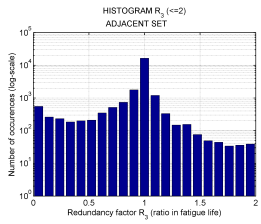

(c) Adjacent set

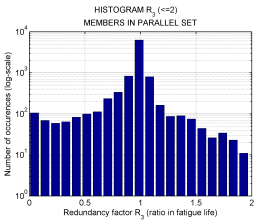

(d) Parallel set

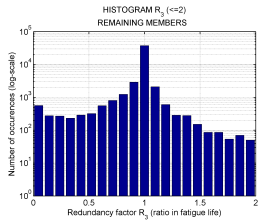

(e) Remaining members

Figure 5.11: Residual Fatigue Redundant Factor for 3L-jacket separated according to member classification

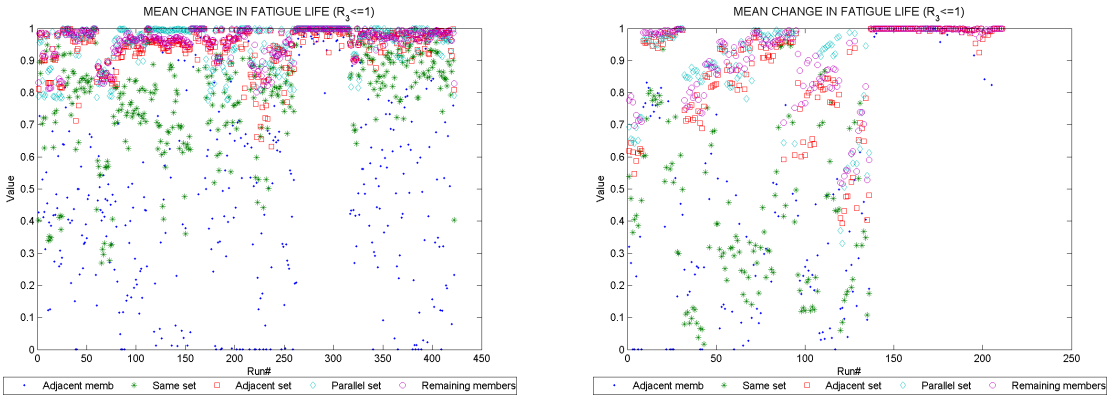

(a) 4L-jacket **(b)** 3L-jacket

Figure 5.12: Mean value for R3 less than or equal to 1.0 for each damage case, according to classification

5.1.3 Fatigue Accelerator Factor

Another approach to describe the changes in fatigue life is to look at the Fatigue Accelerator Factor (FAF), which is defined such that

$$F_{Imp} = \frac{1}{\text{FAF}} \cdot F_{Int} \quad \Leftrightarrow \quad D_{Imp} = \text{FAF} \cdot D_{Int} \tag{5.1}$$

where Imp and Int stands for *impaired* and *intact*, respectively, D is the Miner damage and F is the fatigue life. Thus, this factor is simply the inverse of the R_3 factor, and it will have large values when the fatigue life is vastly reduced. It will therefore give a better impression of what values that are found within the $[0, 0.1\rangle$ interval in the R_3 histogram plots, and it will also be more adequate in describing the largest reduction that occurs.

In figures 5.13 and 5.14, the largest FAF that occurs for each member in a set for *all* damage cases are shown, i.e. each "dot" on the line is a member in the set which the line represents and the x-value for the dot is the most extreme value that the member will experience. The values are presented in an Empirical CDF plot (Kaplan-Meier), so the value for $F(x) = 1$ is the largest observed FAF and the value for $F(x) = 0.5$ is for an even number of observations n equal to the *n/2'th* entry in a sorted list.

From the figures, it can be seen that for the 4L-jacket the caissons and the caisson supports are often largely influenced by the damage scenarios. For the 3L-jacket, there is no similar behaviour for any of the sets, but there is a general trend that a larger FAF is expected. This is clearly shown when looking at the FAF for

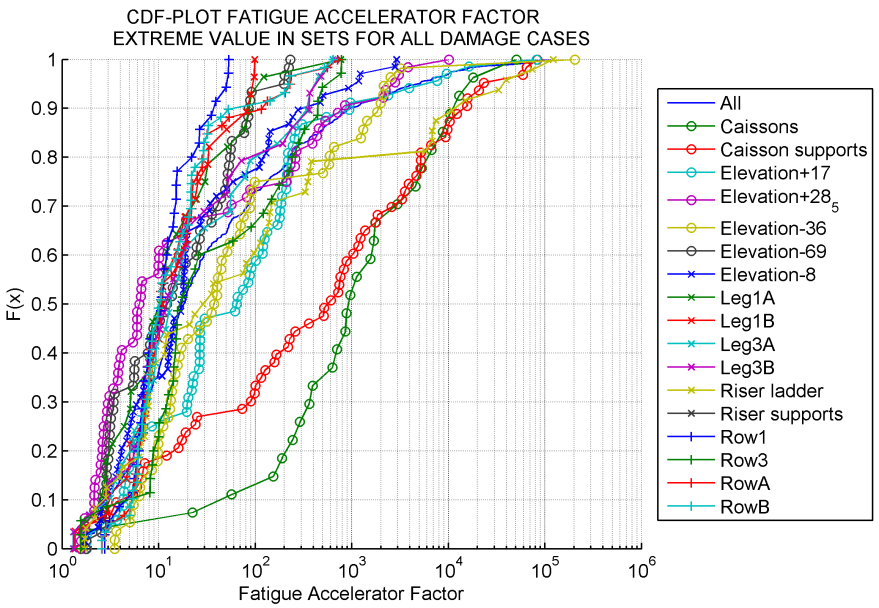

Figure 5.13: Largest Fatigue Accelerator Factor for the sets in the 4L-jacket

$F(x) = 0.5$ for all members. For the 4L-jacket, this corresponds to a value of about 10^1 while the 3L-jacket has a value of about 10^2.

In appendix H, the FAF for each set is shown together with one line per damage location. This way, one can see which damage cases affects which set, and how much they influence the fatigue life in the most extreme cases. For the 4L-jacket, it is seen that damage in the caisson supports usually leads to the highest FAF for most of the sets, but also damage in the same set give large values. Other interesting observations are the start point of the lines. If they start at 10^0, then there exist a damage scenario which does not influence a member in the set under consideration. For the 4L-jacket, most of the lines start at 10^0, while this is not true for the 3L-jacket. This could be explained by the size of the different sets, i.e. somewhat related to the redundancy in the sets and the distribution of "local" elements that acts as supports for appendices and "global" elements which transfer global loads. Otherwise, it is an indicator of the 3L-jacket being less redundant. This difference in the starting points is also visible in figures 5.13 and 5.14

Even though extremely large FAF may occur, there is not given that the fatigue lives will be extremely low. After all, the FAF is only the ratio between the Miner damage before and after damage. Due to structural redundancy, there may exist elements which in the unimpaired condition does not transfer any loads and thus have very long fatigue lives. When in an impaired condition, however, these elements become a part of the load-bearing structure and thus start to transfer loads. But since the elements are intended to carry loads in a damage scenario

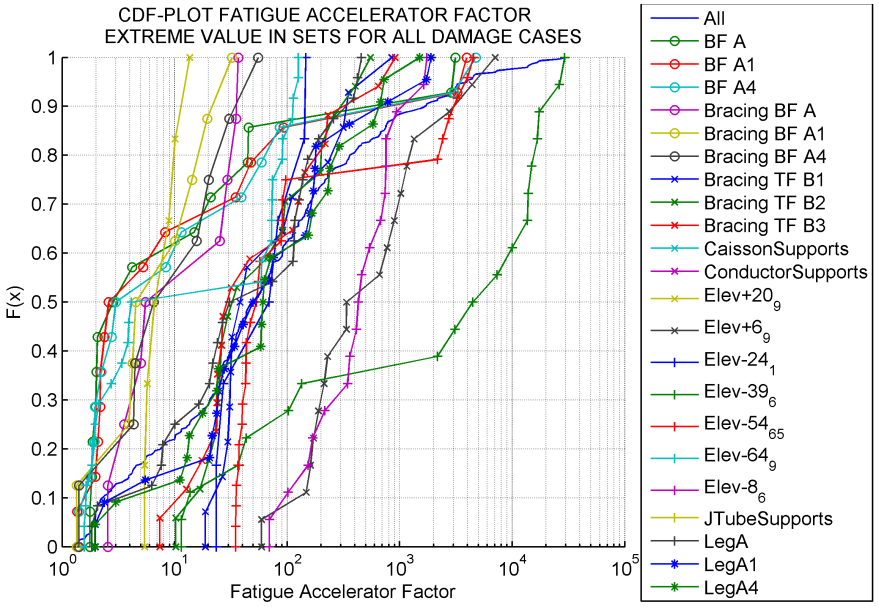

Figure 5.14: Largest Fatigue Accelerator Factor for the sets in the 3L-jacket

4L-jacket	3L-jacket
-0.345	-0.634

Table 5.1: Correlation coefficient between fatigue accelerator factor and Miner damage

(ref. ALS criteria), they will have low stress ranges in the sea states relevant for fatigue. Thus, the fatigue life may be accelerated by a large factor, but the life itself could be well above the minimum requirement according to the FLS criteria. However, these large FAF means that elements which previously was well below the probability of failure criteria from a RBI planning, suddenly becomes critical regarding the risk of failure. This means that there may be a correlation between the FAF and the initial fatigue life (or Miner damage). In figures 5.15 and 5.16, this hypothesis is investigated by plotting the largest FAF against the initial Miner damage. A simple linear regression on the data shows a negative slope for both cases, i.e. a large FAF is expected for a low Miner damage. For the 3L-jacket, there is a more clear trend to support the hypothesis, while there is more spread in the data for the 4L-jacket. This is rather interestingly as the 3L-jacket is the least redundant structure. However, there is still a large spread in the data, making it very difficult to draw a conclusion in any of these cases. A better way of describing the connection between the FAF and the Miner damage is to calculate the correlation coefficient. The result can be seen in table 5.1.

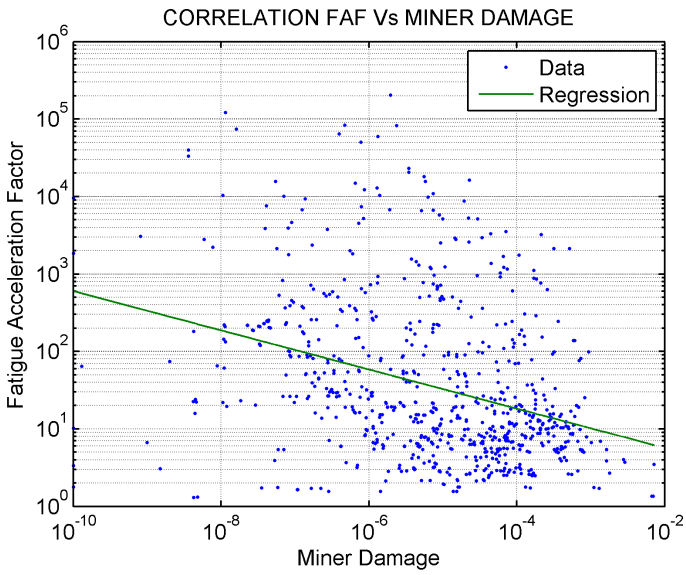

Figure 5.15: Correlation between the FAF and initial Miner damage, 4L-jacket

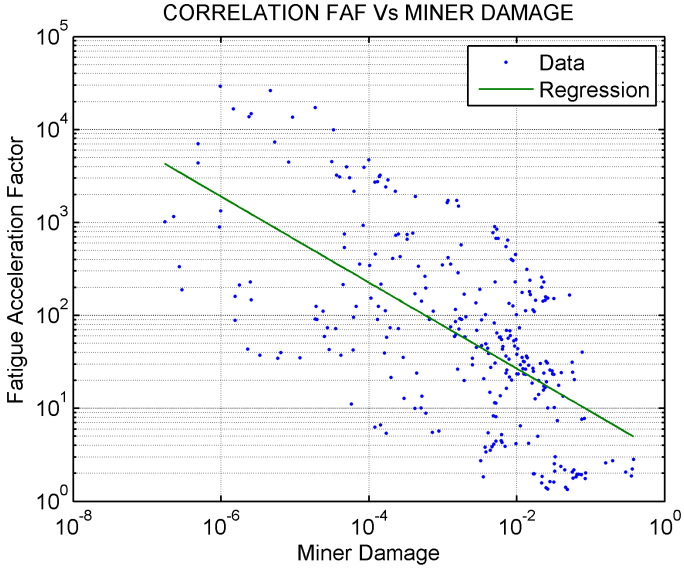

Figure 5.16: Correlation between the FAF and initial Miner damage, 3L-jacket

The largest FAF that occurs in a set with respect to damaged set is summarized in tables 5.2 and 5.3. Here, the correlation between damage location and its effect on the different location can be seen easily, but no information regarding the distribution of the influence is shown. To see this, one must resort to the figures in appendix H. The numbers in the tables are conditional formatted so that green colour means the lowest or no influence (FAF $\cong$ 1) and red means largest influence. The colour map is green-yellow-orange-red. It can be seen once again that the caisson supports are the most critical for the 4L-jacket. It is also noted that the "diagonal" in the matrices, i.e. damage and FAF in the same set, tends to be the worst, but there is also large cross-correlations.

MAXIMUM FATIGUE ACCELERATOR FACTORS

Damage set	Caissons	Caiss supp	Elev +17	Elev +28.5	Elev -36	Elev -69	Elev -8
Caisson supports	5.1E+04	8.3E+04	8.2E+04	1.0E+04	2.0E+05	1.1E+00	2.4E+02
Elevation+17	1.7E+01	4.1E+01	1.3E+02	4.3E+01	1.3E+00	1.4E+00	1.3E+00
Elevation+28_5	4.3E+00	2.6E+02	9.5E+01	2.6E+02	1.3E+00	1.5E+00	1.3E+00
Elevation-36	2.6E+02	2.0E+02	2.3E+00	3.9E+00	2.0E+03	2.0E+00	2.3E+00
Elevation-69	1.0E+00	1.4E+00	1.6E+00	1.4E+00	2.1E+00	8.8E+01	1.1E+00
Elevation-8	1.0E+04	5.2E+03	8.9E+02	1.9E+01	6.4E+01	1.6E+00	2.9E+03
Riser ladder	1.0E+00	1.5E+00	5.3E+01	8.8E+01	8.1E+00	2.7E+01	4.1E+00
Riser supports	1.0E+00	1.0E+00	5.4E+01	1.0E+00	1.2E+00	1.8E+00	4.2E+00
Row1	1.7E+00	1.7E+01	1.1E+01	2.2E+00	9.9E+01	2.3E+02	1.7E+01
Row3	1.6E+00	1.6E+00	1.8E+02	2.7E+02	1.5E+01	5.2E+01	3.0E+00
RowA	2.3E+00	2.7E+00	2.6E+02	4.6E+02	6.3E+00	3.2E+00	7.0E+00
RowB	2.1E+00	5.9E+01	2.4E+02	5.3E+02	3.5E+00	3.4E+00	7.0E+00

	Leg1A	Leg1B	Leg3A	Leg3B	Riser ladd	Row1	Row3	RowA	RowB
Caisson supports	1.8E+00	1.7E+01	1.0E+00	1.1E+00	1.0E+00	2.0E+00	1.1E+00	1.3E+00	2.0E+00
Elevation+17	3.8E+00	4.0E+00	4.1E+00	4.2E+00	4.4E+00	1.4E+00	1.1E+00	2.9E+00	2.9E+00
Elevation+28_5	4.4E+00	5.1E+00	3.2E+00	3.1E+00	3.9E+00	1.1E+00	1.2E+00	6.0E+00	6.2E+00
Elevation-36	4.1E+00	4.0E+00	8.9E+00	6.6E+00	9.0E+04	1.3E+00	1.2E+00	1.4E+00	1.4E+00
Elevation-69	2.8E+00	3.0E+00	1.2E+01	1.1E+01	2.3E+01	1.2E+00	1.2E+00	2.3E+00	2.4E+00
Elevation-8	7.7E+02	9.9E+01	9.3E+00	7.0E+00	6.3E+02	5.2E+00	2.0E+00	1.0E+01	1.1E+01
Riser ladder	1.0E+00	1.0E+00	1.5E+00	1.5E+00	1.2E+05	1.0E+00	1.1E+00	1.7E+00	1.7E+00
Riser supports	1.0E+00	1.0E+00	1.0E+00	1.0E+00	8.8E+00	1.0E+00	1.0E+00	1.0E+00	1.0E+00
Row1	9.0E+01	9.7E+01	3.9E+00	4.3E+00	2.2E+01	5.3E+01	2.6E+00	4.0E+00	4.2E+00
Row3	1.0E+01	1.0E+01	6.4E+02	6.8E+02	4.8E+02	1.2E+01	7.8E+02	8.2E+00	8.6E+00
RowA	8.6E+01	2.6E+00	2.5E+02	2.7E+00	2.1E+00	1.5E+00	1.5E+00	7.1E+02	1.4E+02
RowB	2.6E+00	8.9E+01	2.6E+00	2.4E+02	2.1E+00	1.5E+00	1.5E+00	1.3E+02	6.4E+02

Table 5.2: Maximum fatigue accelerator factors for the 4L-jacket

MAXIMUM FATIGUE ACCELERATOR FACTORS

Damage set	BF A	BF A1	BF A4	Brace BF A	Brace BF A1	Brace BF A4	Brace TF B1	Brace TF B2	Brace TF B3
Bracing BF A	8.4E+00	4.8E+00	4.8E+00	3.8E+00	1.8E+00	1.7E+00	1.3E+00	1.1E+00	1.1E+00
Bracing BF A1	4.9E+00	1.8E+01	7.4E+00	4.0E+00	4.5E+00	3.4E+00	1.1E+00	1.5E+00	1.3E+00
Bracing BF A4	4.7E+00	6.1E+00	1.5E+01	3.0E+00	2.8E+00	4.5E+00	1.3E+00	1.3E+00	1.4E+00
Bracing TF B1	1.2E+00	2.1E+00	2.6E+00	1.2E+00	1.3E+00	1.5E+00	8.5E+02	5.3E+01	2.2E+02
Bracing TF B2	1.6E+00	1.6E+00	1.2E+00	1.5E+00	1.2E+00	1.2E+00	1.9E+01	5.5E+02	3.2E+01
Bracing TF B3	2.8E+00	1.7E+00	2.8E+00	1.4E+00	1.5E+00	1.4E+00	2.5E+01	3.5E+01	9.1E+02
CaissonSupports	1.0E+00	1.0E+00	1.0E+00	1.0E+00	1.0E+00	1.0E+00	1.0E+00	1.0E+00	1.0E+00
ConductorSupports	1.1E+00	1.0E+00	1.1E+00	1.0E+00	1.0E+00	1.0E+00	1.0E+00	1.1E+00	1.0E+00
Elev+20_9	1.0E+00	1.0E+00	1.1E+00	1.0E+00	1.0E+00	1.0E+00	3.4E+00	2.5E+00	2.7E+00
Elev+6_9	1.0E+00	1.0E+00	1.0E+00	1.0E+00	1.0E+00	1.0E+00	1.0E+00	9.1E+00	1.3E+01
Elev-24_1	1.2E+00	1.5E+00	1.5E+00	1.2E+00	1.1E+00	1.1E+00	8.8E+00	6.9E+00	7.0E+00
Elev-39_6	1.4E+00	2.6E+00	3.3E+00	1.6E+00	1.5E+00	1.5E+00	4.7E+01	6.5E+01	4.3E+01
Elev-54_6_5	1.8E+00	1.7E+00	1.7E+00	1.7E+00	1.5E+00	1.4E+00	1.1E+00	1.1E+00	1.1E+00
Elev-64_9	3.1E+03	3.9E+03	4.7E+03	3.7E+01	3.2E+01	5.5E+01	4.1E+00	2.3E+00	2.1E+00
Elev-8_6	1.1E+00	1.1E+00	1.1E+00	1.1E+00	1.1E+00	1.1E+00	3.2E+00	3.0E+00	3.4E+00
JTubeSupports	1.0E+00	1.0E+00	1.0E+00	1.0E+00	1.0E+00	1.3E+00	1.2E+00	1.0E+00	1.0E+00

	Elev +20.9	Elev +6.9	Elev -24.1	Elev -39.6	Elev -54.65	Elev -64.9	Elev -8.6	LegA	LegA1	LegA4
Bracing BF A	1.1E+00	1.0E+00	1.2E+00	1.8E+00	3.5E+01	8.1E+01	1.0E+00	2.0E+00	1.2E+00	1.5E+00
Bracing BF A1	1.0E+00	1.0E+00	1.3E+00	1.1E+01	4.3E+01	1.1E+02	1.0E+00	1.4E+00	2.3E+00	1.9E+00
Bracing BF A4	1.1E+00	1.0E+00	1.3E+00	7.8E+00	5.2E+01	1.3E+02	1.1E+00	1.4E+00	1.7E+00	2.1E+00
Bracing TF B1	1.4E+01	7.0E+03	4.8E+01	2.1E+01	2.5E+00	1.6E+00	1.7E+03	1.3E+02	1.9E+03	1.5E+03
Bracing TF B2	1.0E+01	1.2E+03	1.4E+02	1.6E+01	1.7E+00	1.6E+00	1.7E+02	4.2E+02	3.6E+02	1.1E+02
Bracing TF B3	6.6E+00	1.9E+02	1.5E+02	2.9E+01	3.8E+00	2.7E+00	6.8E+02	4.6E+02	1.0E+02	6.8E+02
CaissonSupports	1.0E+00	1.0E+00	1.0E+00	1.0E+00	1.0E+00	1.0E+00	1.0E+00	1.0E+00	1.0E+00	1.0E+00
ConductorSupports	1.0E+00	1.5E+00	1.9E+00	1.1E+00	1.2E+00	1.0E+00	1.3E+00	1.8E+00	1.2E+00	1.4E+00
Elev+20_9	2.3E+00	1.3E+00	1.0E+00	1.0E+00	1.1E+00	1.0E+00	1.0E+00	2.1E+00	2.7E+00	2.4E+00
Elev+6_9	1.1E+00	3.4E+02	1.1E+00	1.1E+00	1.0E+00	1.0E+00	1.5E+00	4.2E+01	3.8E+01	2.7E+01
Elev-24_1	1.3E+00	1.4E+00	6.2E+01	1.9E+00	1.6E+00	1.2E+00	2.2E+00	7.5E+00	7.7E+00	5.1E+01
Elev-39_6	1.2E+00	1.2E+00	6.0E+00	2.9E+04	3.7E+00	1.6E+00	1.3E+00	2.0E+01	1.8E+02	2.3E+02
Elev-54_6_5	1.0E+00	1.0E+00	1.1E+00	1.9E+00	9.1E+00	1.9E+00	1.0E+00	1.1E+00	1.1E+00	1.2E+00
Elev-64_9	4.1E+00	1.3E+00	2.3E+00	1.9E+01	4.5E+03	7.8E+01	1.3E+00	2.4E+00	4.1E+00	4.1E+00
Elev-8_6	1.0E+00	7.9E+00	2.3E+00	1.3E+00	1.1E+00	1.1E+00	9.4E+02	8.7E+01	1.0E+03	5.6E+01
JTubeSupports	1.0E+00	1.3E+00	1.0E+00	1.0E+00	1.0E+00	1.5E+00	1.0E+00	1.0E+00	1.1E+00	1.1E+00

Table 5.3: Maximum fatigue accelerator factors for the 3L-jacket

5.1.4 Fatigue lives

Instead of looking at changes in fatigue life expressed either through the R_3 or the FAF or any other redundancy factor for that matter, it may be somewhat more interesting to find the lowest fatigue life, as this would be the critical value for the structure as a whole. When only looking at the reduction in fatigue life for a damage case, it is ambiguous which member that is most critical in regards of the remaining fatigue life in the structure. To illustrate, take the following two cases:

1. The member whose damage will lead to a fatigue life reduction (the most extreme) of 1.0 [%]
2. The member whose damage will lead to a fatigue life reduction (the most extreme) of 10.0 [%]

Now say that the critical member in case 1 has an initial fatigue life of 5000 [y], and that the critical member in case 2 has an initial fatigue life of 100 [y]. Then, the impaired fatigue life in case 1 is reduced to 50 [y] while for case 2 the impaired fatigue life is reduced to a merely 10 [y]. So even though the *largest reduction* (largest FAF) is found in case 1, the *lowest fatigue life* occurs in case 2.

A simple worst case fatigue life plot is shown in figure 5.17 for the 4L-jacket, and in figure 5.18 for the 3L-jacket. In these figures, the minimum fatigue life for a joint for *all* damage cases is plotted in a histogram together with the initial life (life is in log-scale). There is a clear shift to the left for both jackets, i.e. towards a lower fatigue life, and it is a rather large portion of the joints which are below 100 [y]. The lowest fatigue life is a merely 1 year for the 4L-jacket, and a merely 3 years for the 3L-jacket. These values are not what one would consider to be acceptable, if one should have a criteria that no second member should fail due to fatigue within an inspection interval. However, it is not said that the structure will collapse should a second member fail, and one also needs to take into account the probability of such an event occurring.

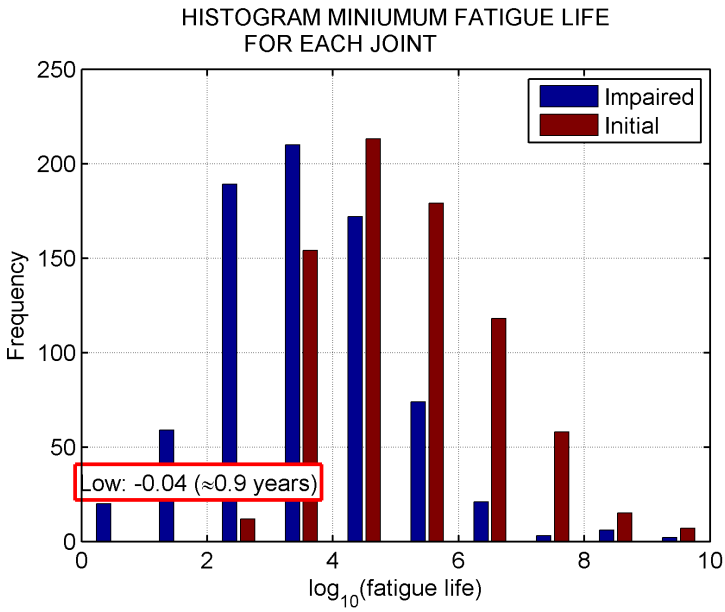

Figure 5.17: Minimum fatigue life for each joint for the initial structure and the impaired structure, 4L-jacket

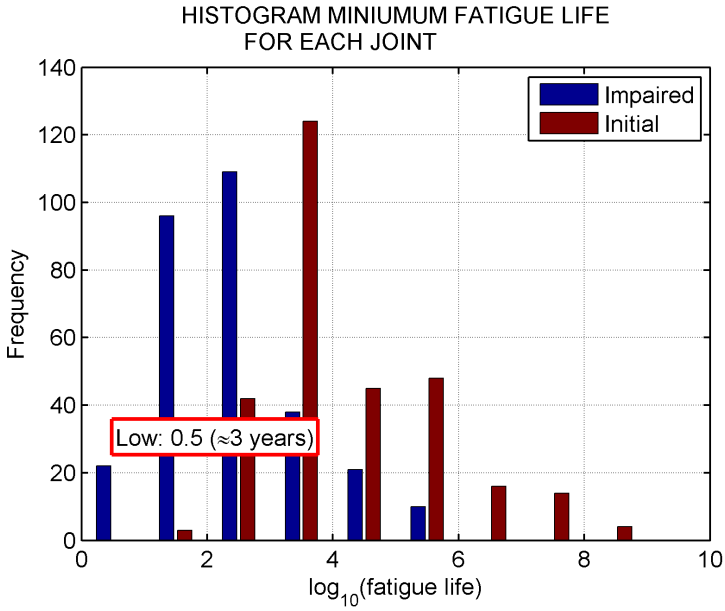

Figure 5.18: Minimum fatigue life for each joint for the initial structure and the impaired structure, 3L-jacket

MIMIMUM FATIGUE LIFE BELOW 10.0 YEARS

Joint	Member	Set	Damage (Set)	Initial	Impaired	FAF
2025	2529	Elevation-36	3538 (Caisson supp)	2.0E+03	9.2E-01	2.1E+03
2025	2535	Caisson supp	3538 (Caisson supp)	1.4E+04	3.9E+00	3.6E+03
2026	920	Caissons	3538 (Caisson supp)	5.5E+03	6.4E+00	8.6E+02
2036	720	Caissons	3526 (Caisson supp)	1.5E+04	9.0E+00	1.7E+03
2046	745	Caissons	3536 (Caisson supp)	3.0E+04	1.0E+01	3.0E+03
2065	2525	Elevation-36	3533 (Caisson supp)	3.2E+03	1.5E+00	2.1E+03
2065	2532	Caisson supp	3533 (Caisson supp)	2.3E+04	6.8E+00	3.3E+03
2066	845	Caissons	3533 (Caisson supp)	4.5E+04	8.5E+00	5.3E+03
2075	2524	Elevation-36	3528 (Caisson supp)	5.1E+05	2.5E+00	2.0E+05
2076	820	Caissons	3528 (Caisson supp)	5.2E+04	5.9E+00	8.7E+03
2085	2523	Elevation-36	3529 (Caisson supp)	4.7E+03	1.5E+00	3.2E+03
2085	2536	Caisson supp	3529 (Caisson supp)	3.4E+04	6.6E+00	5.2E+03
2086	945	Caissons	3529 (Caisson supp)	5.9E+03	6.7E+00	8.8E+02
3011	710	Caissons	3524 (Elevation-8)	5.9E+03	5.3E+00	1.1E+03
3066	810	Caissons	3530 (Elevation-8)	3.9E+03	6.2E+00	6.3E+02
3076	935	Caissons	3530 (Elevation-8)	9.3E+03	5.3E+00	1.8E+03
3090	2045	Leg1A	3530 (Elevation-8)	4.7E+03	6.1E+00	7.7E+02
4010	4526	Elevation+17	3526 (Caisson supp)	4.2E+05	5.2E+00	8.2E+04
4020	4525	Elevation+17	3536 (Caisson supp)	4.4E+04	2.7E+00	1.6E+04
4088	810	Caissons	3528 (Caisson supp)	1.8E+05	9.9E+00	1.8E+04

Table 5.4: Damage cases and members with fatigue life less than 10 years, 4L-jacket

There is also a third factor that needs to be emphasized when looking at the fatigue life, namely the calculated value is not necessarily a "correct" value. As discussed in appendix C Jacket Analysis, non-linearities may play an important role for jacket structures. Take into account the considerable sensitivity for fatigue life with respect to the stress range, and one should see why these numbers must only be taken as a guidance as they will indeed reflect the expected results, but due to the linearisation involved they may be both non-conservative or very conservative, depending on the basis for the linearisation (which in most cases are chosen such that conservatism is obtained).

So far, almost only a graphical visualisation of the result has been presented, and without looking at the individual R_3 plots or XY-plots for each damage case, it is difficult to see what are critical damage cases in regards to fatigue life and which joint or members are exposed. Therefore, a quick summary of all joints which have a fatigue life less than 10 [y] for some damage scenario is shown in tables 5.4 and 5.5. Here, the joint number along with the element number (member) and the set where the low fatigue life occurs is shown together with the actual fatigue lives for the initial- and impaired structure as well as the FAF, and also the location of the damage case along with the damaged element number.

MIMIMUM FATIGUE LIFE BELOW 10.0 YEARS

Joint	Member	Set	Damage (Set)	Initial	Impaired	FAF
104441	303542	Brace TF B2	304451 (Brace TF B2)	4.2E+03	7.6E+00	5.5E+02
104441	104441	LegA	304451 (Brace TF B2)	3.4E+03	8.7E+00	3.9E+02
104441	303642	Brace TF B3	304461 (Brace TF B3)	4.0E+03	6.2E+00	6.5E+02
104441	104441	LegA	304461 (Brace TF B3)	3.1E+03	6.9E+00	4.6E+02
104441	204461	Elev-24.1	304451 (Brace TF B2)	1.3E+03	9.4E+00	1.4E+02
104551	303454	Brace TF B2	304451 (Brace TF B2)	1.4E+03	6.8E+00	2.0E+02
104551	104551	LegA1	304451 (Brace TF B2)	1.2E+03	8.4E+00	1.5E+02
104551	303652	Brace TF B1	304561 (Brace TF B1)	5.6E+03	6.6E+00	8.5E+02
104551	104551	LegA1	304561 (Brace TF B1)	6.3E+03	8.1E+00	7.8E+02
104661	303464	Brace TF B3	304461 (Brace TF B3)	1.3E+03	5.7E+00	2.3E+02
104661	104661	LegA4	304461 (Brace TF B3)	1.1E+03	7.4E+00	1.5E+02
104661	313564	Brace TF B1	304561 (Brace TF B1)	2.2E+03	7.0E+00	3.1E+02
104661	104661	LegA4	304561 (Brace TF B1)	2.0E+03	8.4E+00	2.4E+02
105441	105441	LegA	304451 (Brace TF B2)	9.4E+02	6.2E+00	1.5E+02
105441	305451	Brace TF B2	304451 (Brace TF B2)	3.6E+03	8.9E+00	4.0E+02
105441	105441	LegA	304461 (Brace TF B3)	1.4E+03	5.4E+00	2.6E+02
105441	305461	Brace TF B3	304461 (Brace TF B3)	6.0E+03	6.6E+00	9.1E+02
105551	105551	LegA1	304561 (Brace TF B1)	1.2E+03	7.6E+00	1.6E+02
105551	105551	LegA1	305561 (Brace TF B1)	3.9E+02	9.6E+00	4.1E+01
105661	205466	Elev-8.6	304461 (Brace TF B3)	5.4E+03	7.9E+00	6.8E+02

Table 5.5: Damage cases and members with fatigue life less than 10 years, 3L-jacket

Now it has been indicated that the 4L-jacket is a more redundant structure than the 3L-jacket, and this is somewhat reflected in the tables 5.4 and 5.5. For the 4L-jacket, there is a clear trend that the caisson supports are extremely critical, but also some elements in "Elevation-8" give extremely low fatigue lives. When considering the fact that the caissons are usually supported on four levels without any redundancy (only one support per horizontal elevation), where two of the supports are in the water zone, it is naturally that the force distribution is sensitive towards damage in the supports. Should for instance the support right below the waterline be damaged, the caisson will suddenly have a large span right in the waterline where the external forces acts. A rather large change in the natural period will occur, which could lead to more forces being taken up (depending on the frequency where the wave energy is and the natural frequency of the caisson). On the other hand, the perhaps most critical change would be the static force redistribution to the other supports.

A little study regarding the problems presented in the previous section has been performed. The most critical caisson, i.e. the caisson with support 3538, was imported into USFOS along with all of its supports, see figure 5.19. This way, non-linearities should be captured, but the accuracy of the study is limited since only

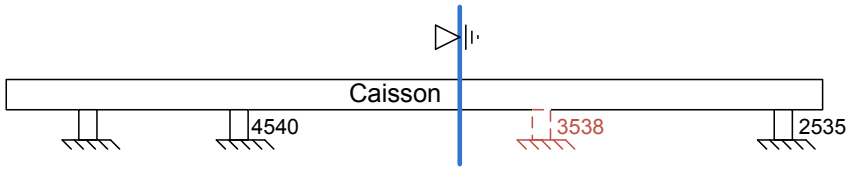

Figure 5.19: Illustration of the caisson used in the caisson support study (note the direction of the waterline)

one sea state was applied, not to mention the missing jacket. However, this study will reflect what is happening under damage case 3538. Boundary conditions for the supports were chosen to be encastré. The caisson were subjected to an irregular sea state with significant wave height of 3 [m] and a spectral peak period of 5 [s]. The changes in axial stress levels for the two neighbouring supports are shown in figure 5.20. A large increase in the moments acting in the supports should be expected due to the location of the resultant wave force. However, in this study only the axial stress levels has been investigated, and one can see that there is an extremely large change for element 4540. A massively increase of 7.5 times the initial stress levels are observed, which by it self would lead to a reduction in fatigue life of $7.5^3 \approx 400$ times. Clearly, there must be large forces going into the structure at places where only small forces used to be, thus explaining the low fatigue lives observed for the damage case 3538 as well as the other caisson support damage cases.

Returning to the 3L-jacket, one see that table 5.5 is not represented by a single caisson nor conductor support at all. Regarding caissons, there is only a single sewage caisson on the 3L-jacket which is extremely small, thus very small forces are attracted by it. However, the 3L-jacket has a set of conductors which are more similar to the caissons in the 4L-jacket, but still they do not give any large reductions (large FAF) as seen in table 5.3. The difference however lies in the fact that the conductors are supported all the way to the mud line as well as being supported with smaller length intervals. On the other hand, a very plausible explanation could simply be that for the 3L-jacket, the joints where the caisson/conductor supports are located are not included in the fatigue check, nor are the caissons them self. Thus, the caisson/conductor support cases cannot be compared across the jackets as it is most likely the joint connection between a brace and a support that inherent the low fatigue life observed.

What can be compared though, is the fact that the 3L-jacket is clearly sensitive to damage in its bracing in the top frame. It has been shown earlier that there is little to none redundancy in the top frames appose to the 4L-jacket and its X-bracing. The damage case 304461 is no stranger so far in this thesis, as it was discussed in section 5.1.2. There it was shown that this damage scenario gave a rather larger number of extreme reductions in fatigue lives, thus it is no surprise that table 5.5 is vastly represented by case 304461 and its relatives 304451 and 304561 which has the exact same trend in the R_3 histogram plot as 304461. What is interesting

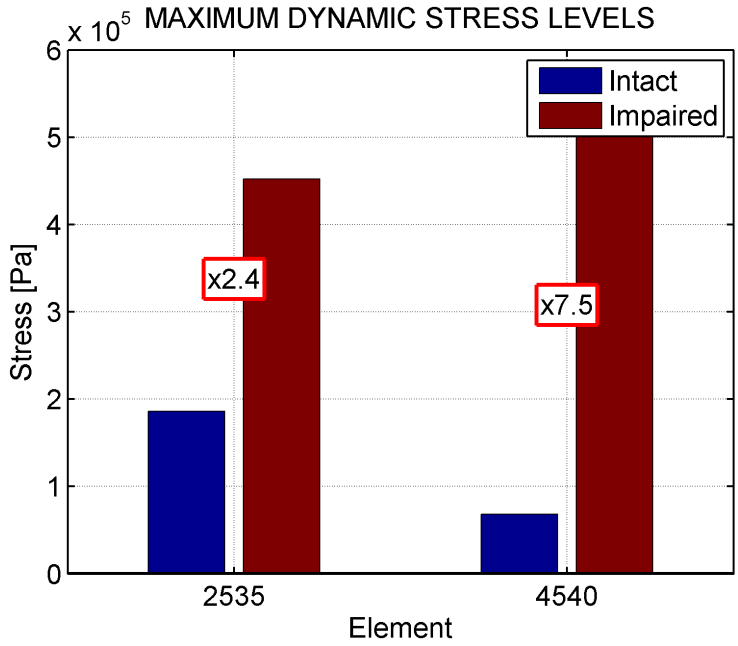

Figure 5.20: Dynamic stress for the caisson support study

however is that not a single vertical brace damage case is present for the 4L-jacket. This may be explained by large redundancy from the X-bracing. Also, the FAF for the cases presented in the tables is in the range $10^1 - 10^5$, thus confirming that the FAF itself is not necessarily a good measure on what is critical in respect to residual fatigue life.

5.1.5 Visualization

In order to visualize how the changes in fatigue life propagates through the structure, since there does not seem to be only very locally effects, an inspection was performed in GeniE by adding all members with a reduction in fatigue life of say, 80 %, 50 % and 10 %, into a GeniE-set. In figure 5.21, an example is shown for the 4L-jacket. The damaged member, element 980, is marked in blue, while the red members are those with fatigue lives less than or equal to 80 %, 50 % or 10 % as specified by the sub-caption. One see that as the threshold limit is reduced, the radii of affected members relative to the damage is also reduced, as one would expect. However, there are still many members in the structure that are influenced by the damage even for a low threshold (large reduction). There is also the rather odd influence in the riser ladder which is still present in the 10 % case. If one look closely, it can be seen three red members which must be related to the horizontal transfer of loads in the diagonal bracing in “Elevation -36” (second to last horizontal level).

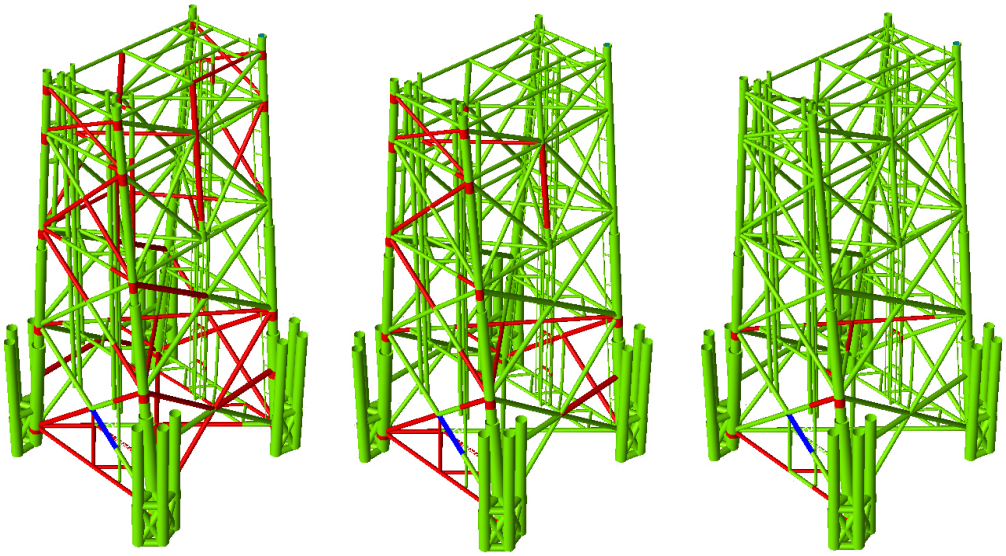

(a) 80 % **(b)** 50 % **(c)** 10 %

Figure 5.21: Members with change in fatigue damage below threshold limit for damage case 980, 4L-jacket

5.2 Probabilistic Fatigue

5.2.1 Log-normal Probability Fit

Another approach to describe the changes in fatigue would be to fit a probabilistic distribution function to the intact fatigue data and the impaired fatigue data. If the fit is good, one would have a way to define an interval of fatigue life which has the same probability of occurrence. Also, one could define a distribution of the fit parameters, and perhaps these distributions could serve as a general description of fatigue redundancy, i.e. one only needs to have an initial distribution of fatigue data, and then calculate the probability of failure based on changes in the parameters. This fit however does not give a way to describe a certain joint, but rather the structure as a whole.

The idea to this way of describing the changes in fatigue came after looking at the distribution of the fatigue life for 4L-jacket, and noting that it seemed to follow a log-normal distribution. Also, a Gamma distribution seemed to be applicable, but after some testing it turned out log-normal was the better fit overall, and thus this distribution was chosen for the 3L-jacket as well without any further investigation. The only confirmation done was a visual inspection that the 3L-jacket also had a similar trend in the distribution of fatigue lives.

Two modifications to the data has been performed pre distribution fitting. First of all, FRAMEWORK has a lower limit of 1.00E-10 in fatigue damage. In order to prevent a large contribution to the parameter estimators from these values which stack up in the top bin, they were simply removed. After all, the fit needs to be good in the "head", not the "tail". Secondly, the fit is for the log dataset, meaning that any fatigue life less than 10 will have negative log-value. This is not applicable for using in a log-normal distribution where all values must be greater than 0. Thus, it was assumed that very few values would fall into this category and should any value do so, it would be set to 0.1 prior to fitting.

4L-jacket

In figure 5.22 the density of the initial fatigue life is shown in a histogram together with the log-normal fit for the initial data as well as the fits for all damage cases. The same is presented in a CDF plot in figure 5.23. It is noted that it is more likely to have a lower fatigue life when the structure is impaired, than under intact situation. However, by inspecting the "head" of the distribution, which in this case is the largest area of interest, one find that the fit is not as good in describing the relative large empirical probabilities observed. This can be seen in figure 5.24. One can also can see from this that not many values was falsely set to 0.1, thus this correction on the data sets should be negligible.

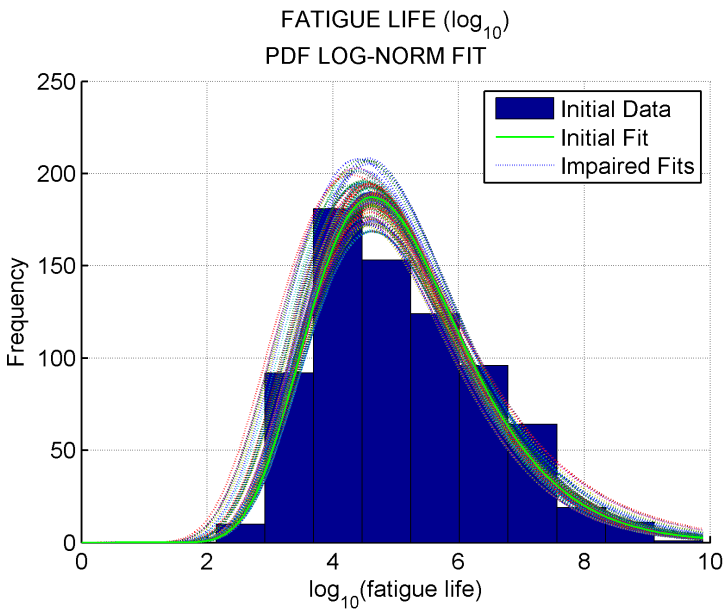

Figure 5.22: Fatigue life density distribution with log-normal fit, 4L-jacket

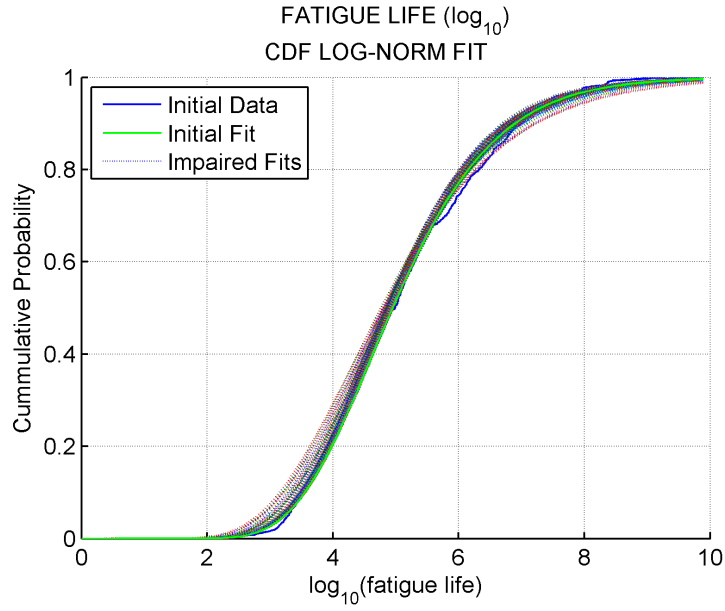

Figure 5.23: Fatigue life cumulative distribution with log-normal fit, 4L-jacket

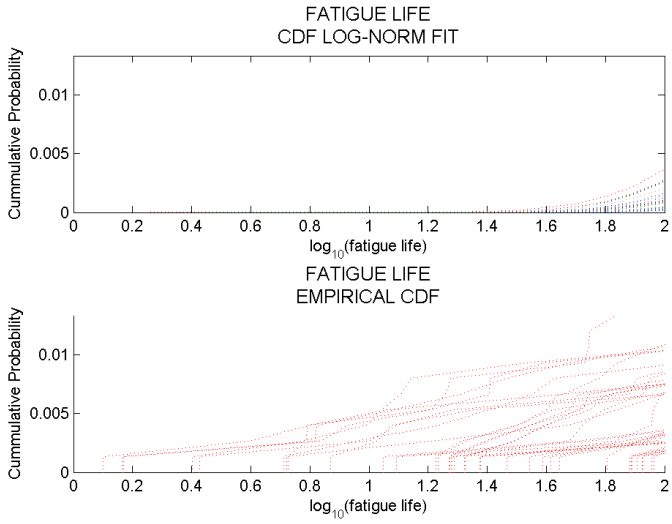

Figure 5.24: Close up of the cumulative probability plot for the fatigue life, 4L-jacket

To test the hypothesis that the data follows a log-normal distribution, a χ^2 test was performed. The result was that even for a low number of α, several fits was rejected. For $\alpha = 0.005$, not even the initial fit for the intact structure was accepted. The test results can be seen in figure 5.25.

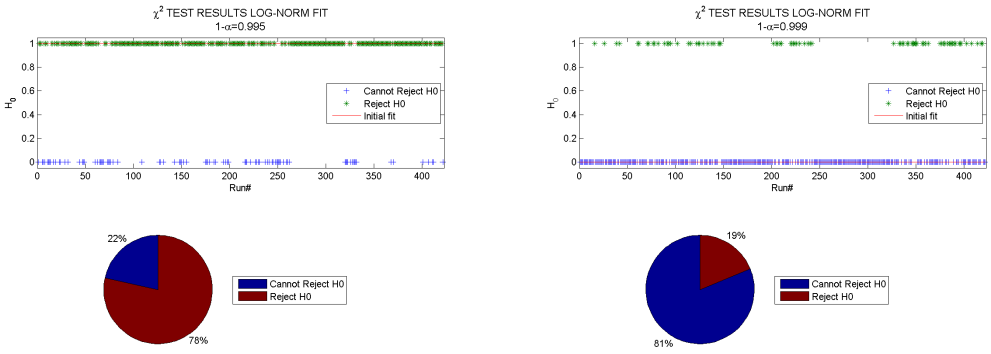

(a) $1 - \alpha = 0.995$ **(b)** $1 - \alpha = 0.999$

Figure 5.25: Results from χ^2 test, 4L-jacket

3L-jacket

In figure 5.26 the PDF results for the 3L-jacket is shown, while the CDF plot is in figure 5.27. A close up is found in figure 5.28.

χ^2 test results is shown in figure 5.29. A key difference between the two jackets is the tendency towards more spread in the individual impaired fit results for the 3L-jacket, thus confirming less redundancy. This is very clear when looking at the CDF-plot. Also, one see that the "head" of the fits are more correct for the 3L-jacket. However, the χ^2 test results are much worse for this jacket.

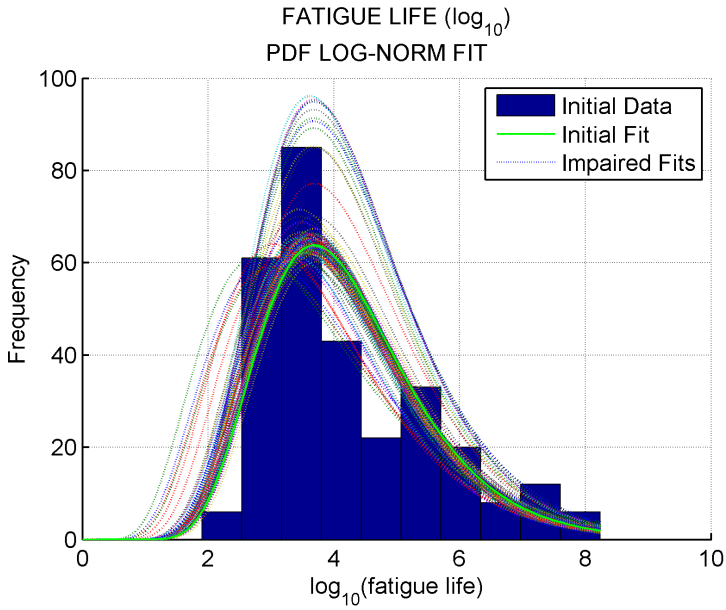

Figure 5.26: Fatigue life density distribution with log-normal fit, 3L-jacket

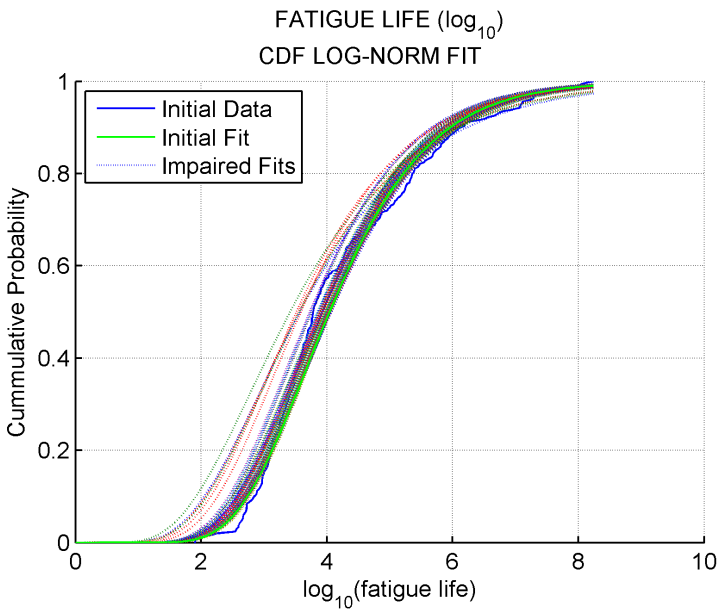

Figure 5.27: Fatigue life cumulative distribution with log-normal fit, 3L-jacket

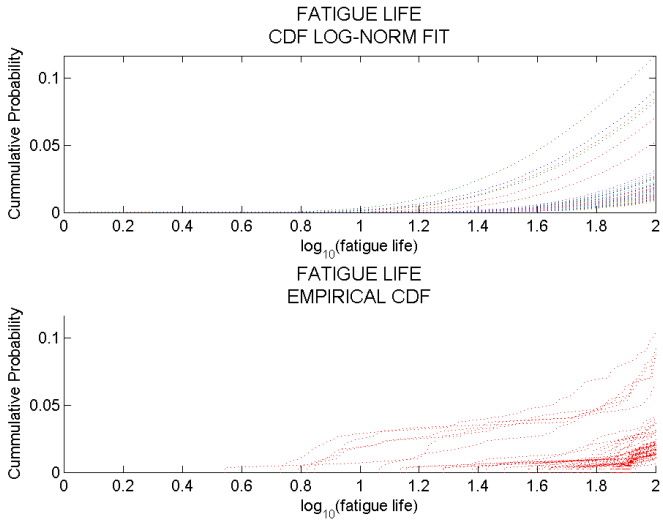

Figure 5.28: Close up of the cumulative probability plot for the fatigue life, 3L-jacket

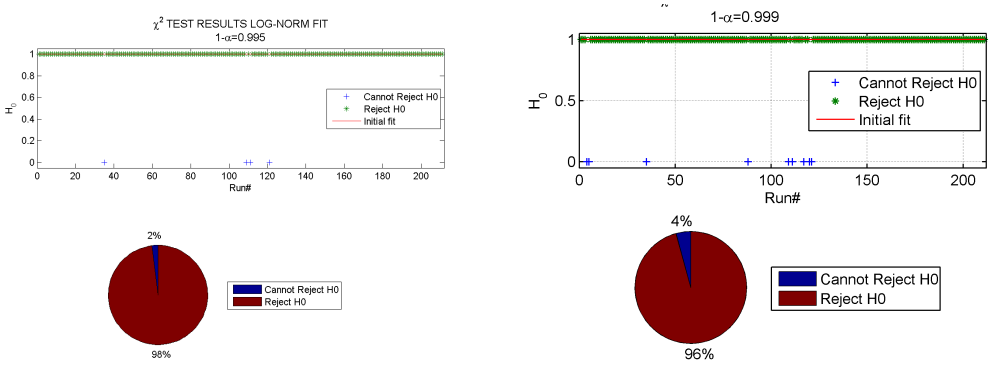

(a) $1 - \alpha = 0.995$ **(b)** $1 - \alpha = 0.999$

Figure 5.29: Results from χ^2 test, 3L-jacket

5.3 Parametric Study Fatigue

In chapter 3.3 there are listed several factors that will influence the fatigue life, and which inherent uncertainty. Thus, changes in the analysis procedure, e.g. stochastic analysis, time domain, etc., and variation in the load modelling, e.g. hydrodynamic coefficients, are all examples that will influence the calculated fatigue life both for the initial structure, as well as for the impaired structure. However, when looking at changes in fatigue life, there is the possibility that these factors have less to say, as they will be on "both sides of the equation". But, changes in dynamics due to damage may be better captured in a non-linear analysis software, so a parametric study of both analysis procedure, theory applied and variables in loading and stress calculation will give a more clear picture of what is relevant.

5.3.1 Wave Spectrum

Only one parametric study has been performed for this thesis, namely to look at the surface modelling of the sea states involved in the analysis, i.e. the difference between a PM spectrum and a JONSWAP spectrum. It has been discussed that a PM spectrum is applicable for fully developed sea states which often are the case for fatigue calculations, while it has been shown that a rather large portion of the sea states in the analysis could be classified as wind-growing seas. The choice of spectrum may therefore be highly relevant. However, the results for the 4L-jacket showed almost no change at all, or at least no alarming differences. Due to this result, the 3L-jacket has not been part of this study.

The absence of changes could be due to the low natural period of the structure, i.e. a large portion of the wave energy is not excited where dynamics are important. The difference in a JONSWAP and PM spectrum could be more pronounced when the eigenvalue is within large wave energy areas. Then, the more concentrated energy around the peak period for the JONSWAP spectrum could become significant. Also, since there are many sea states under consideration, the difference may be cancelled out, e.g. one sea state becomes critical while another becomes negligible.

By performing a visual inspection of the FAF plot and the minimum fatigue life histogram plot, it is very hard to spot any difference between the two wave spectrum. The trends are the same, as well as the extreme values. The two plots for the PM run are shown in figure 5.30. By looking at the minimum fatigue life below 10 [y] once again, and express the difference between the JONSWAP and the PM spectrum as δ=JONSWAP/PM, one get the results in table 5.6. From this table, it can be seen that there are no large difference between the two spectrum, but one fatigue result is not present in the PM run. This member, element 720, had an impaired fatigue life of 1.00E+01 for the JONSWAP spectrum, thus just a slight increase will naturally make it disappear from the table. A closer investigation by increasing the threshold yields an impaired life for this member of 1.00E+01 for the PM spectrum as well, meaning that the difference is only a small numerical round of error.

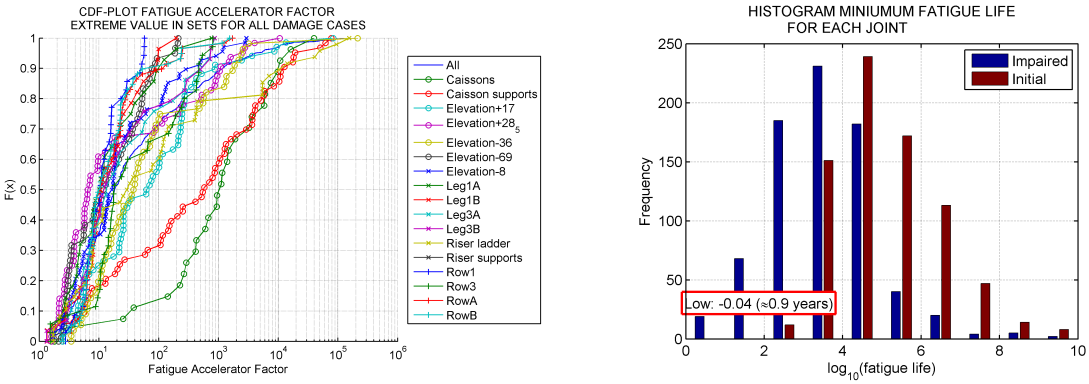

(a) FAF **(b)** Fatiuge life

Figure 5.30: Fatigue accelerator factor and minimum fatigue life for the 4L-jacket using PM-spectrum

MIMIMUM FATIGUE LIFE BELOW 10.0 YEARS

Joint	Member	Set	Damage (Set)	δInitial	δImpaired	δFAF
2025	2529	Elevation-36	3538 (Caisson supp)	100 %	100 %	95 %
2025	2535	Caisson supp	3538 (Caisson supp)	93 %	98 %	100 %
2026	920	Caissons	3538 (Caisson supp)	90 %	98 %	91 %
2036	720	Caissons	3526 (Caisson supp)	83 %	97 %	89 %
2046	745	Caissons	3536 (Caisson supp)	N/A	N/A	N/A
2065	2525	Elevation-36	3533 (Caisson supp)	86 %	100 %	88 %
2065	2532	Caisson supp	3533 (Caisson supp)	88 %	97 %	89 %
2066	845	Caissons	3533 (Caisson supp)	90 %	99 %	91 %
2075	2524	Elevation-36	3528 (Caisson supp)	93 %	100 %	95 %
2076	820	Caissons	3528 (Caisson supp)	88 %	98 %	90 %
2085	2523	Elevation-36	3529 (Caisson supp)	100 %	100 %	100 %
2085	2536	Caisson supp	3529 (Caisson supp)	100 %	100 %	102 %
2086	945	Caissons	3529 (Caisson supp)	92 %	99 %	93 %
3011	710	Caissons	3524 (Elevation-8)	97 %	100 %	92 %
3066	810	Caissons	3530 (Elevation-8)	100 %	97 %	105 %
3076	935	Caissons	3530 (Elevation-8)	121 %	96 %	129 %
3090	2045	Leg1A	3530 (Elevation-8)	96 %	97 %	100 %
4010	4526	Elevation+17	3526 (Caisson supp)	102 %	104 %	99 %
4020	4525	Elevation+17	3536 (Caisson supp)	126 %	104 %	114 %
4088	810	Caissons	3528 (Caisson supp)	120 %	104 %	113 %

Table 5.6: Comparison over damage cases and members with fatigue life less than 10 years for JONSWAP Vs PM spectrum, 4L-jacket

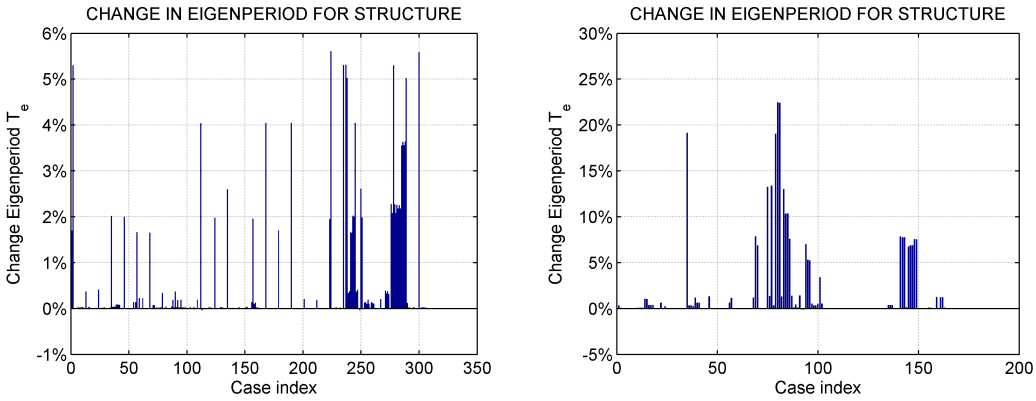

(a) 4L-jacket **(b)** 3L-jacket

Figure 5.31: Changes in natural period for the jackets due to damage

5.4 Eigenvalues

The validity of the assumption of little to no change in the natural period for the jackets is shown in figure 5.31. Note that the case index in these plots does not correspond the case index for the fatigue run. One particular reason for this is the lack of damage in support cases for the eigenvalue run. From the figures it can be seen that the 4L-jacket does not have large changes with its maximum value corresponding to an increase of about 6 %. The 3L-jacket on the other hand shows a significant increase for some cases, with a maximum increase of about 25 %. These cases are traced back to the top frame of the jacket, where there is only a single diagonal bracing.

An overview of which damage cases affect the 3L-jacket the most are given in table 5.7. From this table, one can see resemblance to table 5.5, where the lowest fatigue lives are listed. There is thus a correlation between the large increase in the natural period and low fatigue lives. This could be explained by an increase in dynamic response, but one also have to include local stress distribution into account.

To investigate how much the increase in the natural periods have to say on the response, the Dynamic Amplification Factor (DAF) for a single degree of freedom system (equation (C.1)) has been calculated. The results are shown in figure 5.32 with the calculated DAF normalized against the initial DAF for the intact structure. There is a rather large amplification for higher wave periods due to the increased natural period, and there is therefore reasonable to assume a significantly more dynamic response under impaired conditions. This because the wave energy starts to become significant for wave periods larger than 3 [s] when the wave breaking limit will allow for higher wave amplitudes. As an example, one may look

NATURAL PERIODS (>10%) 3L		
Damage scenario	**Value [s]**	**(Change)**
DAMAGE305561	3.14	(19.1%)
DAMAGE306562	2.98	(13.2%)
DAMAGE306561	2.99	(13.4%)
DAMAGE315562	3.14	(19.0%)
DAMAGE304561	3.23	(22.5%)
DAMAGE314561	3.23	(22.4%)
DAMAGE304451	2.98	(13.0%)
DAMAGE305451	2.91	(10.3%)
DAMAGE305452	2.91	(10.3%)

Table 5.7: Damage cases with an increase in natural period of more than 10 %

at the sea states shown in figure 5.33. The solid line is the natural frequency for the intact structure, and the dashed line is the lowest natural frequency (highest period) that occurs under impaired integrity.

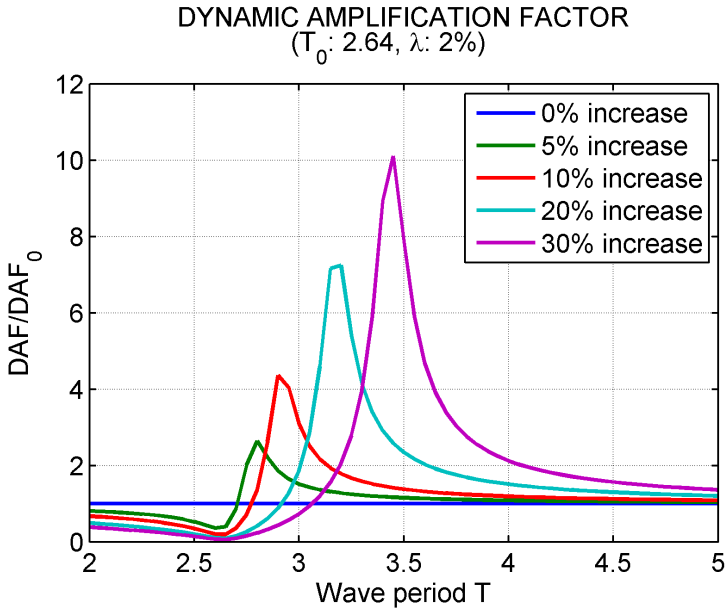

Figure 5.32: Dynamic amplification factor for different increases in natural period

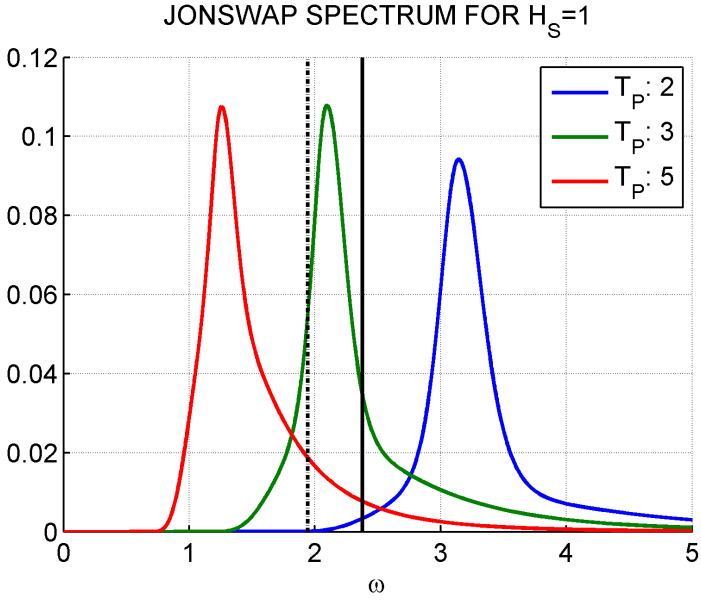

Figure 5.33: JONSWAP wave spectrum for $H_S = 1$ and $T_P = [2, 3, 5]$

Run-name	Direction
Run1	45

(a) 4L-jacket

Run-name	Direction
Run1	0
Run2	30
Run3	45
Run4	60

(c) 3L-jacket

Table 5.8: Connection between run-name in pushover analyses and wave direction applied

5.5 Pushover

The pushover analyses has been performed for several different wave directions. Because of the different fundamental construction of the jackets, the wave directions chosen in the analysis are not exactly the same. The connection between the run-name used for analysis results and the corresponding wave direction applied can be found in table 5.8.

Figures showing all the changes that occur for each respective wave direction can be found in appendix I. A summary of the damage cases which influence the RSR the most can be seen in tables 5.9 and 5.10. Also found in these tables is the calculated R_4 redundancy factor for the specific damage case. It is noted that the 4L-jacket once again proves itself to be more redundant than the 3L-jacket, due to the higher R_4 value. However, there is a lack of wave directions in the 4L-pushover analysis compared to the 3L-jacket. Thus, some care should be taken when comparing the results.

MIMIMUM PEAK LOAD FACTORS				
Case name	**RSR**	**(Change)**	**Run**	**R_4**
DAMAGE2473	3.590	(71.8%)	Run1	3.5
DAMAGE1141	3.937	(78.8%)	Run1	4.7
DAMAGE2472	3.480	(69.6%)	Run1	3.3

Table 5.9: Damage scenarios with the largest reduction in residual strength ratio (less than 80 % of initial), 4L-jacket

MIMIMUM PEAK LOAD FACTORS				
Case name	**RSR**	**(Change)**	**Run**	**R_4**
DAMAGE304561	1.121	(45.5%)	Run5	1.8
DAMAGE314561	1.128	(45.8%)	Run5	1.8
DAMAGE304451	1.043	(42.5%)	Run2	1.7
DAMAGE304461	1.295	(44.5%)	Run7	1.8

Table 5.10: Damage scenarios with the largest reduction in residual strength ratio (less than 50 % of initial), 3L-jacket

6

Concluding remarks

A review of different ways to both define and calculate redundancy has been described. Deterministic and probabilistic approaches has been assessed. The conclusion is that there are several various methods that exists in literature, and that they each behaves differently and can be used accordingly. Due to the random nature of the loads which an offshore structure is subjected to, a probabilistic method is preferred in most cases and in particular the First Order Reliability Method as it has proven to give a good approximation when estimating low probabilities.

Fatigue is an important mechanism when considering the structural integrity. When designing structures, there is not only the extreme environmental loads which must be accounted for, but also the frequently occurring fatigue damage loads. The fatigue life for a jacket structure can be calculated using different approaches. Selection of which method to use is mainly govern by the level of dynamic response for the structure as well as the level of non-linearities which may be relevant. These effects will be closely related to the natural period of the structure. However, non-linearities will be relevant for members close to the free surface for all type of jackets.

Large uncertainty are associated with fatigue life calculations. This is due to the fatigue life being very sensitive to the stress range levels which them self inherent uncertainties, but also due to large spread in empirical testing data which form the basis for SN-curves. Variable amplitude loading creates even more spread in the fatigue life, as the Miner damage will have large spread around unity at failure. Thus, calculated fatigue life ought to have a rather large safety factor depending on the severity should failure occur.

To investigate the effect of damage on the fatigue life for jacket structures, i.e. explore fatigue redundancy, a case study on two different designs has been performed. One case is a four-legged (4L) jacket, while the other is a three-legged (3L) jacket. Members has been removed in a systematic manner, similar as for an ALS redundancy check, prior to a fatigue life calculation using a stochastic fatigue approach. The changes in natural periods due to the impaired integrity has been investigated, and an insight in the ALS redundancy for the jackets has been done by performing a pushover analysis for roughly the same damage cases as in the fatigue analysis.

If there is a large increase in the natural period of the structure due to impaired integrity, one would expect that more external loads are taken up by the structure due to dynamic amplification. It has been noted that the highly redundant 4L-jacket have a slightly increase in the natural period, while the less redundant 3L-jacket have some damage cases which give a rather large increase. Thus, the reduction in fatigue life for these damage cases is expected to be larger than for the rest of the cases.

There is a cross correlation between natural periods and peak load factors. Damage cases with the lowest reserve strength ratio have also the largest increase in the natural period. Since dynamics has not been accounted for in the pushover analyses, this can be explained by relating large reduction in the structural strength to damage in members which form a large part of the structural stiffness.

For the 3L-jacket, there is also a correlation between the minimum peak load factors, largest eigenvalues and the most severe reduction in fatigue life. The large increase in the eigenvalue implies large changes in dynamic behaviour, thus larger stress ranges and hence less fatigue life is expected. However, fatigue life calculations are also sensitive towards local effects, thus for a dynamic analysis it is not easy to separate the local changes in stresses and the global changes in forces. Therefore, a small change in the dynamics for the structure could still have a significant stress redistribution locally, nearby the damage. The number of elements where forces may be redistributed to will affect the level of change in fatigue lives, thus expressing fatigue redundancy.

Large changes in fatigue life is expected for most of the damage cases. This due to the local changes in load path, but also because local changes in structural stiffness can alter the global load path slightly. A stochastic fatigue analysis will capture any changes in the dynamics, both locally and global, thus separating the static redistribution from increased dynamic response is difficult without performing a deterministic analysis.

The large spread in fatigue lives makes it more or less impossible to find a simple linear bias to explain the changes. There will be too much uncertainty involved in such a parameter, even when looking at the mean value for only negative changes. By separating the fatigue lives according to their position relative to the damaged member, more predictable results will be obtained, i.e. largest changes occur close to the damaged member. However, there is difficult to separate influenced members by the classification presented in this thesis. The radii of influenced members as a function of reduction in fatigue life will indeed be smaller for larger changes, but it is not given that the most influenced members are those most nearby to the damage. There is also the effect of appendices which may transfer loads through the structure in ways that are difficult to predict in advance.

The largest FAF is expected in the same set as the damage. However, for the 4L-jacket there is one particular damage case which caused the most critical results. This scenario was damage in the caisson supports. There is also a clear trend that one may expected a larger FAF if the structure is less redundant, as was the case with the 3L-jacket. Although, the most extreme FAF was found in the 4L-jacket. This case is tracked back to a caisson support, and the same case is also found amongst the lowest fatigue lives. However, no general conclusion can be given based on just a single comparison.

Other relevant findings regarding FAF was the confirmation that accelerated fatigue is mostly due to local stress redistribution. No or very little influence is found for members in sets far away from the damaged set. Also, there is a general trend that

the FAF is expected to be large. Values in the range of $10^1 - 10^5$ was not rare for the results in this thesis. However, there is a correlation between a large FAF and a large initial fatigue life. The correlation was stronger for the 3L-jacket than for the 4L-jacket, but due to the difference in the number of data sampling points no general conclusion could be made from this either. It should although be noted that large FAF does not generally mean low fatigue life under impaired integrity.

There is a clear trend that less redundancy leads to lower fatigue life, and this is closely related to increased dynamic response. For the 4L-jacket, the caisson supports represented most of the critical damage sets. These supports may be regarded as non-redundant due to only one support per horizontal elevation. A damage in the supports will therefore lead to an increased free span for the caisson, thus vastly changing dynamics. There is also the fact that the wave load resultant are acting close to the free surface. Hence, should the support at the close to the resultant be damaged, there will be a massive increase in the forces going to the two neighbouring supports.

For the 3L-jacket, the braces in the middle part of the top frame, where there is no deterministic redundancy within the bay, was representing all of the damage scenarios with fatigue life less than 10 years. The conductors on the 3L-jacket, which may be compared with the caissons on the 4L-jacket, are supported on more levels and also supported at the mud line. Thus, this could be the reason why the conductor support cases are not present in the most critical fatigue lives. But perhaps the most important reason is that the supports them self are not among the members in the fatigue check for the 3L-jacket, thus any local increase in the support-brace connection will not be captured. Therefore, some care must be taken when comparing the lowest fatigue life between the two jackets.

Trying to describe changes in fatigue life by looking at the structure as a whole and fitting a log-normal distribution will most likely not give adequate results. Quite a few of the fits in this thesis was not accepted in a χ^2 test, and there was a bad fit for the extreme values. The fits was however better suited for the 4L-jacket than the 3L-jacket, although the 3L-jacket had better fits in the critical area of the distribution.

The choice between a JONSWAP spectrum and a PM spectrum seems to be indifferent regarding fatigue analyses on jackets structures in the North Sea, when the natural period is slightly below 3 seconds. This was at least the case for the 4L-jacket, but once again there can not be drawn a general conclusion due to the lack of data.

To summarize, there has been proven very difficult to explain the changes in fatigue life for a jacket structure with impaired integrity without using a deterministic approach, i.e. calculate the fatigue life for the specific damage case. There are large changes occurring in the structure, and it is clearly a large influence from appendices e.g. the caisson supports. Fatigue life is very sensitive to stress ranges, and impaired integrity may lead to both local changes in dynamics as well as global, and there may also be a significant magnitude on the redistributed loads.

Large changes in fatigue life should thus not be surprising. A jacket structure may be highly redundant from an ALS perspective, i.e. it will survive extreme environmental loads when damaged and still have high residual strength, but the fatigue redundancy could be absent when looking at residual life. After all, it is the hot spot stress range that is governing fatigue damage, not the stress level during progressive collapse.

Any fatigue life in the damaged structure that is less than the inspection interval for the damaged member, would in a deterministic framework mean that a second member failure will occur should the damage case happen in the first place. Since there is fatigue lives which are below five years for some damage cases, and the FAF values are extremely high, it could be said that the structures under consideration have low fatigue redundancy despite for filling the ALS criteria (ULS wave actions when damaged). Although, a large FAF could be a result from a large initial fatigue life due to the weak correlation found in both jackets, and it is not given that large FAF will mean low residual fatigue life and vice versa. Also, the calculated fatigue life values are uncertain due to the linearisation performed.

There most important aspect of this conclusion, however, must be the consideration of the risk associated with the results. Even though the consequence may be high for a low fatigue life, an extremely low probability for this event occurring in the first place would lead to a low risk. It is after all the goal to follow the ALARP principle in such a way that a structure is considered to be safe for everyone affected by it.

7

Further work

Even though several results have been presented in this thesis, there is still a lot more work that could be done in order to get an increased understanding over the factors governing fatigue redundancy, and the associated risk of structural collapse due to fatigue. The following points reflects what the author feels has been left undone, and would be interesting to investigate further.

- Since it the radii of influenced members is reduced as the FAF is increased, i.e. there is a larger reduction in fatigue life for members close to the damaged element, another approach than classifying members according to structural location could be adapted. For instance, there may be more easy to isolate the large changes by looking at maximum changes for either a certain length radius, or by looking at a radius of a certain number of joints.
- A change in fatigue analysis method should be performed. A deterministic analysis will show what changes are due to alteration in the load path, and by comparing to the stochastic analysis one may see if dynamics are important. Using a Stoke's 5th order wave in the deterministic analysis will also capture non-linearities associated with members close to the free surface. A full time domain analysis has the ability of capture all the non-linearities that may be relevant for a jacket structure, thus should give the best results. This would be highly relevant to perform for at least some cases so the low fatigue lives calculated in this thesis could be closer investigated.
- There is still one very important aspect which has not been addressed in the result part of this thesis, namely the probability of failure. Putting the results obtained from this analysis into a probabilistic framework would give a better value regarding whether or not there exists large risk against accelerated fatigue failures, and also create a basis for determining inspection intervals or even design specifications. This probabilistic framework should also combine the risk of failure or structural collapse due to extreme environmental actions and accidental damage events.
- Closely related to the previous point is to address the effect of a second member failure due to the accelerated fatigue damage. This would involve pushover analyses, as well as fatigue analyses. Off course, there is also the probabilistic aspects to take into account, i.e. when looking deterministic at the fatigue life, one could continue with third member failure, fourth member failure etc.
- The caisson and caisson supports are not ideally modelled. The caisson supports are typically a T-stub which acts as a guide for the caisson. Usually, the caisson will be standing freely inside the support with a certain slack. This means that the caisson could vibrate freely, and every change in wave particle

direction would make the caisson slam into the support. This may lead to dynamical vibrations in the support creating several more stress cycles than what is captured when modelling the support-caisson connection as a tubular joint. Thus, studying fatigue life of caissons is at least a master thesis by itself. The modelling done in this thesis should however give adequate results, as it captures load transfer from the caisson to the jacket structure.

- As the fatigue life is very sensitive to the stress range, a closer investigation of how the stress concentration factors
- Investigating whether or not the ALS analysis could form a basis for calculating the FAF is a rather interesting hypothesis. By assuming that axial forces are governing the fatigue life, on could utilize the fact that the fatigue life is inverse proportional to the stress range in the third power and axial stresses are proportional to axial forces. Hence, by denoting the damaged quantities with an asterisk, the following property should hold:

$$\left(\frac{F^*}{F}\right)^3 \propto \frac{FL}{FL^*} \Rightarrow \text{FAF} = \left(\frac{F^*}{F}\right)^3$$

  where F is the axial force and FL is the Fatigue Life.
- Due to the rather large changes in the eigenvalues for the 3L-jacket, more effort should be put into the choice of wave frequencies to create the transfer function. There is also a possibility that the 4L-jacket will be responding to a different choice of step sizes even though the changes in the natural period was less than for the 3L-jacket. Hence, a sensitivity study should be performed to investigate the effect of step size for wave frequencies at or near the eigenvalue.
- Even though there exists lots of data just for these two jackets, and even more could be created by e.g. additional parameter studies, a similar fatigue life calculation should be performed on more jackets in order to investigate the effects of different designs and water depths.

8

Bibliography

[AKSO Internal, 2010] AKSO Internal (2010). Aker Solutions 4L Dynamic And Fatigue Anaysis Report. Internal Report.

[AKSO Internal, 2012] AKSO Internal (2012). Aker Solution 3L FLS Report. Internal Report.

[Berge, 2006] Berge, S. (2006). *Fatigue and Fracture Design of Marine Structures*, volume II. Department of Marine Technology, Trondheim.

[Bishop et al., 1996] Bishop, N. W. M., Feng, Q., Schofield, P., Kirkwood, M. G., and Turner, T. (1996). Spectral Fatigue Analysis of Shallow Water Jacket Platforms. *Journal of Offshore Mechanics and Arctic Engineering*, 118(3):190–197.

[DNV, 2010] DNV (2010). DNV-RP-C203 Fatigue Design of Offshore Steel Structures.

[DNV, 2011] DNV (2011). DNV-RP-H103 Modelling and Analysis of Marine Operations.

[Faltinsen, 1990] Faltinsen, O. M. (1990). *Sea Loads on Ships and Offshore Structures*. Cambridge University Press.

[Frangopol and Curley, 1987] Frangopol, D. M. and Curley, J. P. (1987). Effects of Damage and Redundancy on Structural Reliability. 113(7):1533–1549.

[Frangopol et al., 1992] Frangopol, D. M., Iizuka, M., and Yoshida, K. (1992). Redundancy Measures for Design and Evaluation of Structural Systems. *Journal of Offshore Mechanics and Arctic Engineering*, 114(4):285–290.

[Fu and Frangopol, 1990] Fu, G. and Frangopol, D. M. (1990). Balancing weight, system reliability and redundancy in a multiobjective optimization framework. *Structural Safety*, 7(2-4):165 – 175.

[Furuta et al., 1985] Furuta, H., Shinozuka, M., and Yao, J. (1985). Probabilistic and Fuzzy Representation of Redundancy in Structural Systems. *Presented at the July 1985 First International Fuzzy Systems Associated Congress held at Palma de Mallorca, Spain.*

[Haver, 2011] Haver, S. (2011). Prediction of Characteristic Response for Design Purposes (PRELIMINARY VERSION). Used as course litterature in TMR4195 Design of Offshore Structures, NTNU.

[Melchers, 1999] Melchers, R. E. (1999). *Structural Reliability Analysis and Prediction*. John Wiley & Sons.

[Myrhaug, 2007] Myrhaug, D. (2007). *Marin dynamikk (Marine Dynamics)*. Department of Marine Technology, Trondheim.

[NORSOK-N001, 2010] NORSOK-N001 (2010). N-001 Integrity of offshore structures.

[NORSOK-N003, 2007] NORSOK-N003 (2007). N-003 Action and action effects.

[NORSOK-N004, 2004] NORSOK-N004 (2004). N-004 Design of steel structures.

[NORSOK-N006, 2009] NORSOK-N006 (2009). N-006 Assessment of structural integrity for existing offshore load-bearing structures.

[Næss, 1985] Næss, A. A., editor (1985). *Fatigue Handbook*. Tapir.

[Pinna, 2009] Pinna, R. (2009). Fatigue Analysis of Offshore Structures. Lecture notes in CIVL4171, The University of Western Australia.

[RIFLEX, 2008] RIFLEX (2008). *RIFLEX Theory Manual*.

[Veritas, 1993] Veritas, D. N. (1993). *Framework Theory Manual*. DNV.

[Wikipedia, 2011] Wikipedia (2011). Rainflow-counting algorithm. `http://en.wikipedia.org/wiki/Rainflow-counting_algorithm`.

[Yoshida, 1990] Yoshida, K. (1990). Reliability And Redundancy Of Structural Systems. Master's thesis, University of Colorado.

Appendix

Appendix A

Wave Spectrum

A.1 Sea States

[1]The irregular sea state to be used in a time domain analysis can be described using a wave spectrum. Frequently used wave spectrum on the Norwegian continental shelf are the Pierson-Moskowitz (PM), JONSWAP and Torsethaugen. The sea state can be divided into three categories:

- *Wind sea:* A result from a local wind field
- *Swell sea:* Not caused by local wind field, but can be the result of a decaying wind sea
- *Combined sea:* A combination of swells, and wind generated waves.

One also have differ between a *fully developed wind sea* and a *growing wind sea.* The three spectrum above have different properties according to the previous mentioned definitions. A PM spectrum describes a fully developed wind sea, JONSWAP describes a growing wind sea and Torsethaugen is a combined growing wind sea. Whether or not to use a fully developed sea state assumption can be found by comparing the spectral peak period and significant wave height for the sea state. If these parameters are in the vicinity of the relationship given by equation (A.1), one may assume fully developed sea state.

$$T_P = 5\sqrt{H_S} \tag{A.1}$$

In order to fully describe the characteristics of a sea state, it may be necessary with several surface realizations using Monte Carlo simulation for the random phase angle in each sinusoidal wave component. Care must be taken when one choose the number of wave components subtracted from the spectrum. If one chooses, say, 100 wave components for $\omega \in [0, 3]$ the signal, i.e. the surface elevation, will repeat itself after $T = 2\pi/\Delta\omega \approx 200[s]$ [RIFLEX, 2008].

A.2 JONSWAP

The JONSWAP (Joint North Sea Wave Project) spectrum is a result of several registered wave heights in the south-eastern part of the North Sea in the period 1968-1969. The most common way of defining the spectrum is:

[1]This text is mainly based on [Haver, 2011]

$$S(f) = 0.3125 H_S^2 T_P \left(\frac{f}{f_P}\right)^{-5} \exp\left\{-1.25\left(\frac{f}{f_P}\right)^{-4}\right\} (1-0.287\ln\gamma)\gamma^{\exp\left\{-0.5\left(\frac{f-f_P}{f_P\sigma}\right)^2\right\}} \tag{A.2}$$

where $f_P = T_P^{-1}$, the spectral width parameter is given by

$$\sigma = \begin{array}{l} 0.07,\ f \leq f_P \\ 0.09,\ f > f_P \end{array} \tag{A.3}$$

and the peak enhancement factor can be found from

$$\gamma = 42.2\left(\frac{2\pi H_S}{g T_P^2}\right)^{\frac{6}{7}} \tag{A.4}$$

where $g = 9.81 m/s^2$ is the gravitational acceleration. However, the range of γ is between 1 and 7 [Myrhaug, 2007]. To simplify one may use an average value for γ of 3.3 [DNV, 2011].

A.3 Pierson-Moskowitz

The PM spectrum is based on data from the North-Atlantic during the 1950s, and was originally parametrized in terms of the average wind speed measured 19.5 [m] above sea level. However, later it has been expressed in terms of H_s and T_p. The spectrum is given by

$$S(f) = 0.3125 H_S^2 T_P^{-4} f^{-5} \exp\left\{-1.25\left(T_p f\right)^{-4}\right\} \tag{A.5}$$

The PM spectrum has the same total energy for a given sea state as the JONSWAP spectrum, but the energy is more spread along all wave frequencies for the PM spectrum as appose to JONSWAPs concentration of energy around the peak period [Myrhaug, 2007].

Appendix B

Limit States

When designing an offshore structure it is important to ensure that the structure, or its elements, does not encounter a failure mode, i.e. ensure the structure will fulfil its design specifications. These failure modes are denoted by Limit States, and can be divided into different groups, e.g. serviceability criteria and ultimate capacity criteria.

B.1 The Four Limit States

In the NORSOK standards four different notations are used to define the failure modes. These are the Serviceability Limit State (SLS), Ultimate Limit State (ULS), Accidental damage Limit State (ALS) and Fatigue Limit State (FLS). A brief introduction to the different states are given in the following.

B.1.1 SLS

This limit state is meant to make sure the structure fulfils the functional requirements adequately, e.g. the structural deformations should not garble the functionality and accelerations should stay inside the comfort zone for the crew on board. Load levels typically correspond to expected maximum monthly or annual value.

B.1.2 ULS

The ultimate limit state is important regarding structural safety. This control shall ensure that the structure can withstand the foreseen loads with a sufficient safety margin. The load levels typically correspond to an annual exceedance probability of 10^{-2}. The ULS check is divided into two scenarios:

Case a: Permanent and variable actions are governing

Case b: Environmental loads are governing.

B.1.3 FLS

Fatigue limit state is also important regarding structural safety as it shall ensure that the integrity of the structure remains intact during the lifetime of the structure, i.e. ensure adequate fatigue life.

Appropriate safety factors to be used for fatigue life is found in NORSOK N-001. When classifying accessibility for inspection, welds in joints below 150 m water depth are assumed inaccessible. The design factors are shown in table B.1.

Classification of structural components based on damage consequence	Access for inspection and repair		
	No access or in the splash zone	Accessible	
		Below splash zone	Above splash zone
Substantial consequences	10	3	2
Without substantial consequences	3	2	1

"Substantial consequences" in this context means that failure of the joint will entail
danger of loss of human life;
significant pollution;
major financial consequences.

Table B.1: Design factors to be used in fatigue analysis, [NORSOK-N001, 2010]

B.1.4 ALS

The accidental damage limit state is intended to ensure that an accidental scenario does not lead to total collapse of a structure. The scenarios include fires, explosions and collisions, but also extremely rare environmental actions should be included as given by Norwegian rules and regulations. Characteristic load levels in ALS correspond to an annual exceedance probability of 10^{-4}. ALS check should be performed in two levels: After the structure has been subjected to the loads of an 10^{-4} event, it should still survive environmental actions corresponding to ULS levels.

B.2 Actions and Action Effects

All forces acting on the structure shall be taken into account when performing ULS, ALS or FLS check. These forces can be divided into four subsections: permanent, variable, environmental and deformation actions. The limit states are normally controlled by the following equation:

$$\gamma_p x_p + \gamma_v x_v + \gamma_e x_e \leq \frac{y_c}{\gamma_m} \tag{B.1}$$

where x_i are the loads, γ_i are the partial action factor, y_c is the characteristic load capacity and the subscripts p, v, e, m stand for permanent, variable, environmental and material, respectively. The partial action factors to be used according to NORSOK is given in table B.2.

Limit state	Action combinations	Permanent actions (G)	Variable actions (Q)	Environmental actions (E) [d]	Deformation actions (D)[e]
ULS	a[a]	1,3	1,3	0,7	1,0
ULS	b	1,0	1,0	1,3	1,0
SLS		1,0	1,0	1,0	1,0
ALS	Abnormal effect[b]	1,0	1,0	1,0	1,0
ALS	Damaged condition[c]	1,0	1,0	1,0	1,0
FLS		1,0	1,0	1,0	1,0

[a] For permanent actions and/or variable actions, an action factor of 1,0 shall be used where this gives the most unfavourable action effect
[b] Actions with annual probability of exceedance = 10^{-4}
[c] Environmental actions with annual probability of exceedance = 10^{-2}
[d] Earthquake shall be handled as environmental action within the limit state design for ULS and ALS (abnormal effect)
[e] Applicable for concrete structures

Table B.2: Partial action factors for the limit states, [NORSOK-N001, 2010]

The different types of loadings can shortly be classified accordingly to the following. More details are given in NORSOK N-003. .

- Permanent
  Actions that does not change in magnitude, e.g. structural weight, permanent ballast, equipment weight, pretension etc.
- Variable
  Actions that changes due to operation of the structure, e.g. people, stored goods, helicopter, fendering, mooring etc.
- Environmental
  Actions induced by environmental processes, e.g. earthquake, wind, waves, current, ice etc.
- Deformation
  Actions caused by structural deformation, e.g. temperature expansion, mismatches during fabrication etc.

When performing an ALS or ULS check one does not combine all the environmental actions corresponding to a return period of 10 000 years or 100 years, respectively. This would be an extremely conservative assumption, and thus in table B.3 the different combinations one should use according to NORSOK N-003 are given.

A short summary describing how the different actions shall be applied in the different limit states are given in table B.4.

Limit state	Wind	Waves	Current	Ice	Snow	Earthquake	Sea level [a]
Ultimate Limit State	10^{-2}	10^{-2}	10^{-1}	-	-	-	10^{-2}
	10^{-1}	10^{-1}	10^{-2}	-	-	-	10^{-2}
	10^{-1}	10^{-1}	10^{-1}	10^{-2}	-	-	m
	-	-	-	-	10^{-2}	-	m
	-	-	-	-	-	10^{-2}	m
Accidental Limit State	10^{-4}	10^{-2}	10^{-1}	-	-	-	m*
	10^{-2}	10^{-4}	10^{-1}	-	-	-	m*
	10^{-1}	10^{-1}	10^{-4}	-	-	-	m*
	-	-	-	10^{-4}	-	-	m
	-	-	-	-	-	10^{-4}	m

[a] m - mean water level
m* - mean water level, including the effect of possible storm surge
Seismic response analysis should be carried out for the most critical water level.

Table B.3: Combination of environmental actions for the ULS and ALS, [NORSOK-N003, 2007]

	TEMPORARY CONDITIONS					NORMAL OPERATIONS				
	Serviceability limit state	Fatigue limit state	Ultimate limit state	Accidental limit state: Abnormal effect	Accidental limit state: Damaged conditions	Serviceability limit state	Fatigue limit state	Ultimate limit state	Accidental limit state: Abnormal effect	Accidental limit state: Damaged condition
Permanent actions	EXPECTED VALUE									
Variable functional actions	SPECIFIED VALUE									
Environmental actions	Dependant on operational requirements	Expected action history	Value dependent on measures taken			Dependent on operational requirements	Expected action history	Annual probability of exceedance = 10^{-2}	Annual probability of exceedance = 10^{-4}	Annual probability of exceedance = 10^{-2}
Deformation actions	EXPECTED EXTREME VALUE									
Accidental actions	Not applicable			Dependent on measures taken		Not applicable			Annual probability of exceedance = 10^{-4}	Not applicable

Table B.4: Characteristic actions and action combinations, [NORSOK-N003, 2007]

B.2.1 Hydrodynamic Actions

The hydrodynamic loading on slender members, i.e. wave length to diameter ratio greater than 5, can be found by Morrison's equation (B.2).

$$dF = \rho \frac{\pi D^2}{4} C_M a_x dz + \frac{1}{2} \rho C_D D (u - \dot{r}) |u - \dot{r}| dz \tag{B.2}$$

where dF is the force on a strip dz, ρ is the density of the fluid, D is the diameter of the cylinder, C_M is the mass coefficient, a_x is the horizontal water particle acceleration, C_D is the drag coefficient, u is the horizontal wave particle speed and $\dot{r}$ is the time derivative of the response, i.e. the response velocity.

In NORSOK N-003 one find appropriate values for the drag coefficient C_D and mass coefficient C_M, depending on the Keulegan-Carpenter number ($KC = U \cdot T/D$) and relative roughness. Members 2 [m] above the mean water level may be considered smooth during operation stage, while all members are smooth at the installation stage. For surface piercing framed structures like jackets, a Stokes 5th order wave could be applied when performing an extreme action static analysis in order to capture correct wave kinematics up to the free surface. However, a kinematics factor should be introduced on the wave particle velocity to account for wave spreading and irregularities in real sea states. For the North Sea conditions, this factor is 0.95.

In extreme sea states one usually have KC>30 and values to be used for drag and mass coefficients are found in table B.5a. In more moderate sea state which are relevant for fatigue analysis, flow conditions may reach KC<30 and values are then given in table B.5b.

If the structure to be analysed is expected to have large dynamics, then the action effects should be assessed by means of time domain simulation. The surface elevation process should then be modelled with second order wave kinematics. One may also approximate the second order surface by a Fourier series, and for each component use Wheeler stretching to obtain the kinematics.

The sea surface may be modelled by a Gaussian process, but then one needs to compensate for non-conservatisms by calibrating the hydrodynamic coefficients. If extremes are under considerations one should make sure a reasonable load level is obtained for the largest waves, while for fatigue a reasonable load level for the most important fatigue accumulating waves. As a first approach one may use C_D equal to 1.15 and C_M from table B.5a, A Gaussian sea surface is normally sufficiently accurate for fatigue analysis.

KC>30		
	Smooth	Rough
C_D	0.65	1.05
C_M	1.60	1.20

(a)

KC<30		
	Smooth	Rough
C_D	0.65	0.80
C_M	2.00	2.00

(b)

Table B.5: Drag and mass coefficients for slender tubular members

Appendix C

Jacket Analysis

A jacket structure is a framed structure commonly used in offshore applications, and its consists mainly of tubular members. It members are of a slender nature, and thus it will be a drag dominated structure. Usually, a jacket is a stiff structure and very often it may be assumed to behave quasi-static, i.e. one may neglect the mass and damping term in the equation of motion and is only left with the static relationship $F = kx$. As a general rule, if the largest natural period is less than 2 [s], then the structure can be regarded as quasi-static. Dynamics will not be important when calculating extreme response, but can if necessary be included with a DAF [Haver, 2011].

C.1 Static and Dynamic

C.1.1 DAF

For a single degree of freedom system, the DAF is given by equation (C.1).

$$DAF = \frac{1}{\sqrt{\left[1 - \left(\frac{T_n}{T}\right)^2\right]^2 + \left[2\lambda\frac{T_n}{T}\right]^2}} \tag{C.1}$$

where T_n/T is the ratio between the natural period and the excitation period, and λ is the damping ratio between system damping and critical damping. This equation is likely to overestimate the effect of dynamics when used in connection with extreme waves. If a significant dynamic amplification factor is obtained, say DAF >1.1, then time domain simulations utilizing realistic irregular storm wave histories as input should be used in order to investigate the effects of dynamic.

Lately there has been developed a more sophisticated that has proven to be adequate. The procedure is as follows:

- Find the worst sea state along the contour line
- Simulate, say, 30 3-hour realizations of this sea state using different random seeds
- Perform a quasi-static and a dynamic analysis for the simulated sea states
- Find maximum response value in each sea state
- Assume the largest 3-hour value follow a Gumbel distribution, and fit the observed maxima to this type of distribution
- Find which q-probability the design wave approach values are equal to the Gumbel fitted quasi-static response, X_{stat}

- Use this q-probability to find the dynamic response from the Gumbel model for dynamics, X_{dyn}
- The *equivalent* DAF can then be found as $EDAF = X_{dyn}/X_{stat}$
- Applying this EDAF on the design wave approach, dynamics will be accounted for

One should notice that the EDAF is a generalized dynamic amplification factor, and does not necessarily represent the amplification for a random wave event.

C.1.2 Non-linear Response

One important dynamic effect which is relevant for fatigue calculations is a sum-frequency phenomena known as springing. This is a steady-state response which jacket structures could encounter if their natural period is within 2-6 [s]. The effect will in principle be captured if the structure is analysed in time-domain.

For drag dominated structures, the non-linearities associated with the drag term in the Morrison equation have an important effect; The loading does not follow the regularities associated with the surface elevation. This is illustrated in figure C.1a. The force function can be approximated by a Fourier series, and the result using six components is shown in figure C.1b.

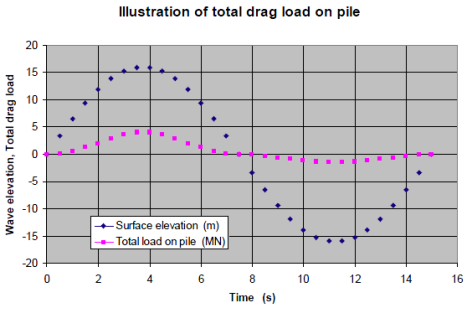

(a) Time history of drag load on a pile and the corresponding surface elevation

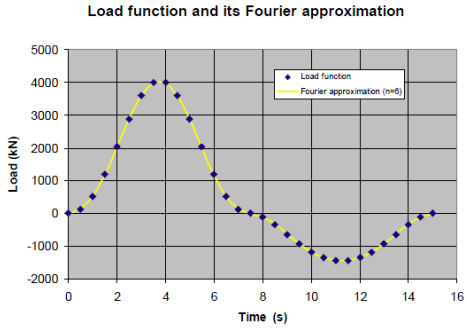

(b) Foruier approximation of the drag load

Figure C.1: Illustration of drag load on pile, [Haver, 2011]

If one inspect the various Fourier components for the load approximation, one will notice that there is a significant energy, i.e. load force, for the ω, 2ω and 3ω component, see figure C.2. Thus, even if the wave period is far away from the natural period there can still be a very large response, i.e. resonance due to one of the loading frequencies will hit the natural period of the structure. This type of loading is known as *super harmonic loading*.

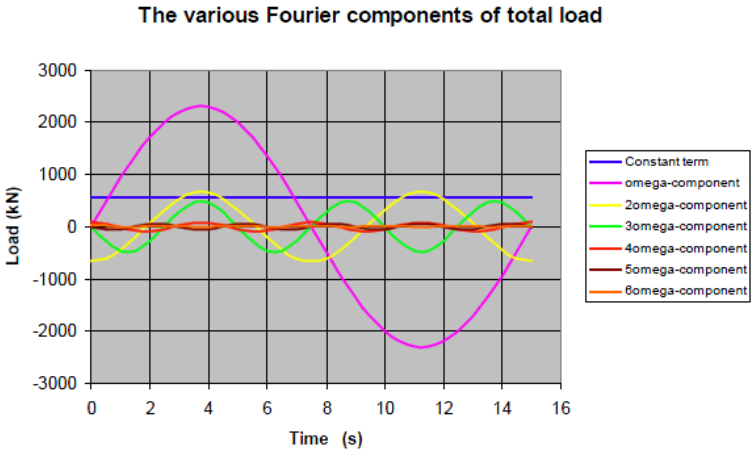

Figure C.2: Various Fourier components for the drag load in figure C.1b, [Haver, 2011]

Also, it could be worth mentioning the relative importance of the current for drag dominated structures. For a rather extreme wave, the horizontal particle speed could be taken as, say, 8 [m/s] while the an extreme current could be taken as typically 1.4 [m/s]. Now, it does not seem like the current will have a large impact on the drag load relative to the wave particle speed, but by remembering that the drag load is proportional to the velocities squared, one see that the cross term, i.e. wave velocity multiplied by current velocity, has a large contribution: $(u_w + u_c)^2 = 8^2 + 2 \cdot 8 \cdot 1.4 + 1.4^2 = 64 + 22.4 + 1.96$.

Appendix D

Batch Script

This chapter describes the batch analysis run which the author created in order to run the several hundred analyses without hundreds of working hours doing the same manually.

D.1 Cygwin

To run several hundred analyses without creating several hundred input files and running them manually, a Cygwin script was written for running the fatigue analyses. Since damage was simulated by changing the E-modulus, only one subroutine needed to be implemented when creating the model. Thus no large changes was required for the input files.

The SESAM program sequence used to calculate fatigue life, *PREFRAME* $\rightarrow$ *PRESEL* $\rightarrow$ (*WAJAC*) $\rightarrow$ *SESTRA* $\rightarrow$ *FRAMEWORK*, are controlled through *MANAGER*. The Cygwin script generates a folder structure, input files for PREFRAME and MANAGER and a Windows batch file in order to run all the analyses in parallel, thus utilizing all available processor cores. The input consists of files for the SESAM programs, e.g. journal files (*.jnl) and input files (*.inp), a loopdata.inp file containing the cases and template files for MANAGER and PREFRAME. The script and the batch run set-up is not universal, and must be modified for every jacket to be analysed. A post-processing of the results from FRAMEWORK is done with MATLAB.

The batch run itself is summarised and visualised in figure D.1. The Cygwin script generates input files for MANAGER and PREFRAME, which are unique for each run. MANAGER acts as a master program which calls on the sub-programs and associates the correct input-file(s) to the programs. There are two *.bat files: One that creates the initial result for the undamaged structure, and one which runs all the impaired scenarios. Since the wave loads for the impaired cases are identical to the initial wave load, WAJAC is only run once. The L*.fem files containing wave loads is therefore copied into the run folder for each damaged case. The final fatigue result files are copied to their respective result folders, where MATLAB can read and process the results. MATLAB must be run manually after all analyses are done.

Figure D.1: Batch program execution flow chart

Appendix E

MATLAB script

MATLAB is listed as a post-processor in chapter D. The scripts written for this has not been optimized, and the basic principle has been to investigate the data, not writing a proper post-processing script. Thus, there is a lot of redundancy in the script that can be avoided if only the relevant parts of the scripts are put together to a complete package. Since this was not the purpose of this master thesis, i.e. create a post-processing program, none of the scripts are given in the appendices, but a simple flowchart and a description of the files will be given in the following.

E.1 SESAM Post

The flowchart for the post-processing is shown in figure E.1. First, the script needs input in form of whether or not it should start from the beginning, or use the previous read data. It is also possible to skip most of the plot creating subroutines as these can be very time consuming when having lots of data. Then, the script reads in data from the fatigue life analyses (if it should start from scratch). The loop data file used in the batch run is needed in order to find and sort the results to the correct damage case. There is a possibility to remove some values from the *.LIS files should there be data of no interest in the files. The sets in which the members belong to are defined in ASCII files, created by the user in advance, and the script separates the data accordingly. Then, plots showing the change in fatigue life is made. Further, the script starts to process the result according to damage case, so that each damage case gets its own plot, e.g. XY-plot. Then, the GeniE java script files are made. These files will create the sets with members whose reduction in fatigue life is less than a given threshold, ref. figure 5.21. After this, the script calculates fatigue accelerator factors according to the sets which members belong to and the location of the damage. Then, minimum fatigue life for each joint is found. Finally, the script takes input from the user to define what is a parallel set and what is an adjacent set. From the input file elem_node_connection.dat, the script automatically finds the adjacent members to the damaged element. All variables are saved in a binary MATLAB file, so that should one want to modify only a part of the script or add a small part, it is not necessary to start all over again. There is also a logfile.m script running in the background that creates a log, where relevant data is written out, e.g. what sets are defined as parallel.

E.1.1 Adjacent and Parallel sets

In the following, the log files from the MATLAB run is shown. Here, it can be seen what sets that has been chosen as adjacent etc. to create the results presented in this thesis.

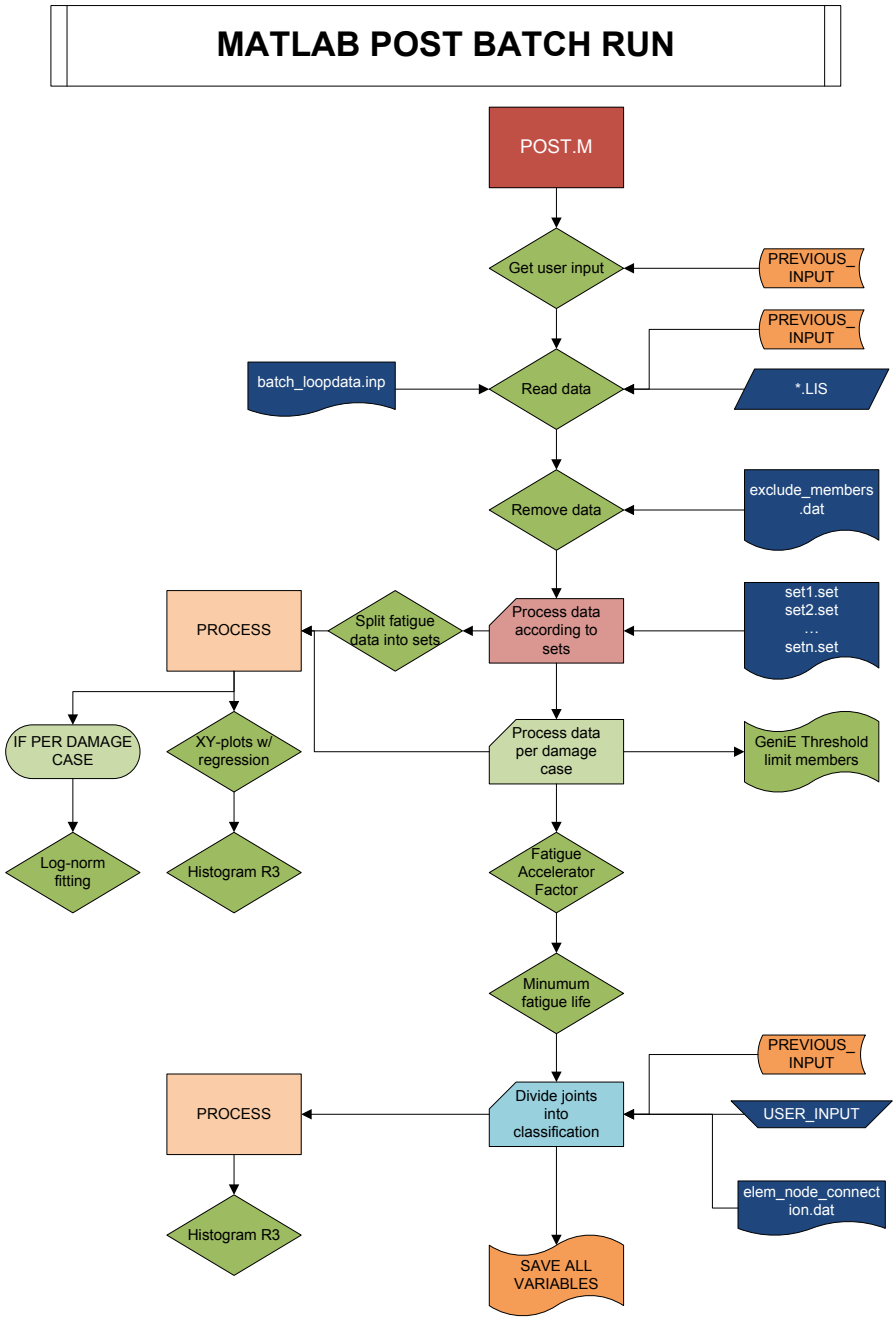

Figure E.1: MATLAB post processing flow chart

4L-jacket:

```
################################################
Log started 01-Jun-2012 at 19:55:28

 ___________________________________________________________
|          POST LIS FILES: A Post-Processing Script         |
|              for Fatigue Damage Calculated By             |
|                     SESAM - FRAMEWORK                     |
|-----------------------------------------------------------|
| Written by: Arve Flesche                                  |
| Date      : 01.06.2012                                    |
| Version   : 0.4.5                                         |
|                                                           |
|           AKER SOLUTIONS MMO AS C&T BERGEN                |
|___________________________________________________________|


[19:55:31]   Starting from scratch...
[19:55:33]   Will create Plots!
[19:55:42]   Reading input...
[19:55:42]   Loopdata instances sucessfully read...
[19:55:42]   Initial Fatigue Life sucessfully found...
[19:55:52]   Damaged case *.LIS files sucessfully found...
[19:55:52]   Initial Fatigue Life sucessfully read...
[19:57:59]   Damaged Fatigue Life sucessfully read...
[19:58:42]   Defining connections between sets with damage, and adjacent, parallel etc. sets...
[19:58:42]   Available sets:
#1:  Caissons
#2:  Caisson supports
#3:  Elevation+17
#4:  Elevation+28_5
#5:  Elevation-36
#6:  Elevation-69
#7:  Elevation-8
#8:  Leg1A
#9:  Leg1B
#10: Leg3A
#11: Leg3B
#12: Riser ladder
#13: Riser supports
#14: Row1
#15: Row3
#16: RowA
#17: RowB
[19:58:44]   ¤PARALLEL SETS¤
[19:58:45]   Using old input:
10 11 15 0  0  0  0  0
4  5  6  7  0  0  0  0
3  5  6  7  0  0  0  0
3  4  6  7  0  0  0  0
3  4  5  7  0  0  0  0
3  4  5  6  0  0  0  0
8  9  10 11 14 15 16 17
8  9  10 11 14 15 16 17
10 11 12 13 15 0  0  0
1  2  8  9  14 0  0  0
17 0  0  0  0  0  0  0
19 0  0  0  0  0  0  0
[19:58:46]   ¤ADJACENT SETS¤
[19:58:47]   Using old input:
1  8  9  14 0  0  0  0  0
1  2  12 0  0  0  0  0  0
1  2  12 0  0  0  0  0  0
1  2  12 0  0  0  0  0  0
12 0  0  0  0  0  0  0  0
1  2  12 0  0  0  0  0  0
3  4  5  6  7  13 0  0  0
12 0  0  0  0  0  0  0  0
3  4  5  6  7  8  9  16 17
3  4  5  6  7  10 11 16 17
3  4  5  6  7  8  10 14 15
3  4  5  6  7  9  11 14 15
[19:58:47]   ¤REMAINING SETS¤
Damage set: Caisson suppor has remaining sets: 3  4  5  6  7  12 13 16 17
Damage set: Elevation+17 has remaining sets:   8  9  10 11 13 14 15 16 17
Damage set: Elevation+28_5 has remaining sets: 8  9  10 11 13 14 15 16 17
Damage set: Elevation-36 has remaining sets:   8  9  10 11 13 14 15 16 17
Damage set: Elevation-69 has remaining sets:   1  2  8  9  10 11 13 14 15 16 17
Damage set: Elevation-8 has remaining sets:    8  9  10 11 13 14 15 16 17
Damage set: Riser ladder has remaining sets:   1  2
```

```
80  Damage set: Riser supports has remaining sets: 1  2  3  4  5  6  7
81  Damage set: Row1 has remaining sets:           1  2
82  Damage set: Row3 has remaining sets:           12 13
83  Damage set: RowA has remaining sets:           1  2  9  11 12 13
84  Damage set: RowB has remaining sets:           1  2  8  10 12 13
```

3L-jacket:

```
################################################
Log started 03-Jun-2012 at 17:01:13

 ------------------------------------------------------------
|          POST LIS FILES: A Post-Processing Script          |
|              for Fatigue Damage Calculated By              |
|                     SESAM - FRAMEWORK                      |
|------------------------------------------------------------|
| Written by: Arve Flesche                                   |
| Date      : 01.06.2012                                     |
| Version   : 0.4.5                                          |
|                                                            |
|           AKER SOLUTIONS MMO AS C&T BERGEN                 |
|____________________________________________________________|

[17:01:15]   Starting from scratch...
[17:01:18]   Will create Plots!
[17:01:23]   Reading input...
[17:01:23]   Loopdata instances sucessfully read...
[17:01:23]   Initial Fatigue Life sucessfully found...
[17:01:26]   Damaged case *.LIS files sucessfully found...
[17:01:27]   Initial Fatigue Life sucessfully read...
[17:01:55]   Damaged Fatigue Life sucessfully read...
[17:39:32]   Defining connections between sets with damage, and adjacent, parallel etc. sets...
[17:39:32]   Available sets:
#1:  BF A
#2:  BF A1
#3:  BF A4
#4:  Bracing BF A
#5:  Bracing BF A1
#6:  Bracing BF A4
#7:  Bracing TF B1
#8:  Bracing TF B2
#9:  Bracing TF B3
#10: CaissonSupports
#11: ConductorSupports
#12: Elev+20_9
#13: Elev+6_9
#14: Elev-24_1
#15: Elev-39_6
#16: Elev-54_6_5
#17: Elev-64_9
#18: Elev-8_6
#19: JTubeSupports
#20: LegA
#21: LegA1
#22: LegA4
[17:39:34]   ¤PARALLEL SETS¤
[17:39:34]   Using old input:
0  0  0  0  0  0
0  0  0  0  0  0
0  0  0  0  0  0
20 0  0  0  0  0
22 0  0  0  0  0
21 0  0  0  0  0
20 0  0  0  0  0
0  0  0  0  0  0
13 14 15 16 17 18
12 14 15 16 17 18
12 13 15 16 17 18
12 13 14 16 17 18
12 13 14 15 17 18
12 13 14 15 16 18
12 13 14 15 16 17
0  0  0  0  0  0
[17:39:57]   ¤ADJACENT SETS¤
[17:39:58]   Using old input:
1  2  3  5  6  16 17 0  0  0  0  0  0
1  2  3  4  6  16 17 0  0  0  0  0  0
1  2  3  4  5  16 17 0  0  0  0  0  0
2  3  8  9  10 12 13 14 15 18 19 21 22
1  2  7  9  11 12 13 14 15 18 20 21 0
1  3  7  8  11 12 13 14 15 18 19 20 22
7  12 13 14 15 18 0  0  0  0  0  0  0
8  9  12 13 14 15 18 0  0  0  0  0  0
7  8  9  10 19 20 22 0  0  0  0  0  0
7  8  9  10 11 19 20 22 0  0  0  0  0
7  8  9  10 11 20 22 0  0  0  0  0  0
```

```
7  8  9  10 11 19 20 22 0  0  0  0  0
1  2  3  4  5  6  11 19 0  0  0  0  0
1  2  3  4  5  6  19 0  0  0  0  0  0
7  8  9  10 11 19 20 22 0  0  0  0  0
3  7  9  12 13 15 16 17 18 22 0  0  0
[17:39:58]   ¤REMAINING SETS¤
Damage set: Bracing BF A has remaining sets:  7  8  9  10 11 12 13 14 15 18 19 20 21 22
Damage set: Bracing BF A1 has remaining sets: 7  8  9  10 11 12 13 14 15 18 19 20 21 22
Damage set: Bracing BF A4 has remaining sets: 7  8  9  10 11 12 13 14 15 18 19 20 21 22
Damage set: Bracing TF B1 has remaining sets: 1  4  5  6  11 16 17
Damage set: Bracing TF B2 has remaining sets: 3  4  5  6  10 16 17 19
Damage set: Bracing TF B3 has remaining sets: 2  4  5  6  10 16 17
Damage set: CaissonSuppor has remaining sets: 1  2  3  4  5  6  8  9  11 16 17 19 21 22
Damage set: ConductorSupp has remaining sets: 1  2  3  4  5  6  7  10 16 17 19 20 21 22
Damage set: Elev+20_9 has remaining sets:     1  2  3  4  5  6  11 21
Damage set: Elev+6_9 has remaining sets:      1  2  3  4  5  6  21
Damage set: Elev-24_1 has remaining sets:     1  2  3  4  5  6  19 21
Damage set: Elev-39_6 has remaining sets:     1  2  3  4  5  6  21
Damage set: Elev-54_6_5 has remaining sets:   7  8  9  10 20 21 22
Damage set: Elev-64_9 has remaining sets:     7  8  9  10 11 20 21 22
Damage set: Elev-8_6 has remaining sets:      1  2  3  4  5  6  21
Damage set: JTubeSupports has remaining sets: 1  2  4  5  6  8  10 11 14 20 21
```

Appendix F

Fatigue Life XY Plots and Histogram

This chapter shows the changes in fatigue life presented as a XY-plot and a histogram. The histogram shows the "fatigue" redundancy factor R_3. The plots that are presented shows the fatigue life for all members in a set, and each figure contains data points from all damage cases i.e. each blue dot in the XY-plot is a brace-chord connection and is either the brace side or the chord side (two dots in total per joint). In the XY-plots, there are two red lines showing the 50 [%] change limits according to initial fatigue life, as well as a linear regression line for all data points. The histograms is simply the data in the XY-plot presented in a different manner, and is only for R_3 values in the range [0-2].

F.1 4L

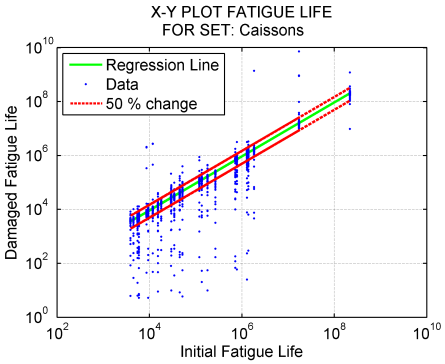

(a) XY Plot for set Caissons

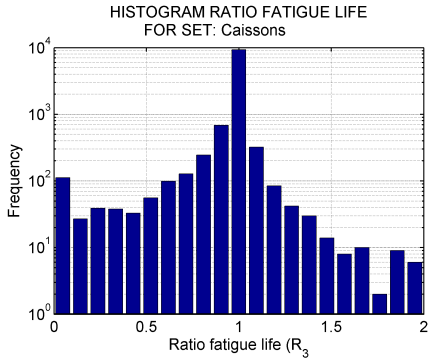

(b) Histogram for set Caissons

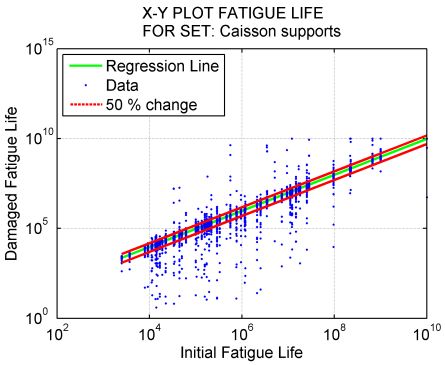

(c) XY Plot for set Caissonsupports

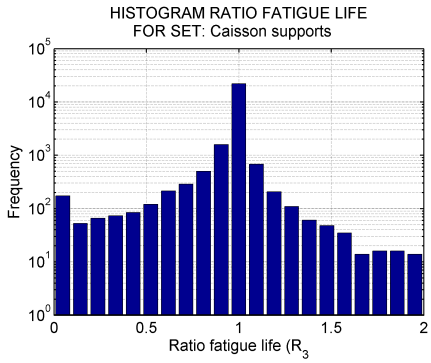

(d) Histogram for set Caissonsupports

Figure F.1: Fatigue life changes in XY-plots and histograms

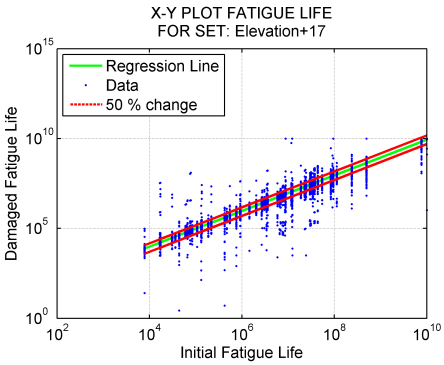

(a) XY Plot for set Elevation+17

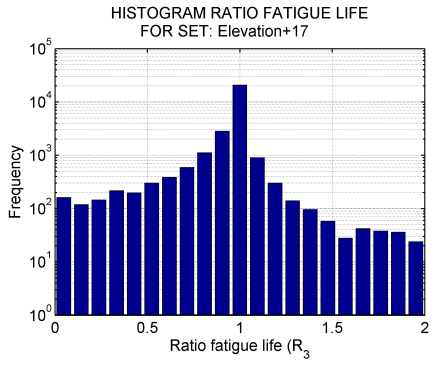

(b) Histogram for set Elevation+17

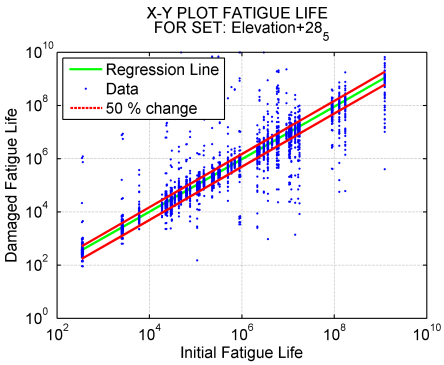

(c) XY Plot for set Elevation+28.5

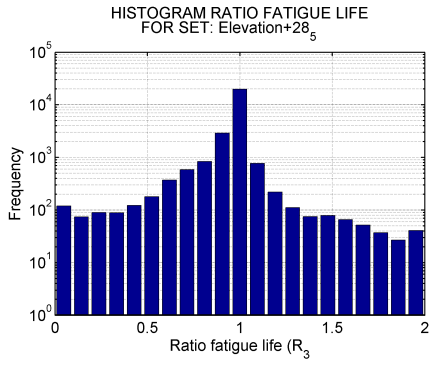

(d) Histogram for set Elevation+28.5

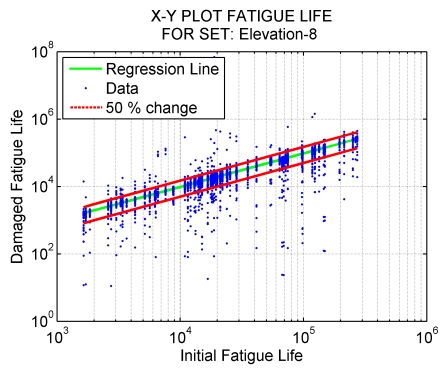

(e) XY Plot for set Elevation-8

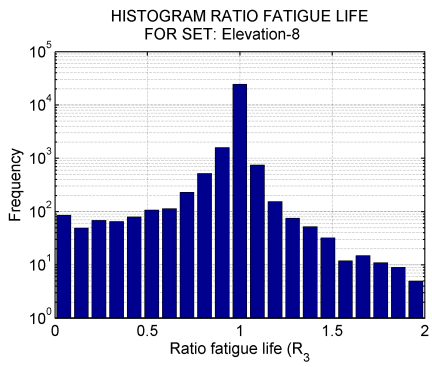

(f) Histogram for set Elevation-8

Figure F.2: Fatigue life changes in XY-plots and histograms

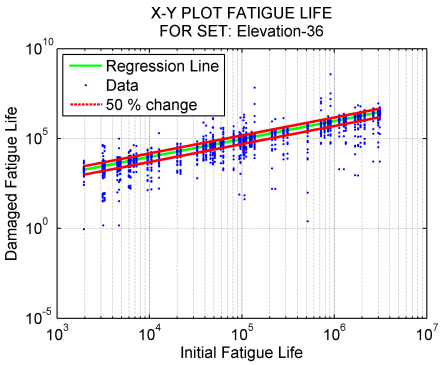

(a) XY Plot for set Elevation-36

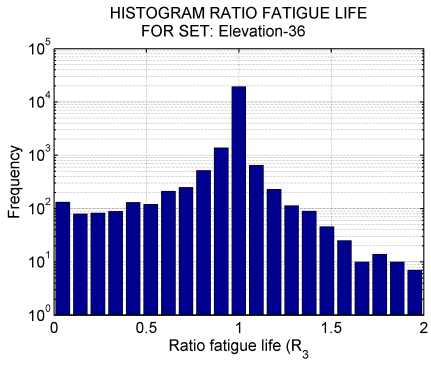

(b) Histogram for set Elevation-36

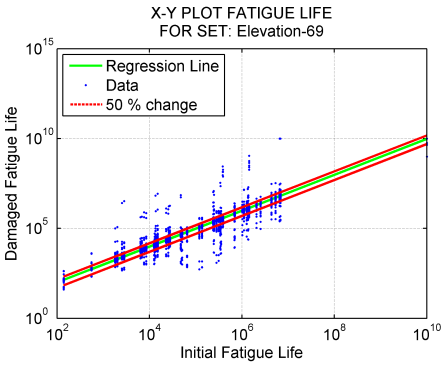

(c) XY Plot for set Elevation-69

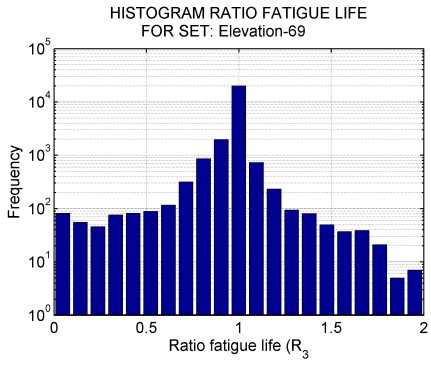

(d) Histogram for set Elevation-69

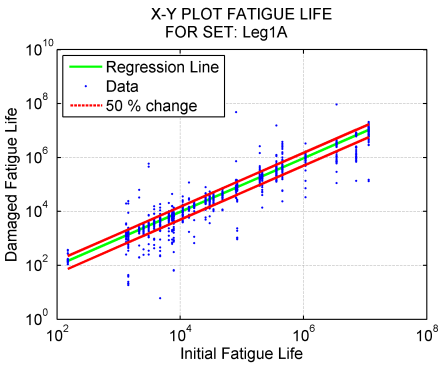

(e) XY Plot for set Leg1A

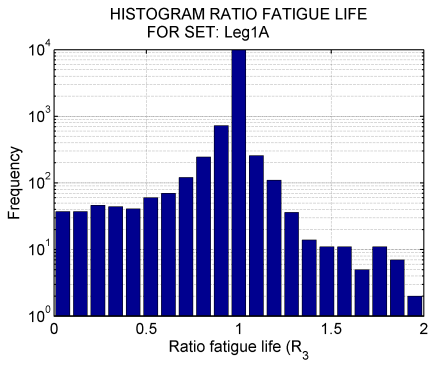

(f) Histogram for set Leg1A

Figure F.3: Fatigue life changes in XY-plots and histograms

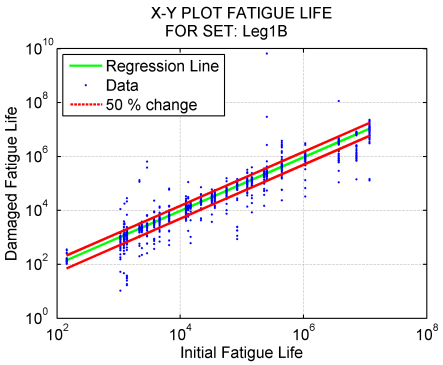

(a) XY Plot for set Leg1B

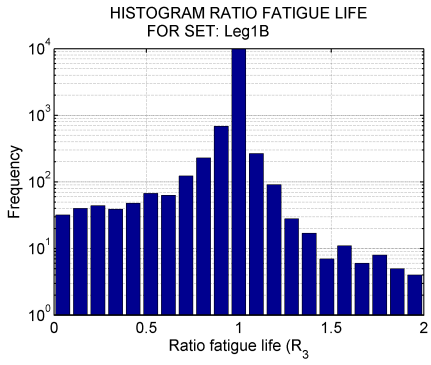

(b) Histogram for set Leg1B

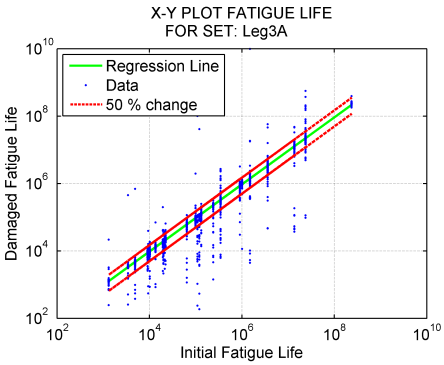

(c) XY Plot for set Leg3A

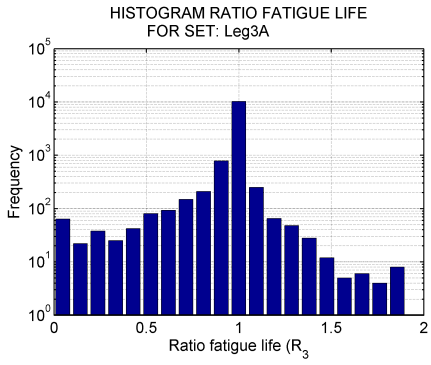

(d) Histogram for set Leg3A

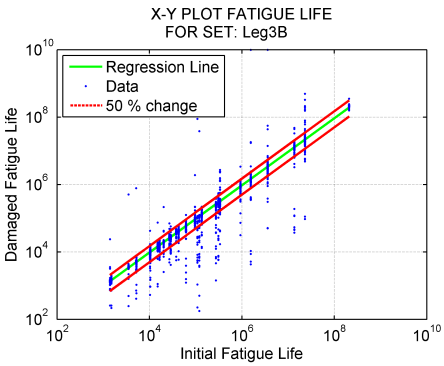

(e) XY Plot for set Leg3B

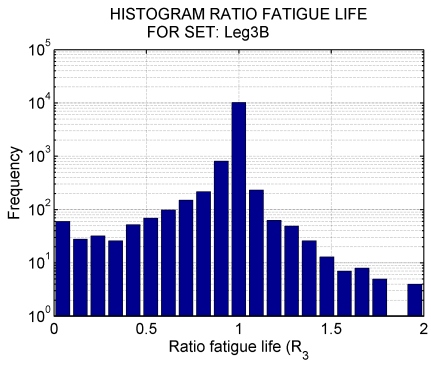

(f) Histogram for set Leg3B

Figure F.4: Fatigue life changes in XY-plots and histograms

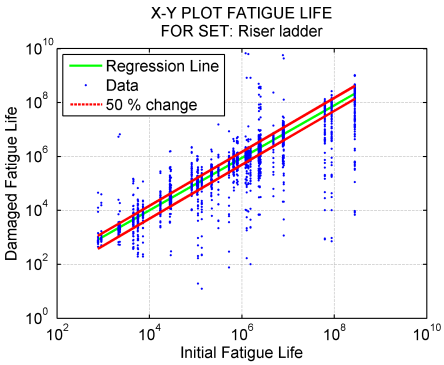

(a) XY Plot for set Riserladder

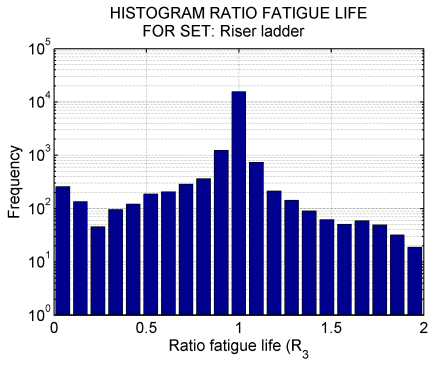

(b) Histogram for set Riserladder

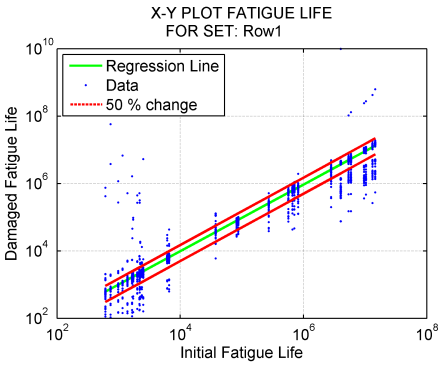

(c) XY Plot for set Row1

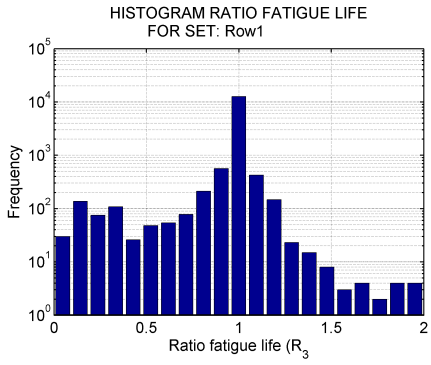

(d) Histogram for set Row1

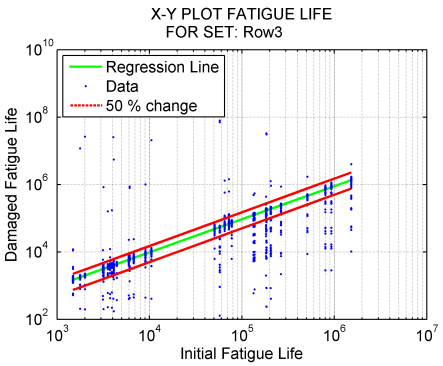

(e) XY Plot for set Row3

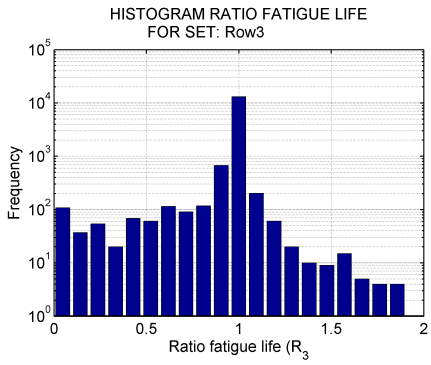

(f) Histogram for set Row3

Figure F.5: Fatigue life changes in XY-plots and histograms

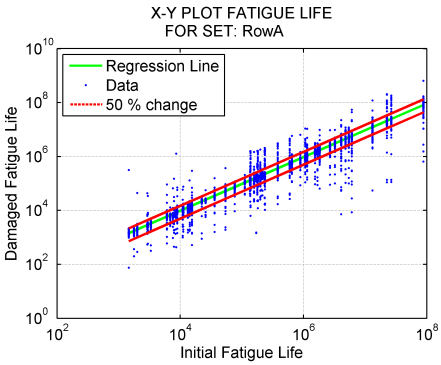

(a) XY Plot for set RowA

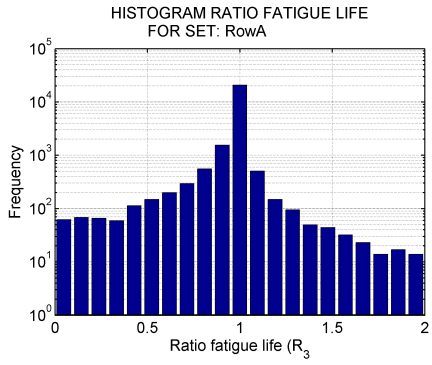

(b) Histogram for set RowA

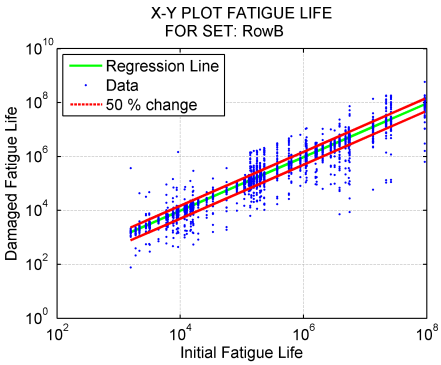

(c) XY Plot for set RowB

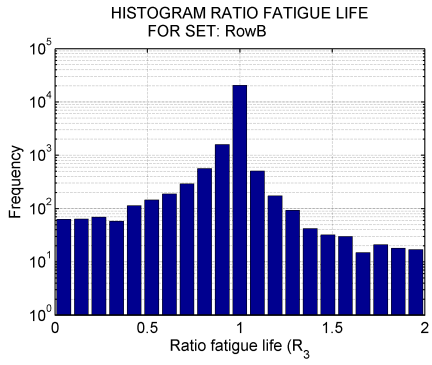

(d) Histogram for set RowB

Figure F.6: Fatigue life changes in XY-plots and histograms

F.2 3L

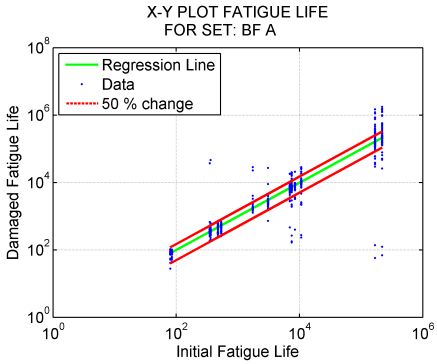

(a) XY Plot for set BFA

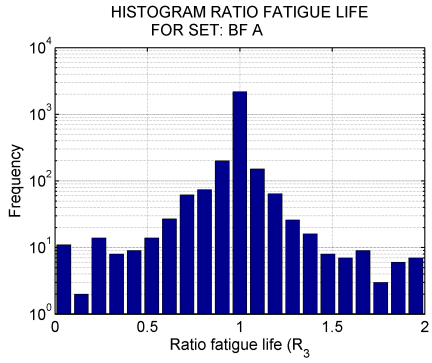

(b) Histogram for set BFA

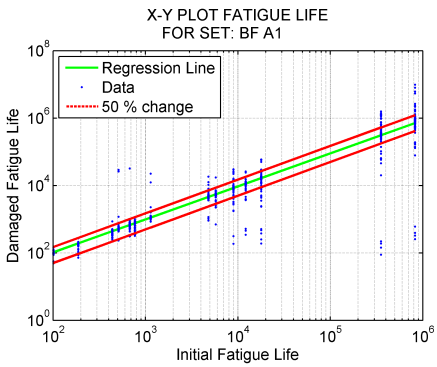

(c) XY Plot for set BFA1

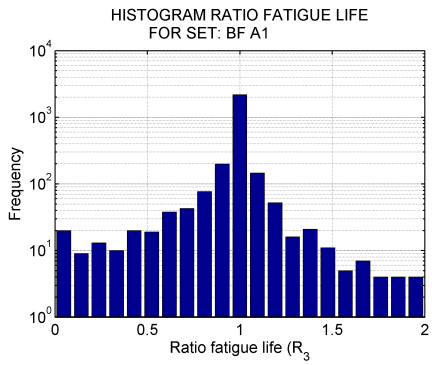

(d) Histogram for set BFA1

Figure F.7: Fatigue life changes in XY-plots and histograms

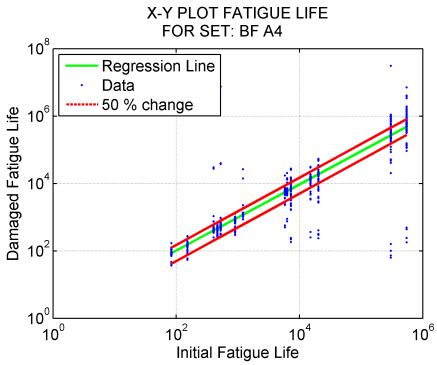

(a) XY Plot for set BFA4

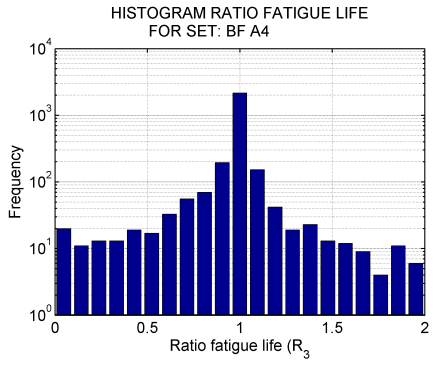

(b) Histogram for set BFA4

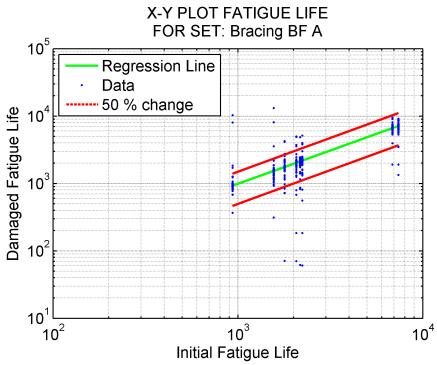

(c) XY Plot for set BracingBFA

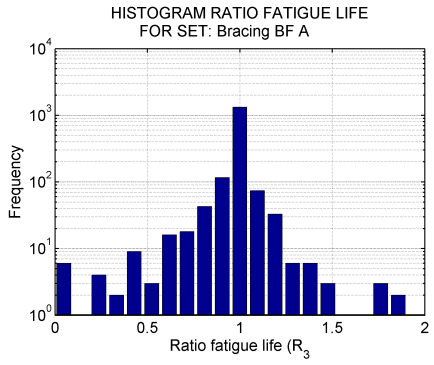

(d) Histogram for set BracingBFA

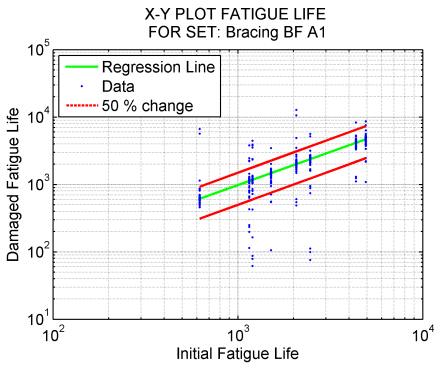

(e) XY Plot for set BracingBFA1

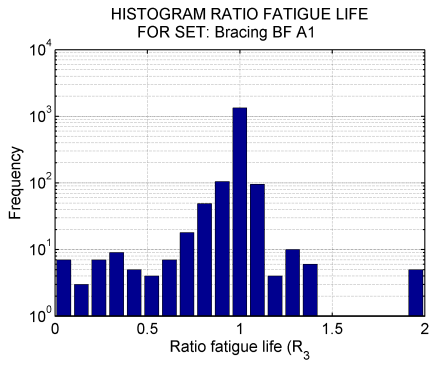

(f) Histogram for set BracingBFA1

Figure F.8: Fatigue life changes in XY-plots and histograms

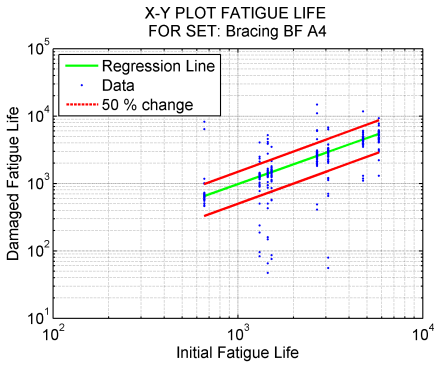

(a) XY Plot for set BracingBFA4

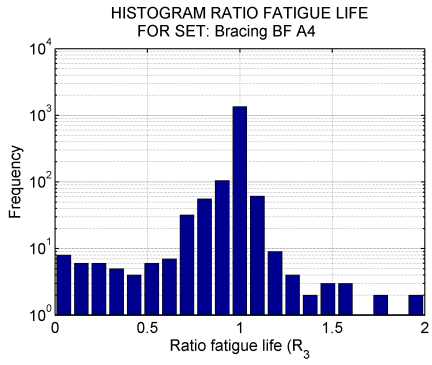

(b) Histogram for set BracingBFA4

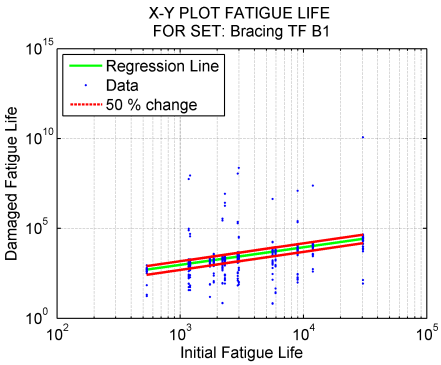

(c) XY Plot for set BracingTFB1

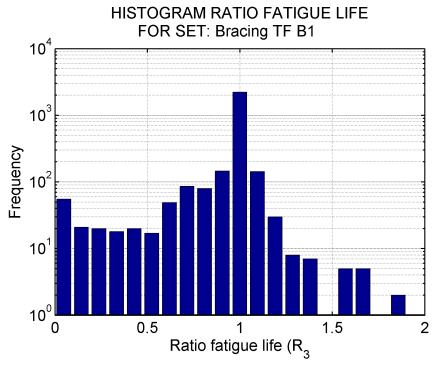

(d) Histogram for set BracingTFB1

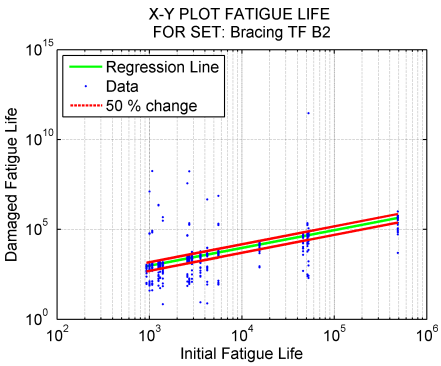

(e) XY Plot for set BracingTFB2

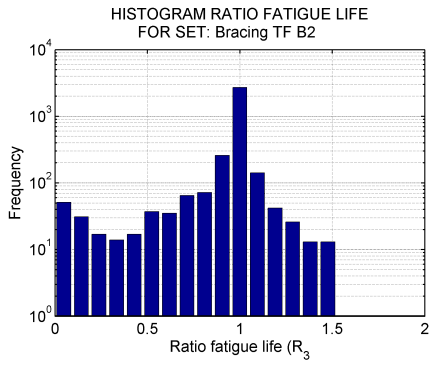

(f) Histogram for set BracingTFB2

Figure F.9: Fatigue life changes in XY-plots and histograms

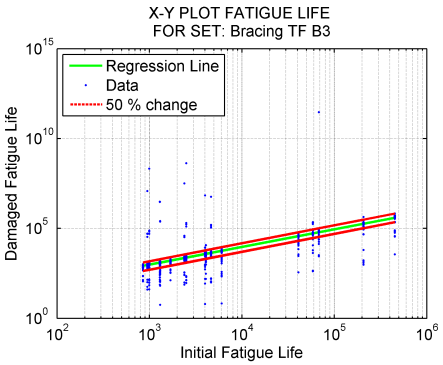

(a) XY Plot for set BracingTFB3

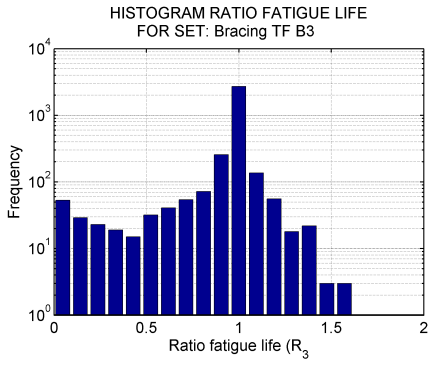

(b) Histogram for set BracingTFB3

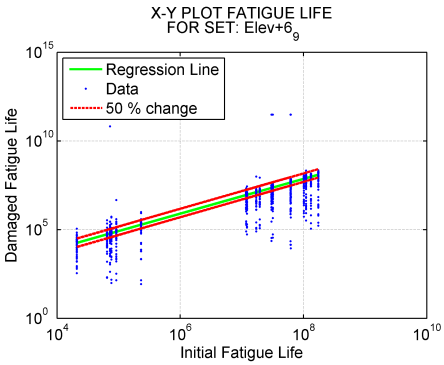

(c) XY Plot for set Elev+6.9

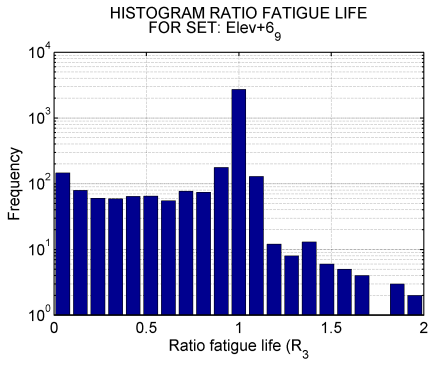

(d) Histogram for set Elev+6.9

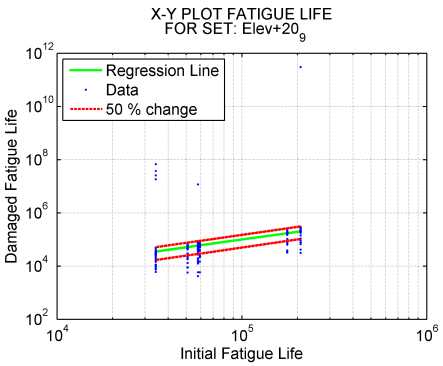

(e) XY Plot for set Elev+20.9

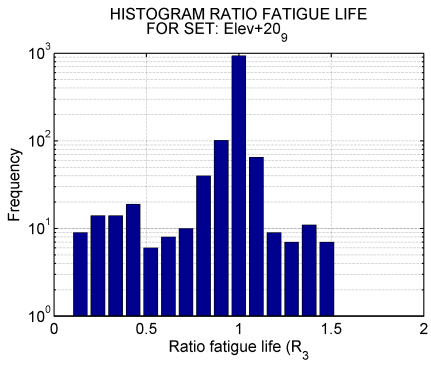

(f) Histogram for set Elev+20.9

Figure F.10: Fatigue life changes in XY-plots and histograms

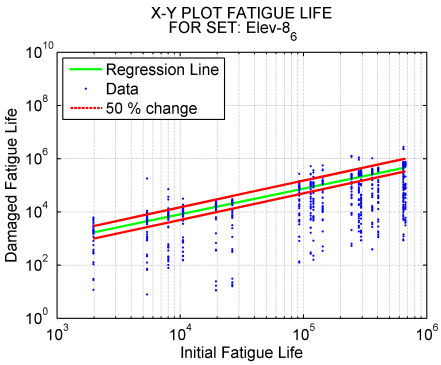

(a) XY Plot for set Elev-8.6

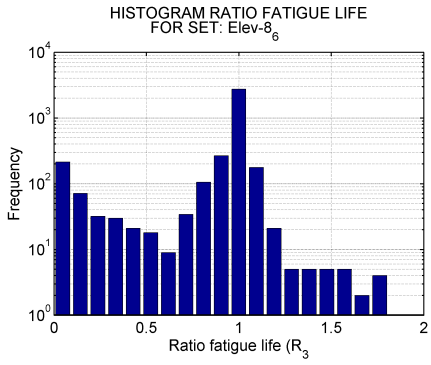

(b) Histogram for set Elev-8.6

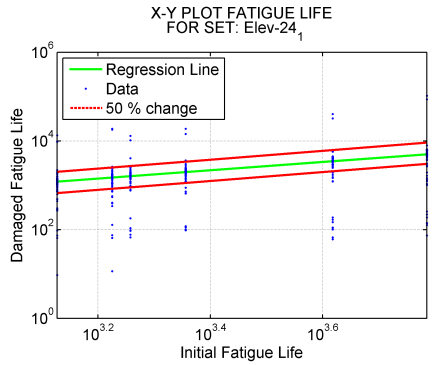

(c) XY Plot for set Elev-24.1

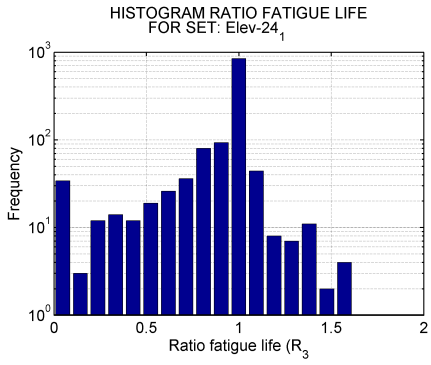

(d) Histogram for set Elev-24.1

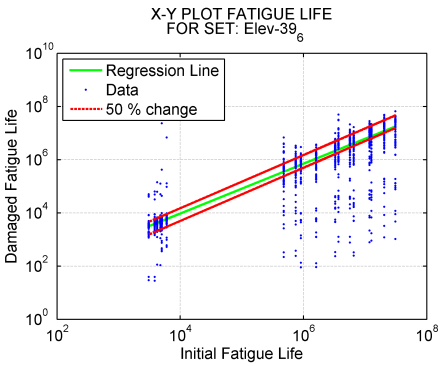

(e) XY Plot for set Elev-39.6

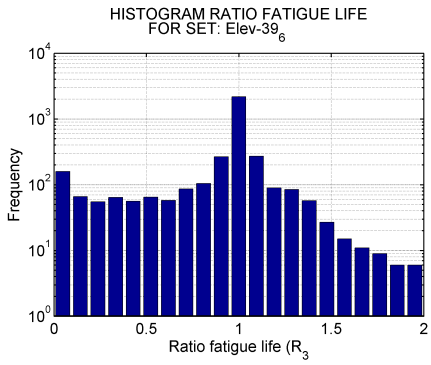

(f) Histogram for set Elev-39.6

Figure F.11: Fatigue life changes in XY-plots and histograms

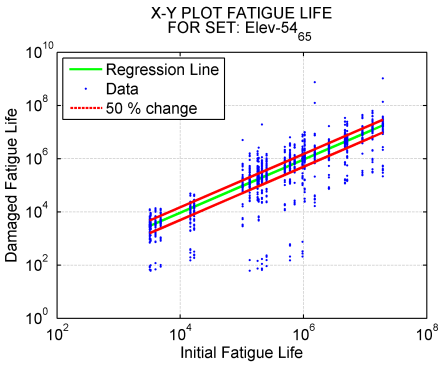

(a) XY Plot for set Elev-54.65

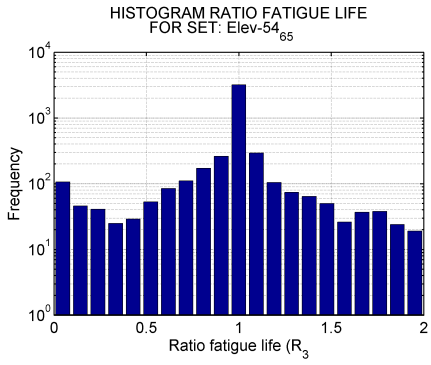

(b) Histogram for set Elev-54.65

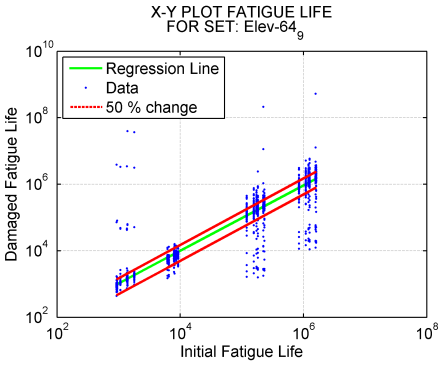

(c) XY Plot for set Elev-64.9

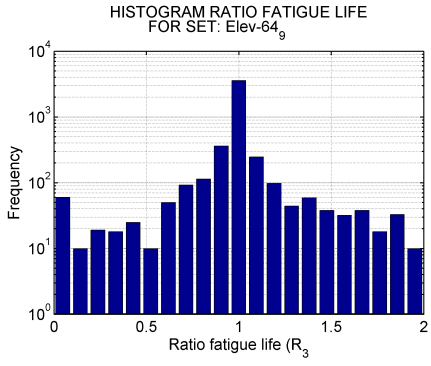

(d) Histogram for set Elev-64.9

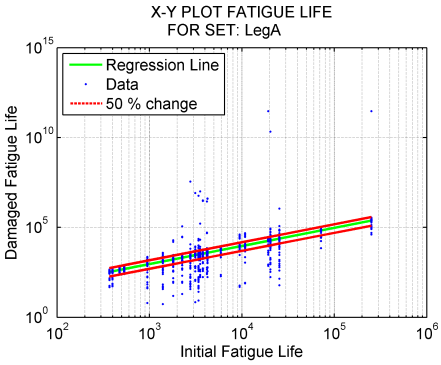

(e) XY Plot for set LegA

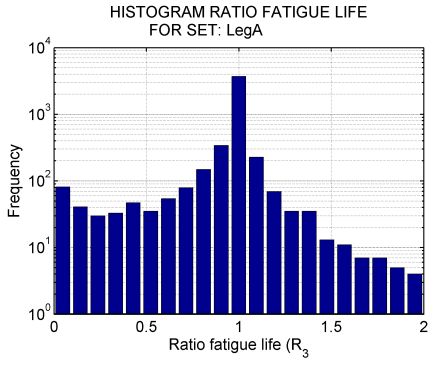

(f) Histogram for set LegA

Figure F.12: Fatigue life changes in XY-plots and histograms

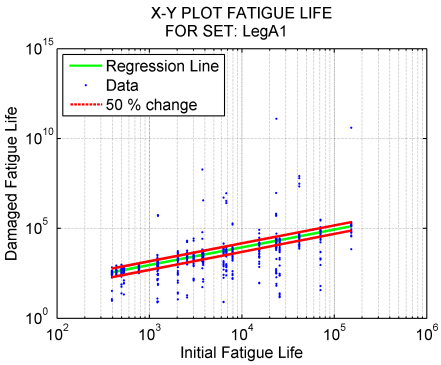

(a) XY Plot for set LegA1

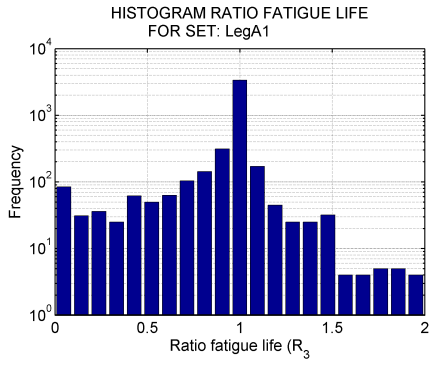

(b) Histogram for set LegA1

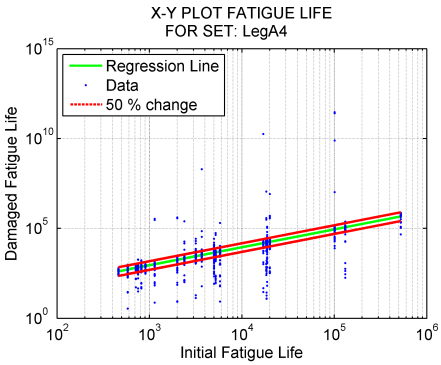

(c) XY Plot for set LegA4

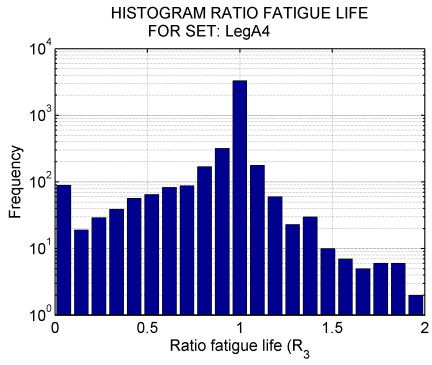

(d) Histogram for set LegA4

Figure F.13: Fatigue life changes in XY-plots and histograms

Appendix G

Residual Fatigue Redundant Factor

In this chapter, the R_3 is plotted in histograms where the different changes throughout the structure has been divided into the classification as described in section 5.1.2. Only values in the range [0-2] are plotted.

G.1 4L

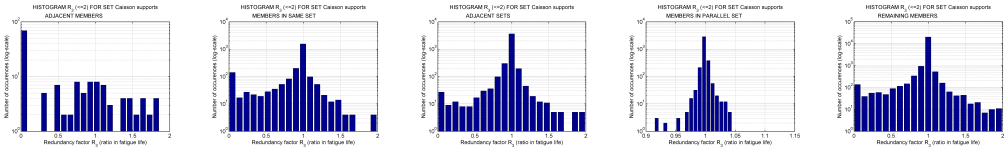

(a) Adjacent members **(b)** Same set **(c)** Adjacent set **(d)** Parallel set **(e)** Remaining members

Figure G.1: R3 Factor (4L-jacket), damage in Caissonsupports

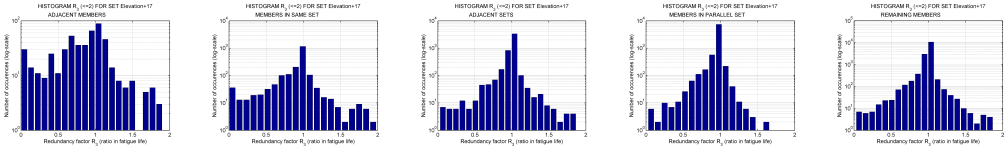

(a) Adjacent members **(b)** Same set **(c)** Adjacent set **(d)** Parallel set **(e)** Remaining members

Figure G.2: R3 Factor (4L-jacket), damage in Elevation+17

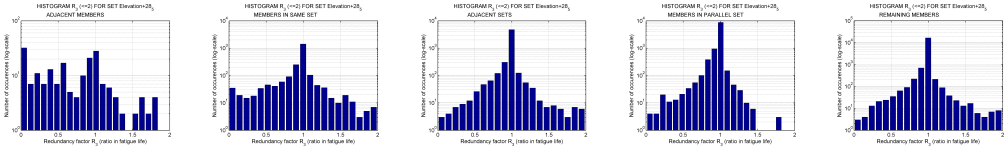

(a) Adjacent members **(b)** Same set **(c)** Adjacent set **(d)** Parallel set **(e)** Remaining members

Figure G.3: R3 Factor (4L-jacket), damage in Elevation+28.5

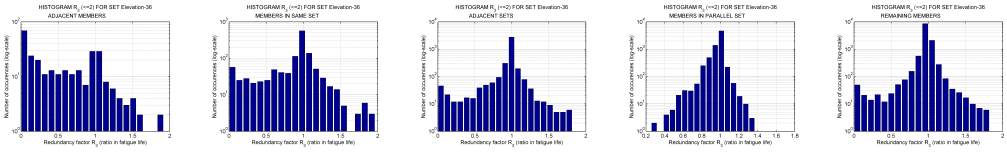

(a) Adjacent members **(b)** Same set **(c)** Adjacent set **(d)** Parallel set **(e)** Remaining members

Figure G.4: R3 Factor (4L-jacket), damage in Elevation-36

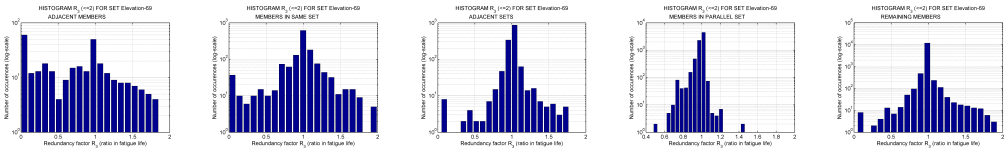

(a) Adjacent members **(b)** Same set **(c)** Adjacent set **(d)** Parallel set **(e)** Remaining members

Figure G.5: R3 Factor (4L-jacket), damage in Elevation-69

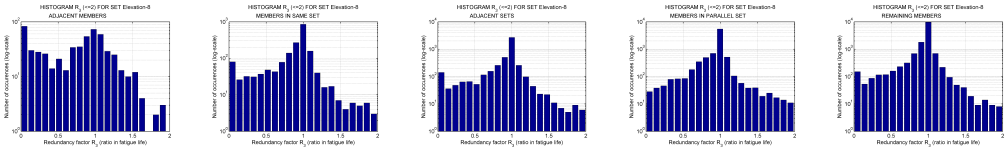

(a) Adjacent members **(b)** Same set **(c)** Adjacent set **(d)** Parallel set **(e)** Remaining members

Figure G.6: R3 Factor (4L-jacket), damage in Elevation-8

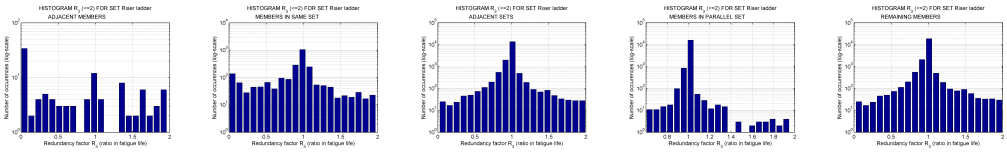

(a) Adjacent members **(b)** Same set **(c)** Adjacent set **(d)** Parallel set **(e)** Remaining members

Figure G.7: R3 Factor (4L-jacket), damage in Riserladder

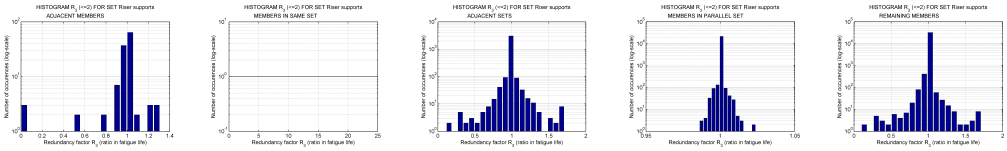

(a) Adjacent members **(b)** Same set **(c)** Adjacent set **(d)** Parallel set **(e)** Remaining members

Figure G.8: R3 Factor (4L-jacket), damage in Risersupports

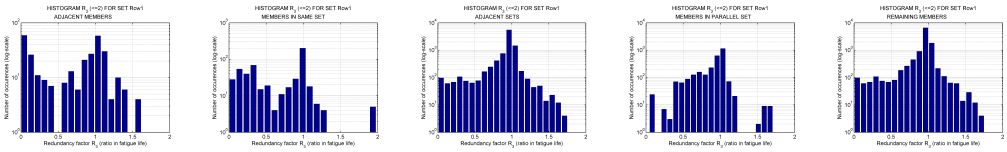

(a) Adjacent members **(b)** Same set **(c)** Adjacent set **(d)** Parallel set **(e)** Remaining members

Figure G.9: R3 Factor (4L-jacket), damage in Row1

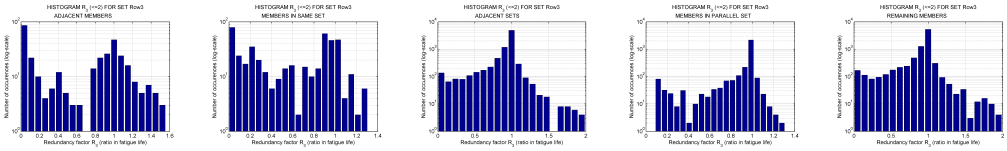

(a) Adjacent members **(b)** Same set **(c)** Adjacent set **(d)** Parallel set **(e)** Remaining members

Figure G.10: R3 Factor (4L-jacket), damage in Row3

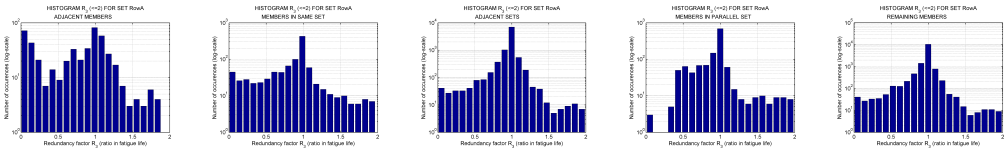

(a) Adjacent members **(b)** Same set **(c)** Adjacent set **(d)** Parallel set **(e)** Remaining members

Figure G.11: R3 Factor (4L-jacket), damage in RowA

G.2 3L

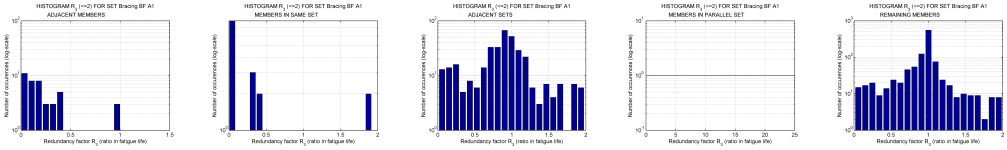

(a) Adjacent members **(b)** Same set **(c)** Adjacent set **(d)** Parallel set **(e)** Remaining members

Figure G.12: R3 Factor (3L-jacket), damage in BracingBFA1

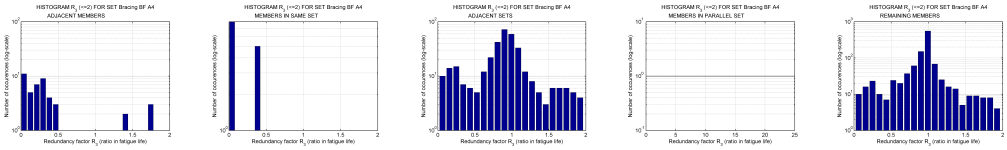

(a) Adjacent members **(b)** Same set **(c)** Adjacent set **(d)** Parallel set **(e)** Remaining members

Figure G.13: R3 Factor (3L-jacket), damage in BracingBFA4

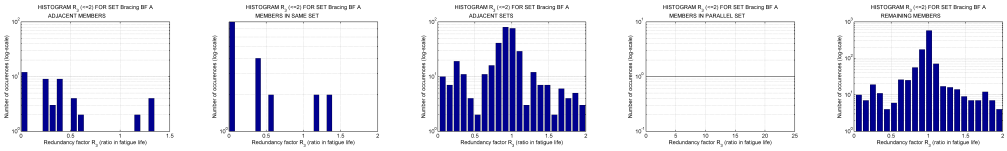

(a) Adjacent members **(b)** Same set **(c)** Adjacent set **(d)** Parallel set **(e)** Remaining members

Figure G.14: R3 Factor (3L-jacket), damage in BracingBFA

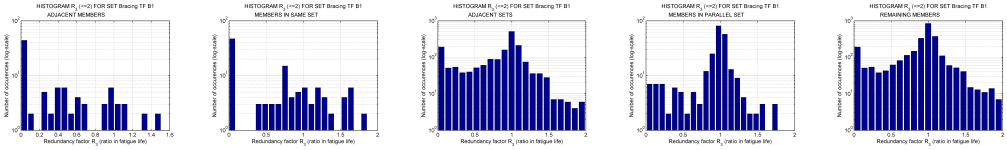

(a) Adjacent members **(b)** Same set **(c)** Adjacent set **(d)** Parallel set **(e)** Remaining members

Figure G.15: R3 Factor (3L-jacket), damage in BracingTFB1

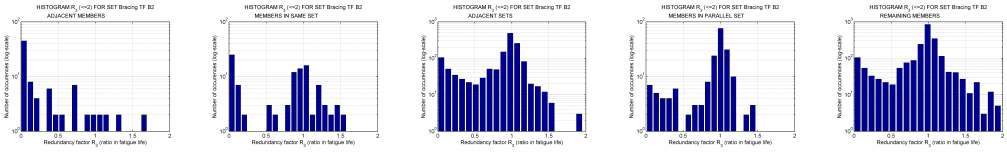

(a) Adjacent members **(b)** Same set **(c)** Adjacent set **(d)** Parallel set **(e)** Remaining members

Figure G.16: R3 Factor (3L-jacket), damage in BracingTFB2

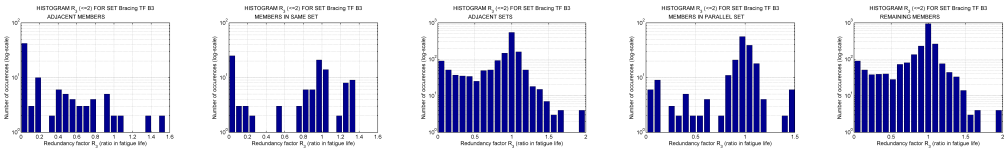

(a) Adjacent members **(b)** Same set **(c)** Adjacent set **(d)** Parallel set **(e)** Remaining members

Figure G.17: R3 Factor (3L-jacket), damage in BracingTFB3

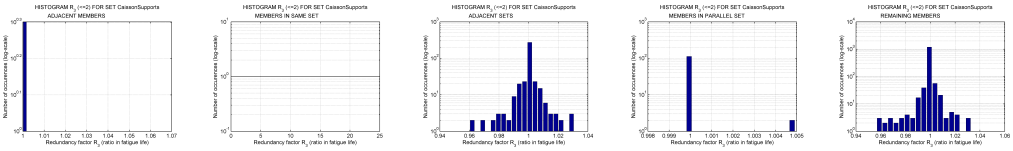

(a) Adjacent members **(b)** Same set **(c)** Adjacent set **(d)** Parallel set **(e)** Remaining members

Figure G.18: R3 Factor (3L-jacket), damage in CaissonSupports

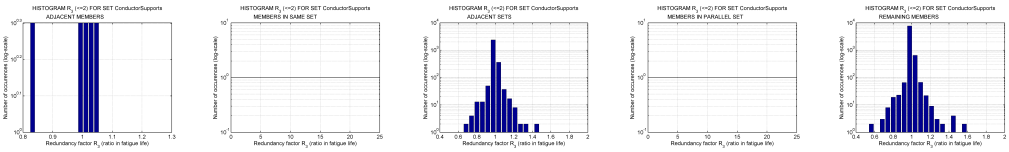

(a) Adjacent members **(b)** Same set **(c)** Adjacent set **(d)** Parallel set **(e)** Remaining members

Figure G.19: R3 Factor (3L-jacket), damage in ConductorSupports

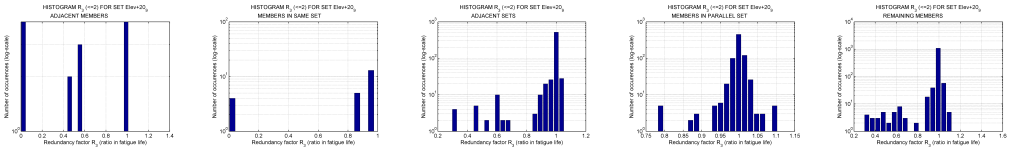

(a) Adjacent members **(b)** Same set **(c)** Adjacent set **(d)** Parallel set **(e)** Remaining members

Figure G.20: R3 Factor (3L-jacket), damage in Elev+20.9

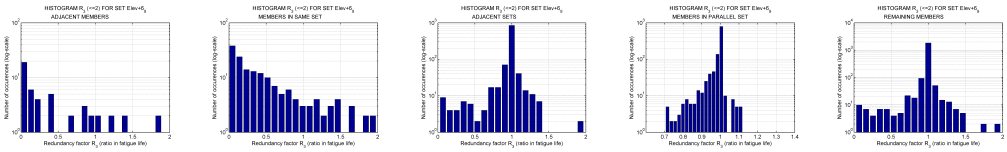

(a) Adjacent members **(b)** Same set **(c)** Adjacent set **(d)** Parallel set **(e)** Remaining members

Figure G.21: R3 Factor (3L-jacket), damage in Elev+6.9

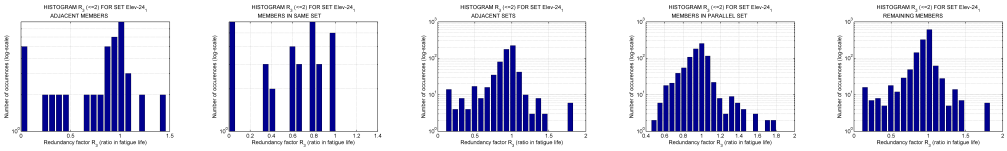

(a) Adjacent members **(b)** Same set **(c)** Adjacent set **(d)** Parallel set **(e)** Remaining members

Figure G.22: R3 Factor (3L-jacket), damage in Elev-24.1

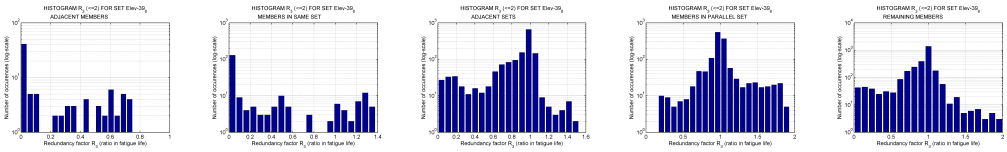

(a) Adjacent members **(b)** Same set **(c)** Adjacent set **(d)** Parallel set **(e)** Remaining members

Figure G.23: R3 Factor (3L-jacket), damage in Elev-39.6

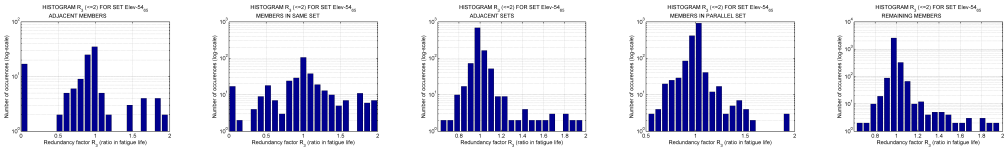

(a) Adjacent members **(b)** Same set **(c)** Adjacent set **(d)** Parallel set **(e)** Remaining members

Figure G.24: R3 Factor (3L-jacket), damage in Elev-54.6.5

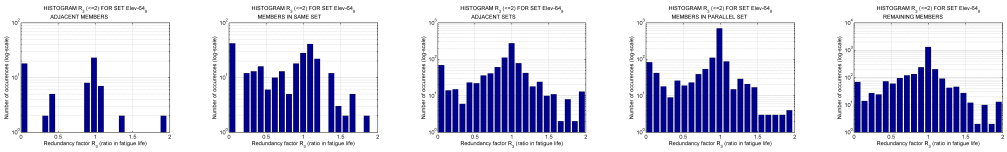

(a) Adjacent members **(b)** Same set **(c)** Adjacent set **(d)** Parallel set **(e)** Remaining members

Figure G.25: R3 Factor (3L-jacket), damage in Elev-64.9

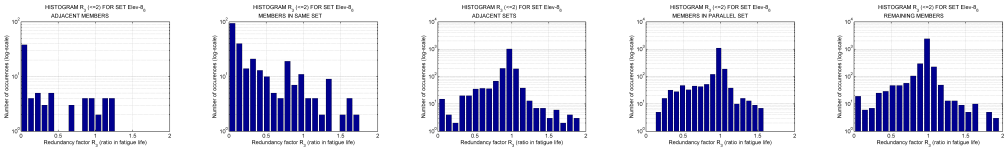

(a) Adjacent members **(b)** Same set **(c)** Adjacent set **(d)** Parallel set **(e)** Remaining members

Figure G.26: R3 Factor (3L-jacket), damage in Elev-8.6

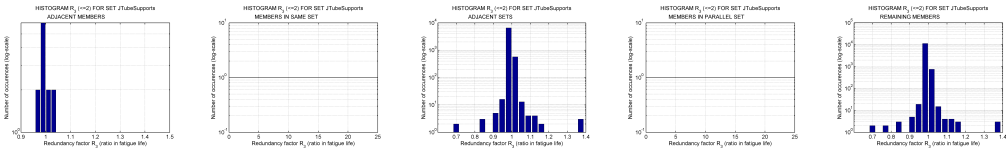

(a) Adjacent members **(b)** Same set **(c)** Adjacent set **(d)** Parallel set **(e)** Remaining members

Figure G.27: R3 Factor (3L-jacket), damage in JTubeSupports

Appendix H

Fatigue Accelerator Factor

In the following figures, the worst FAF that occurs in a set is plotted so that each "dot" on the lines represent one member. Each line represents a damage case, where the location of the damage is given in the legend.

H.1 4L

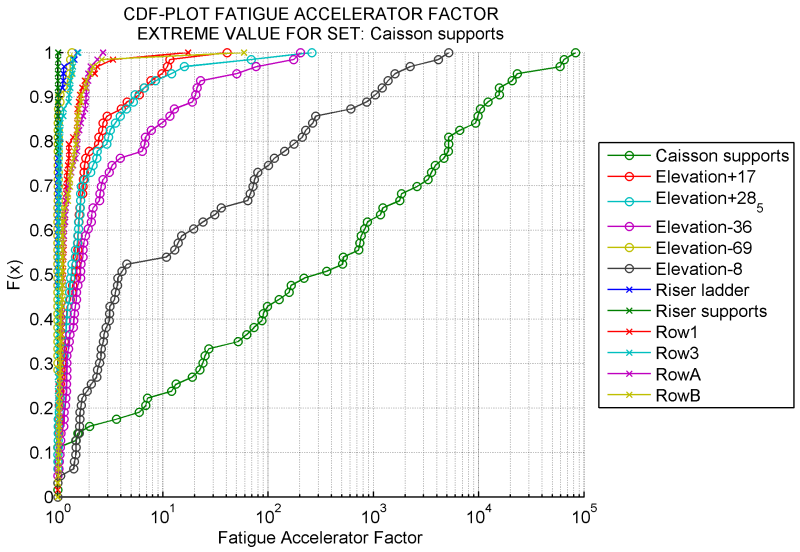

Figure H.1: Largest Fatigue Accelerator Factor for set Caisson supports

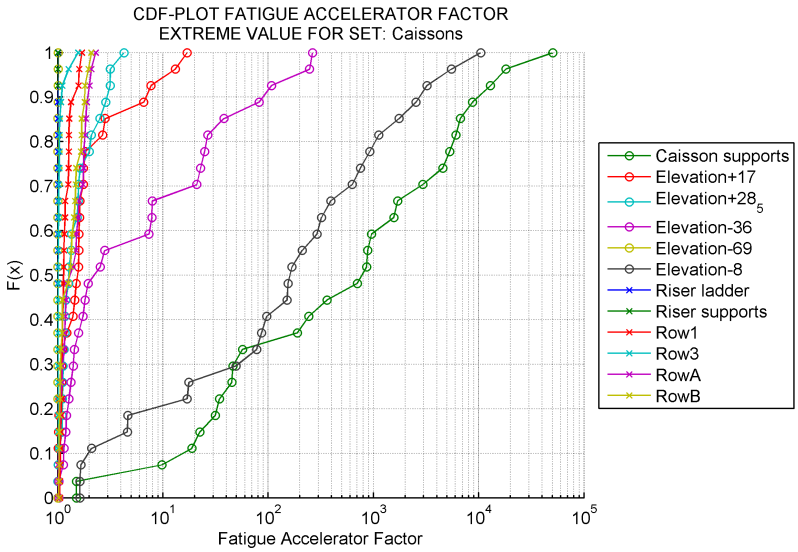

Figure H.2: Largest Fatigue Accelerator Factor for set Caissons

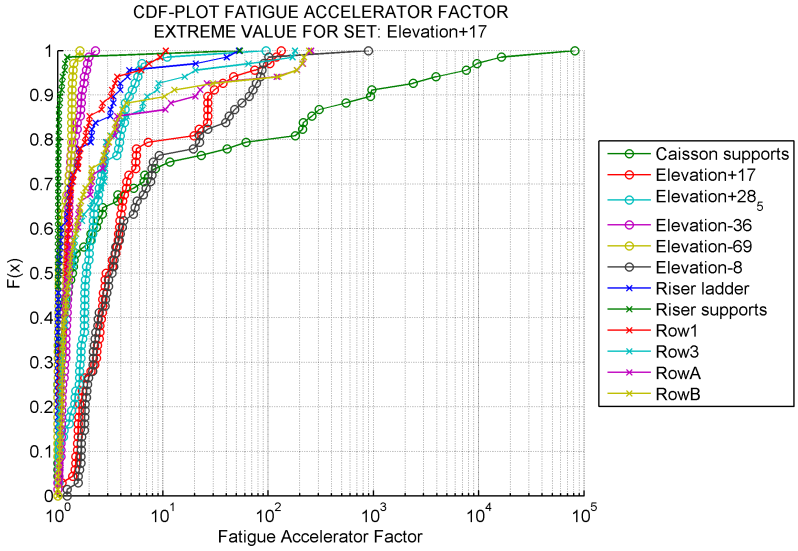

Figure H.3: Largest Fatigue Accelerator Factor for set Elevation+17

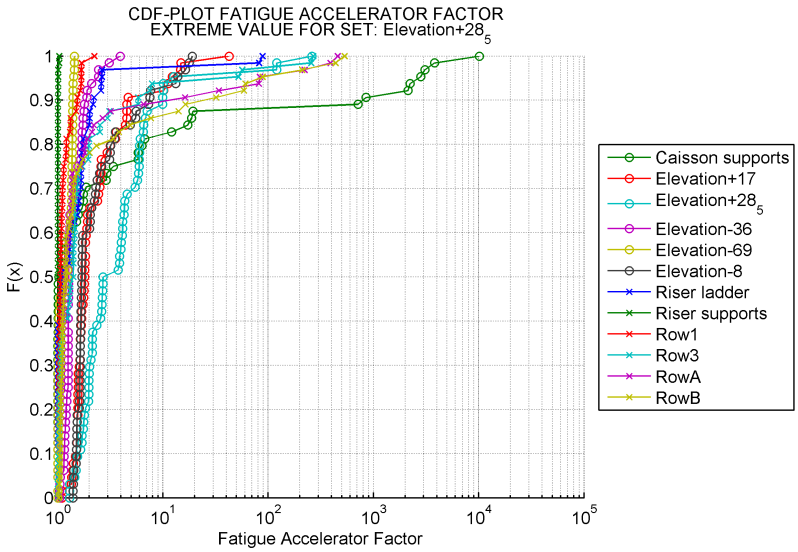

Figure H.4: Largest Fatigue Accelerator Factor for set Elevation+28.5

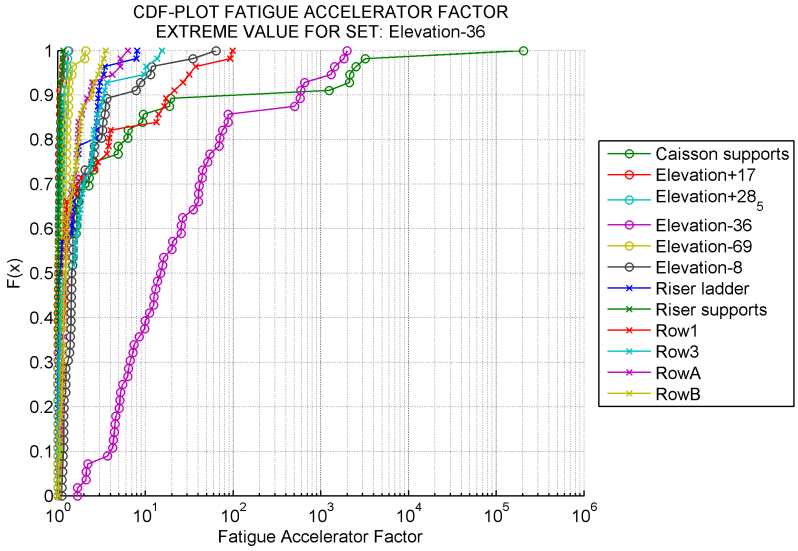

Figure H.5: Largest Fatigue Accelerator Factor for set Elevation-36

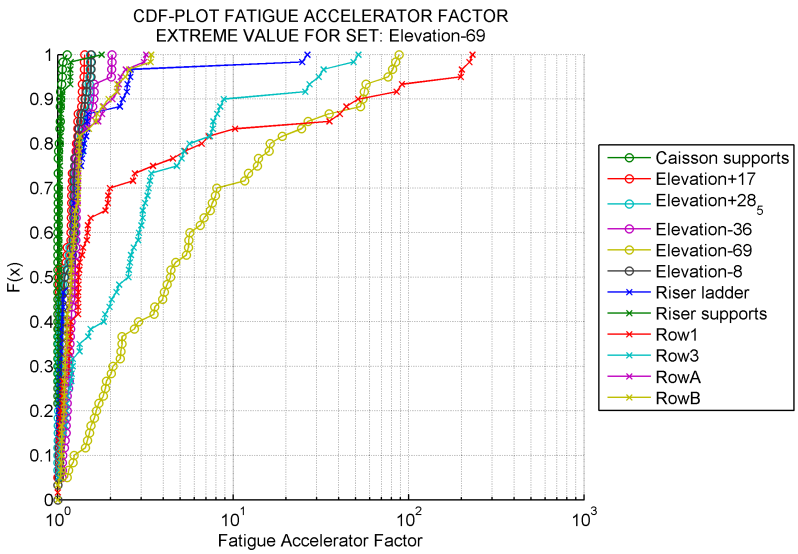

Figure H.6: Largest Fatigue Accelerator Factor for set Elevation-69

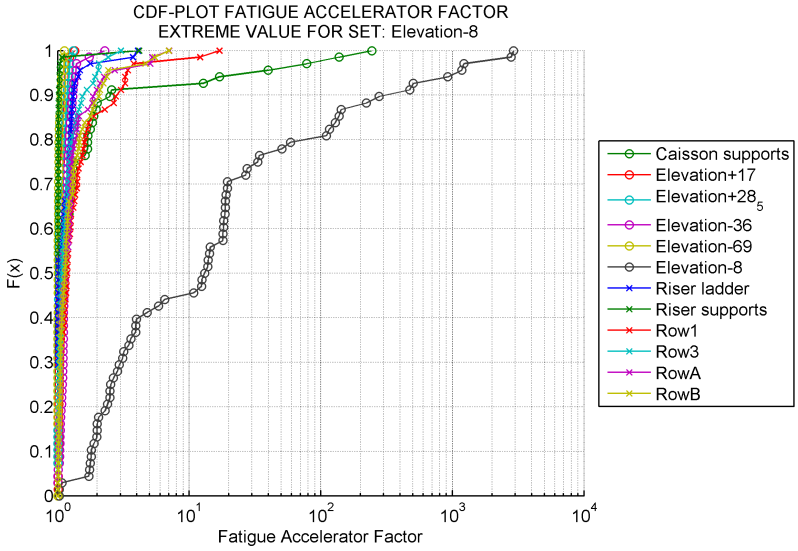

Figure H.7: Largest Fatigue Accelerator Factor for set Elevation-8

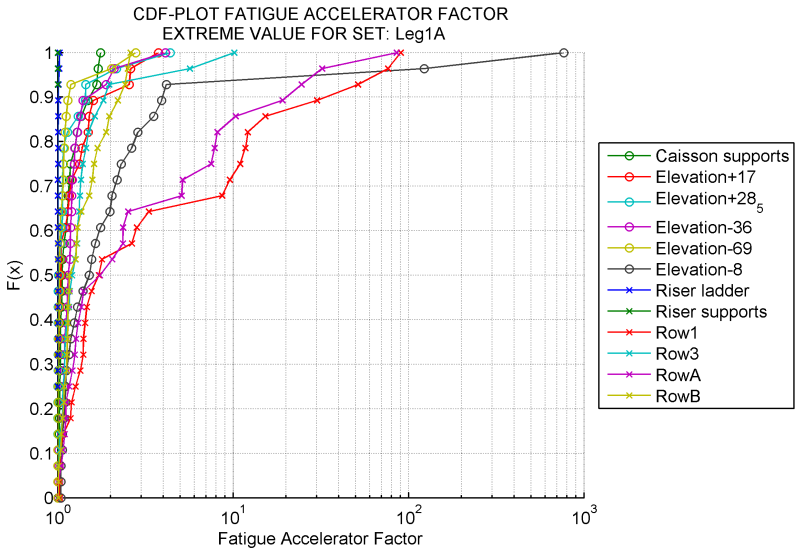

Figure H.8: Largest Fatigue Accelerator Factor for set Leg1A

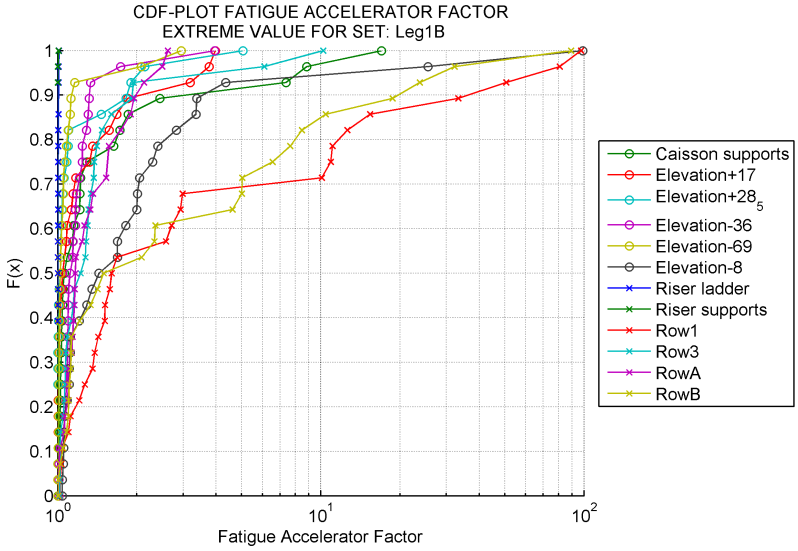

Figure H.9: Largest Fatigue Accelerator Factor for set Leg1B

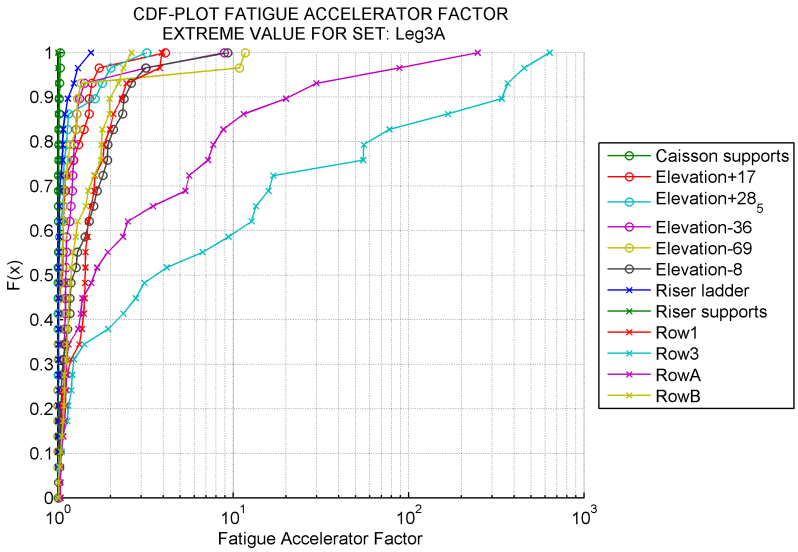

Figure H.10: Largest Fatigue Accelerator Factor for set Leg3A

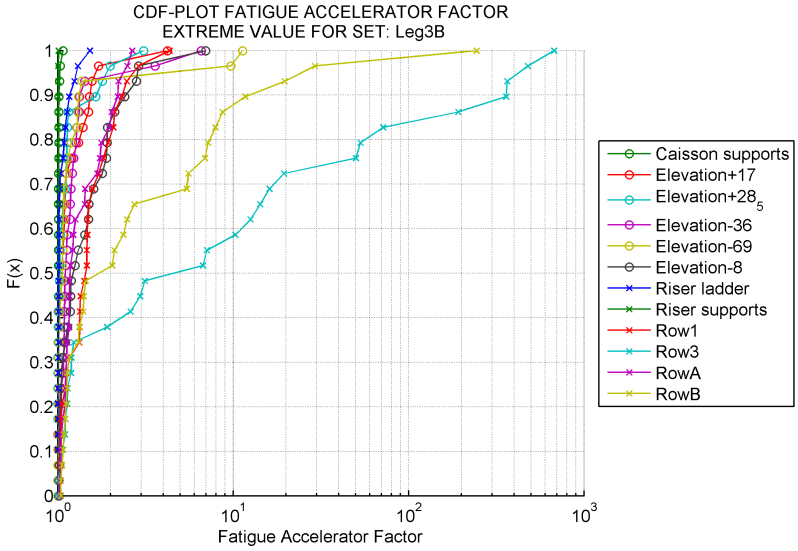

Figure H.11: Largest Fatigue Accelerator Factor for set Leg3B

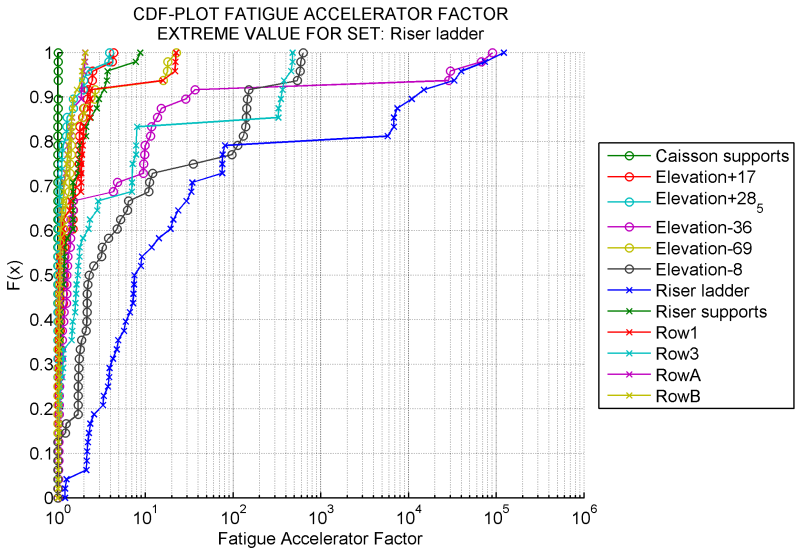

Figure H.12: Largest Fatigue Accelerator Factor for set Riser ladder

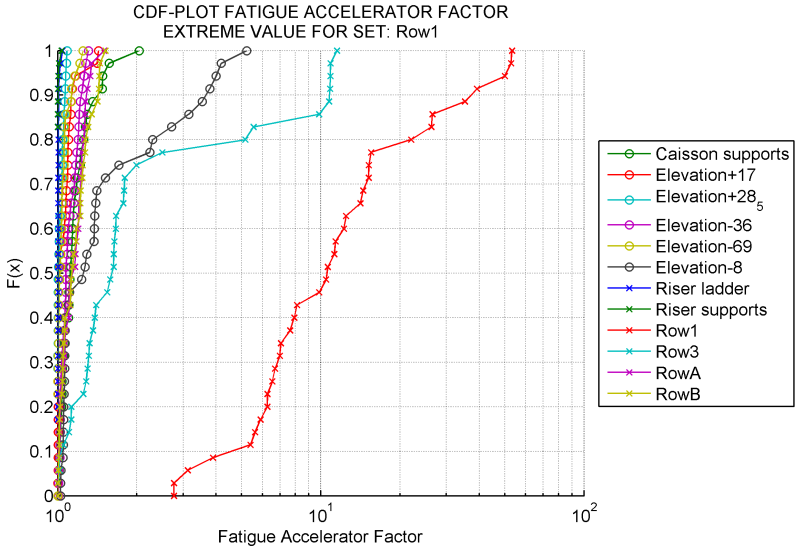

Figure H.13: Largest Fatigue Accelerator Factor for set Row1

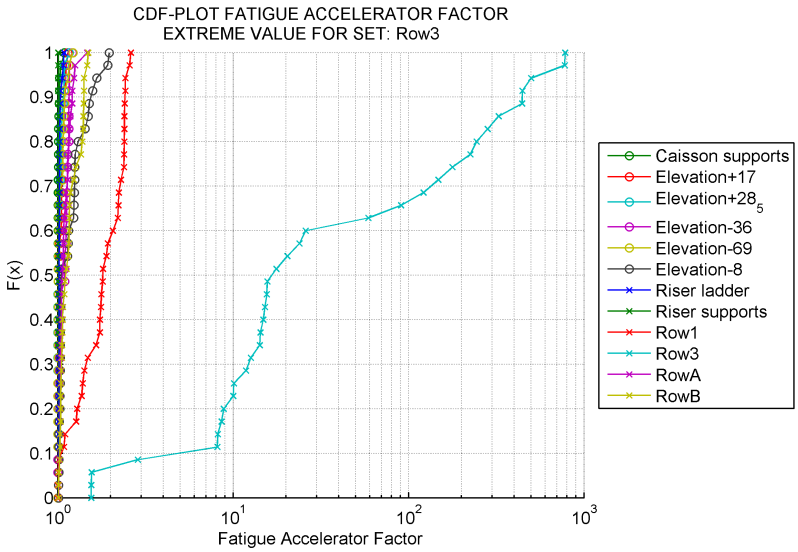

Figure H.14: Largest Fatigue Accelerator Factor for set Row3

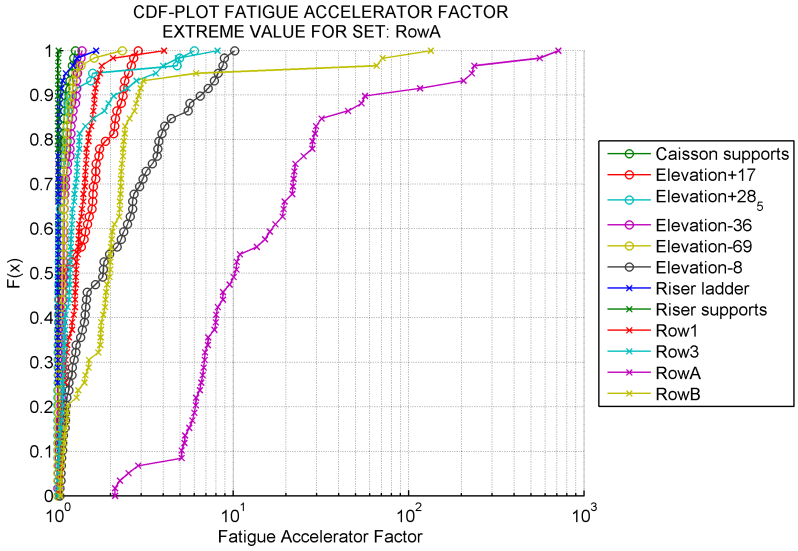

Figure H.15: Largest Fatigue Accelerator Factor for set RowA

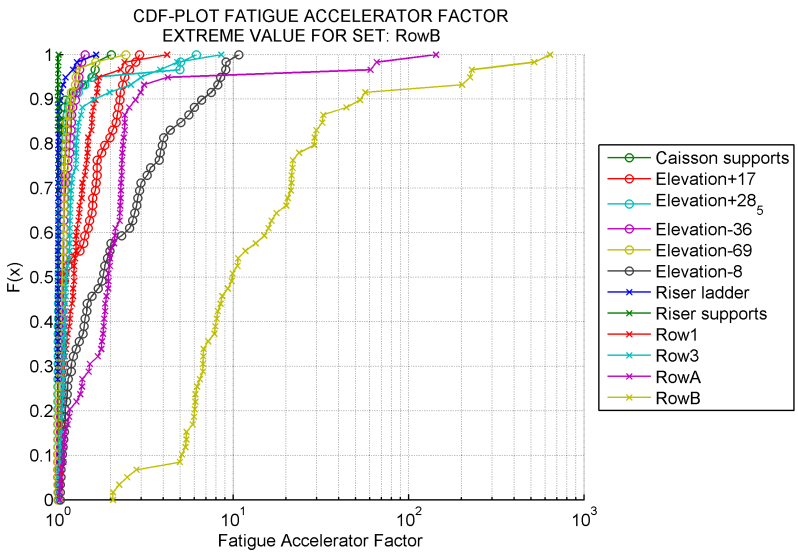

Figure H.16: Largest Fatigue Accelerator Factor for set RowB

H.2 3L

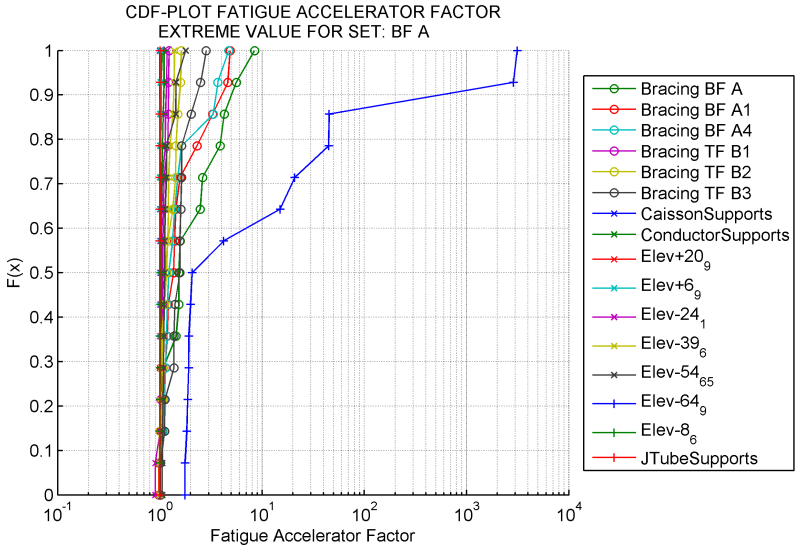

Figure H.17: Largest Fatigue Accelerator Factor for set BF A

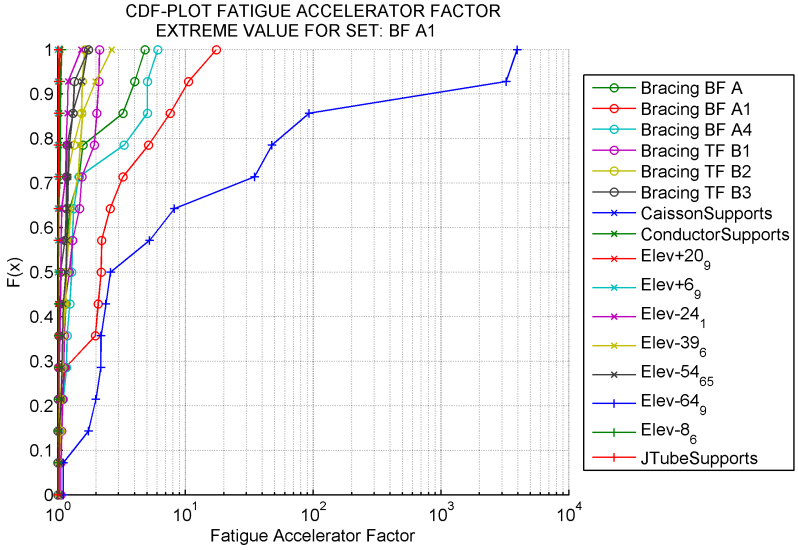

Figure H.18: Largest Fatigue Accelerator Factor for set BF A1

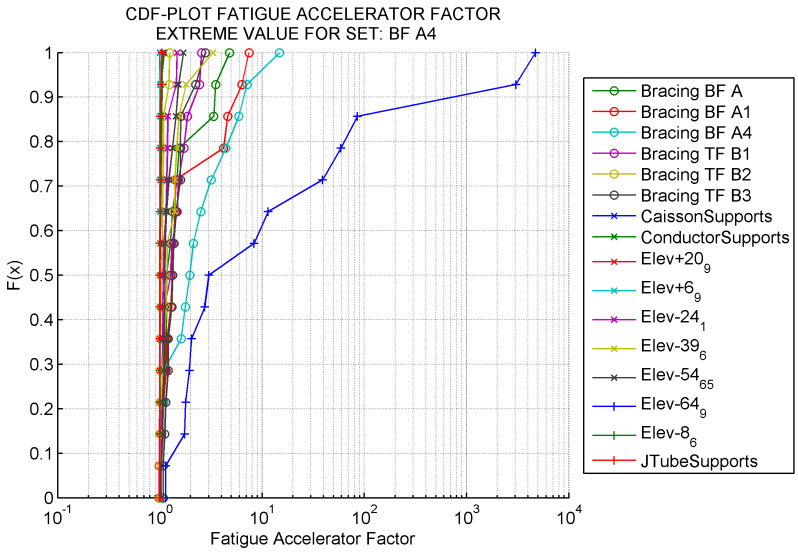

Figure H.19: Largest Fatigue Accelerator Factor for set BF A4

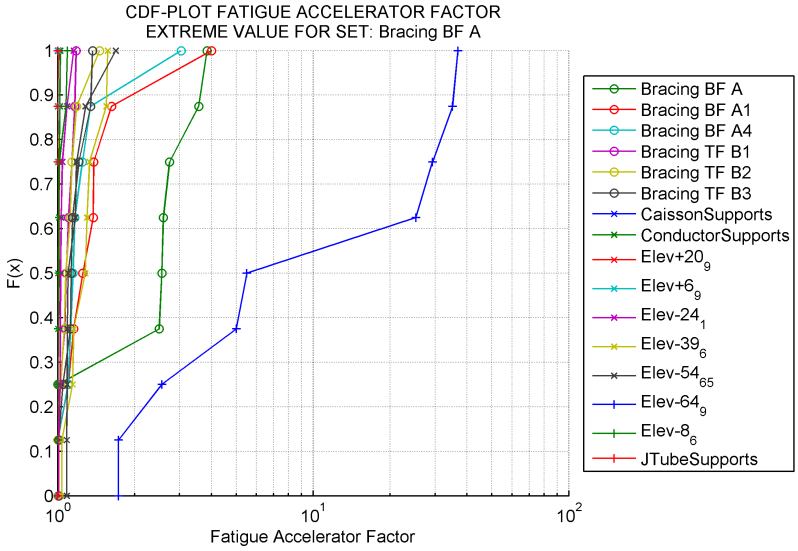

Figure H.20: Largest Fatigue Accelerator Factor for set Bracing BF A

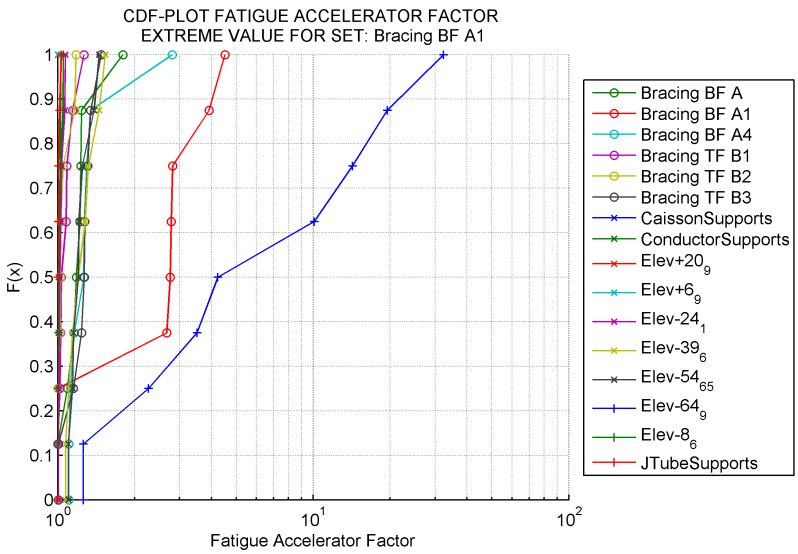

Figure H.21: Largest Fatigue Accelerator Factor for set Bracing BF A1

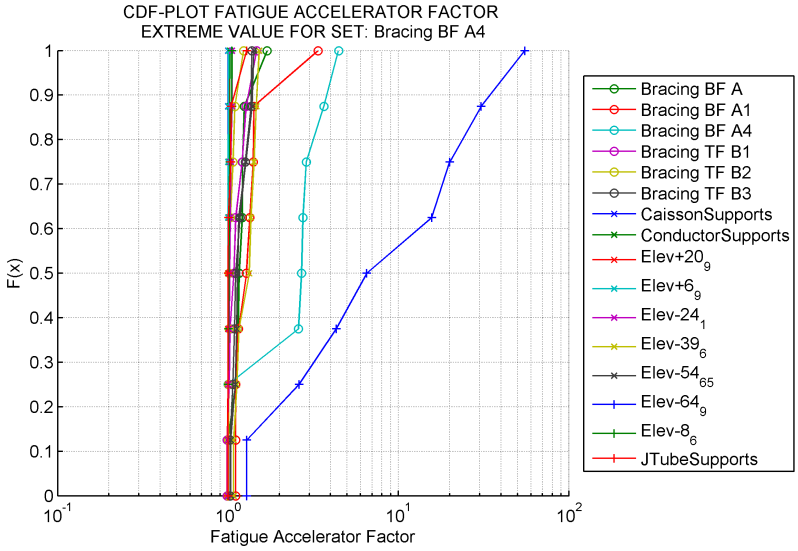

Figure H.22: Largest Fatigue Accelerator Factor for set Bracing BF A4

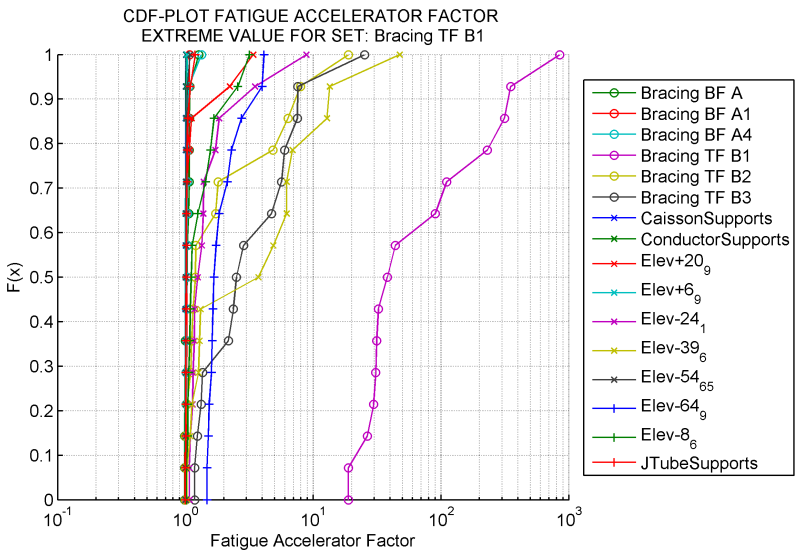

Figure H.23: Largest Fatigue Accelerator Factor for set Bracing TF B1

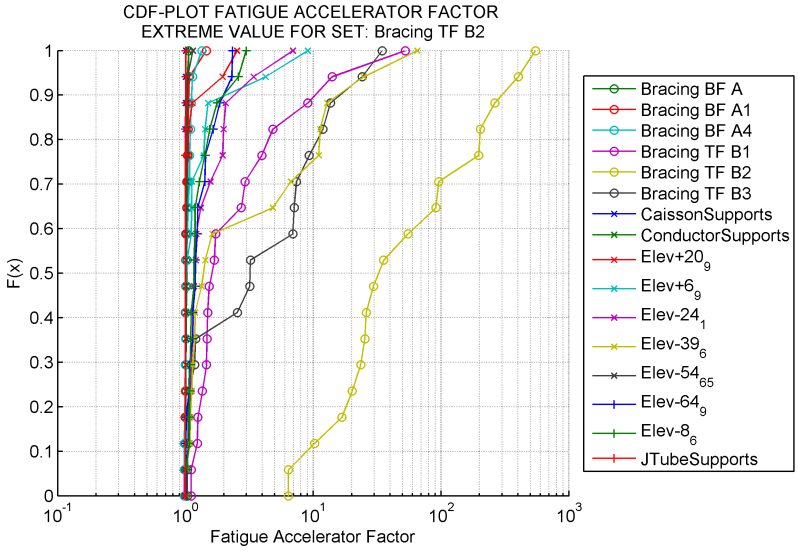

Figure H.24: Largest Fatigue Accelerator Factor for set Bracing TF B2

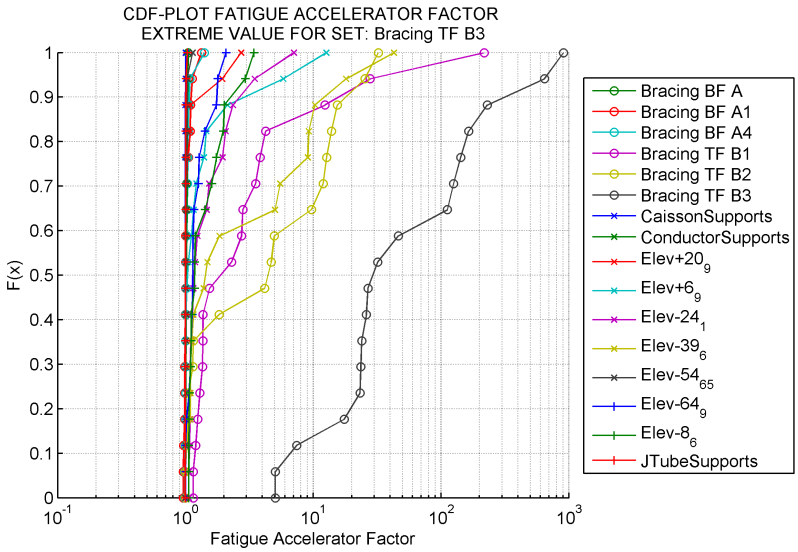

Figure H.25: Largest Fatigue Accelerator Factor for set Bracing TF B3

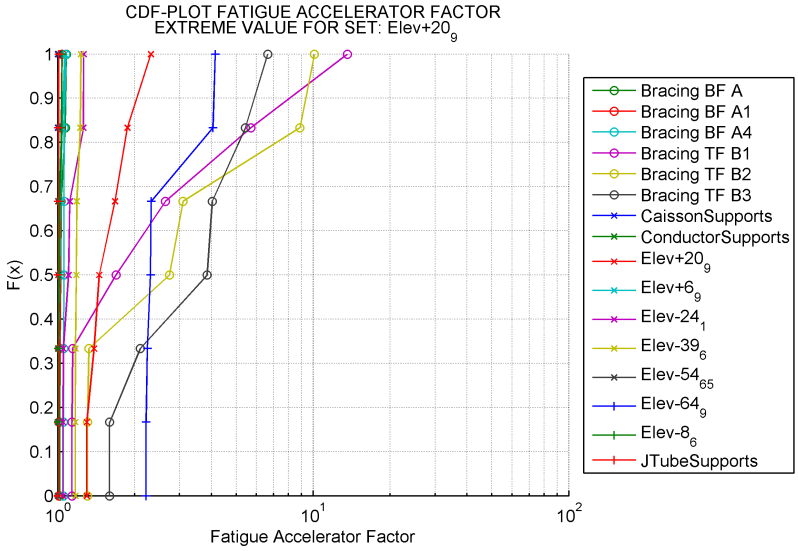

Figure H.26: Largest Fatigue Accelerator Factor for set Elev+20.9

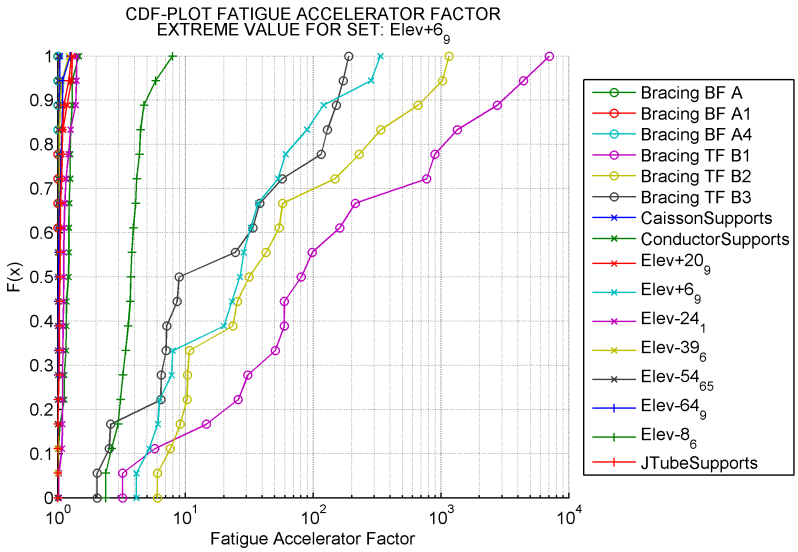

Figure H.27: Largest Fatigue Accelerator Factor for set Elev+6.9

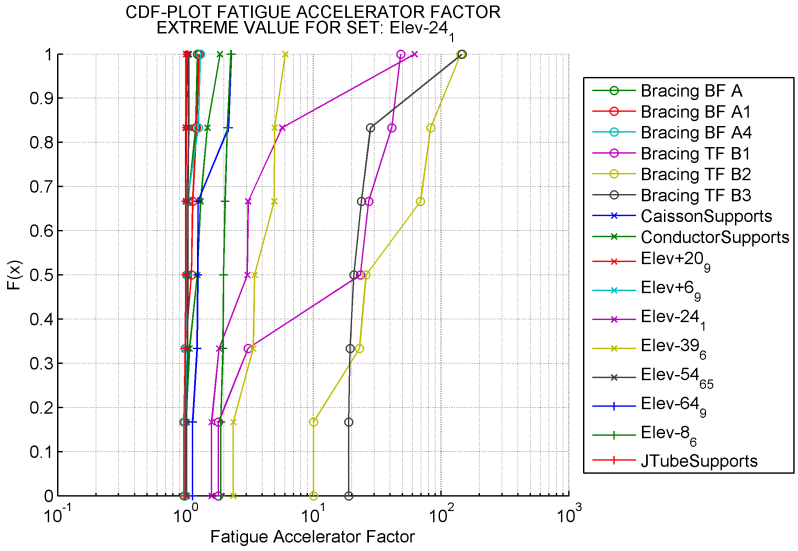

Figure H.28: Largest Fatigue Accelerator Factor for set Elev-24.1

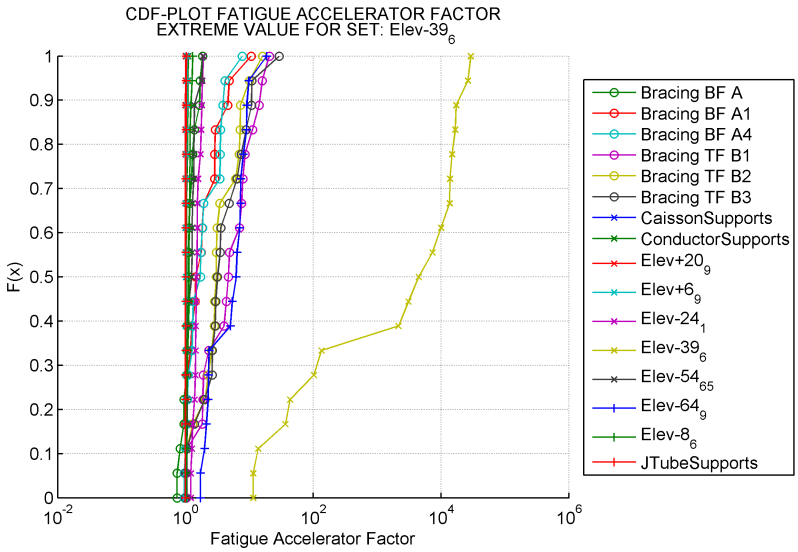

Figure H.29: Largest Fatigue Accelerator Factor for set Elev-39.6

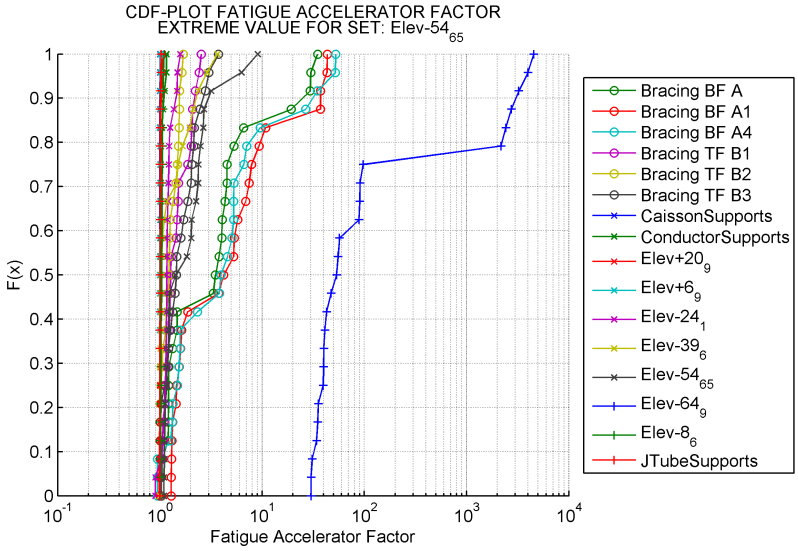

Figure H.30: Largest Fatigue Accelerator Factor for set Elev-54.6.5

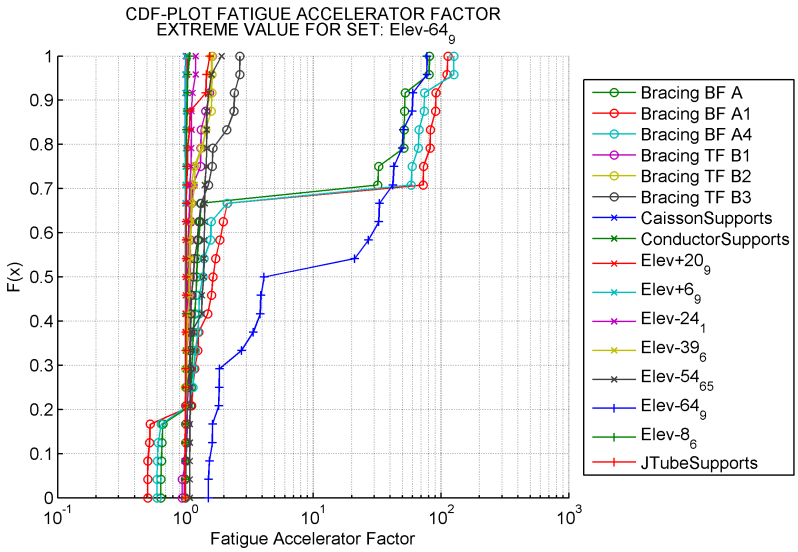

Figure H.31: Largest Fatigue Accelerator Factor for set Elev-64.9

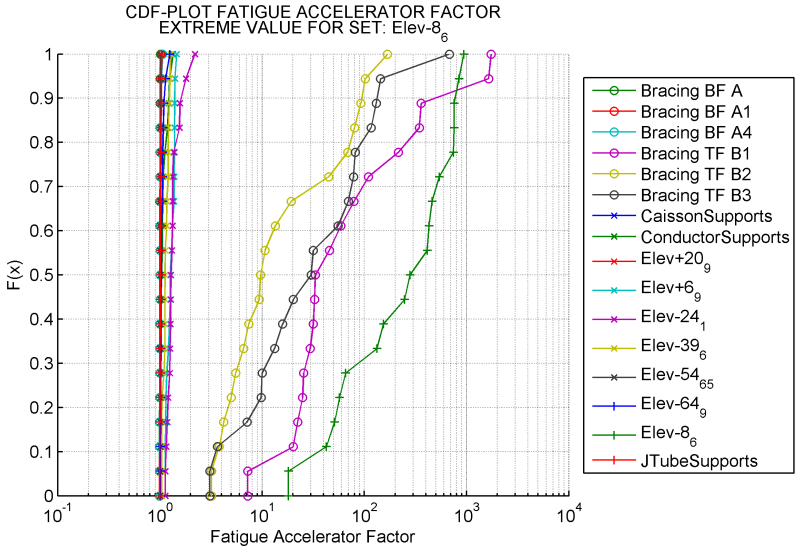

Figure H.32: Largest Fatigue Accelerator Factor for set Elev-8.6

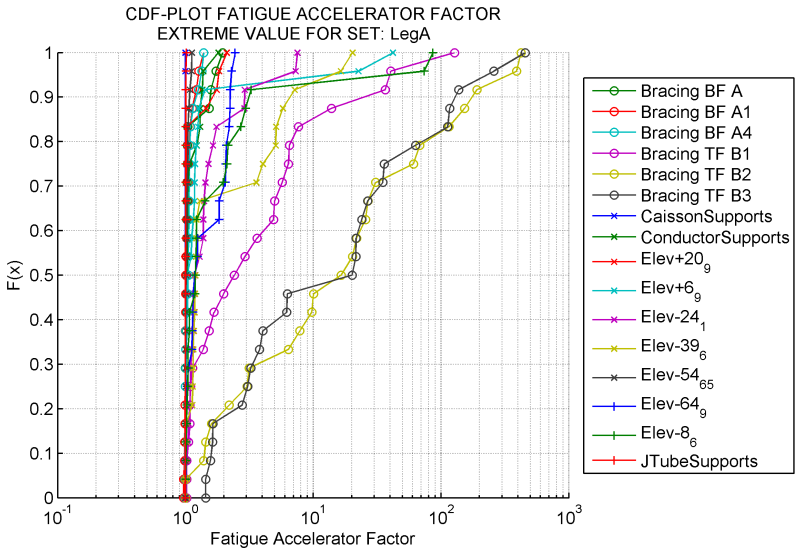

Figure H.33: Largest Fatigue Accelerator Factor for set LegA

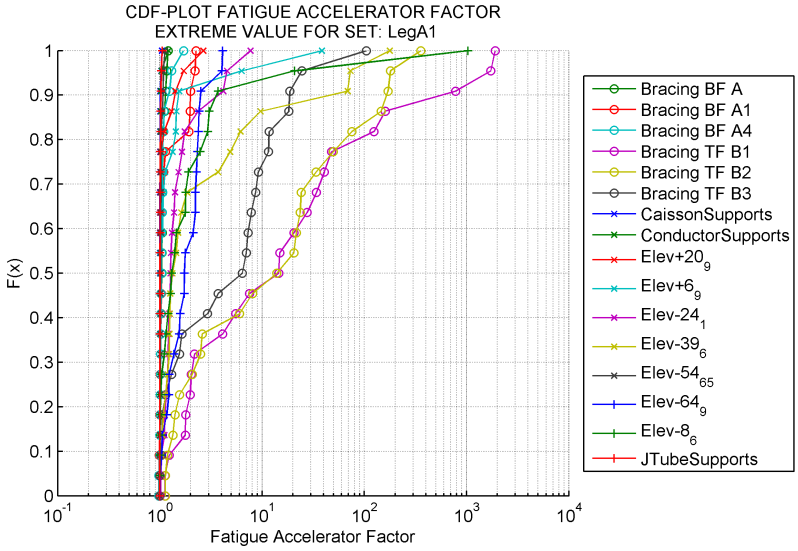

Figure H.34: Largest Fatigue Accelerator Factor for set LegA1

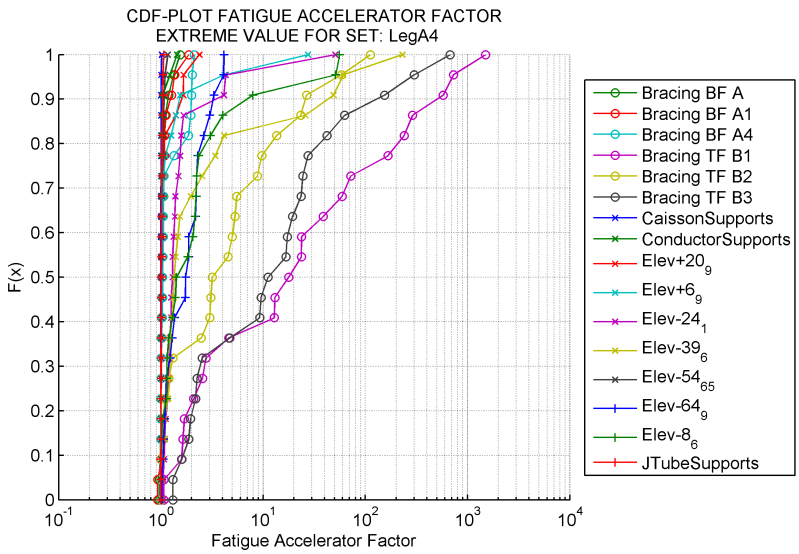

Figure H.35: Largest Fatigue Accelerator Factor for set LegA4

Appendix I

Pushover RSR

The following figures shows how much the damage scenarios affect the RSR of the structure. The x-axis is the damage case index, while the y-axis represents the impaired RSR reduction expressed as a percent of the initial RSR, e.g. a value of 10 % means the impaired RSR is 90 % of the intact RSR.

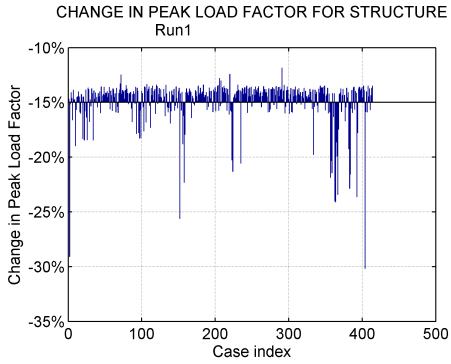

(a) Run 1

Figure I.1: Changes in RSR due to impaired integrity, 4L-jacket

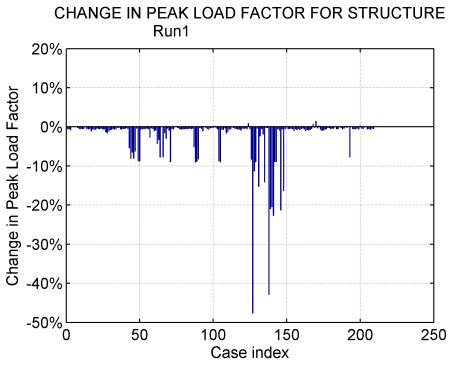

(a) Run 1

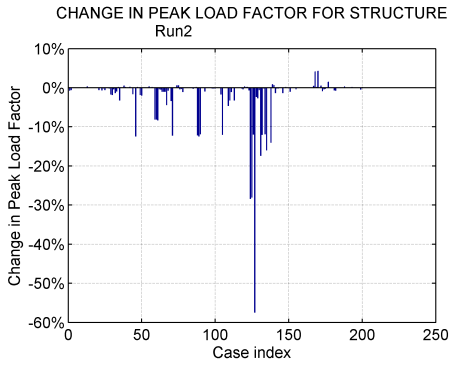

(b) Run 2

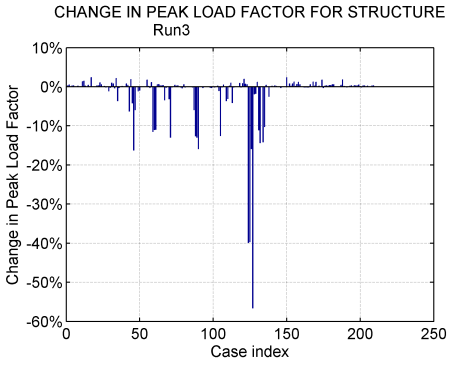

(c) Run 3

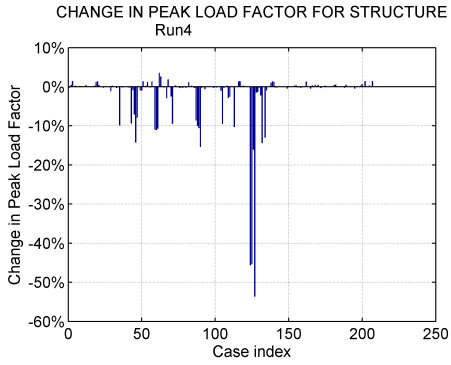

(d) Run 4

Figure I.2: Changes in RSR due to impaired integrity, 3L-jacket